

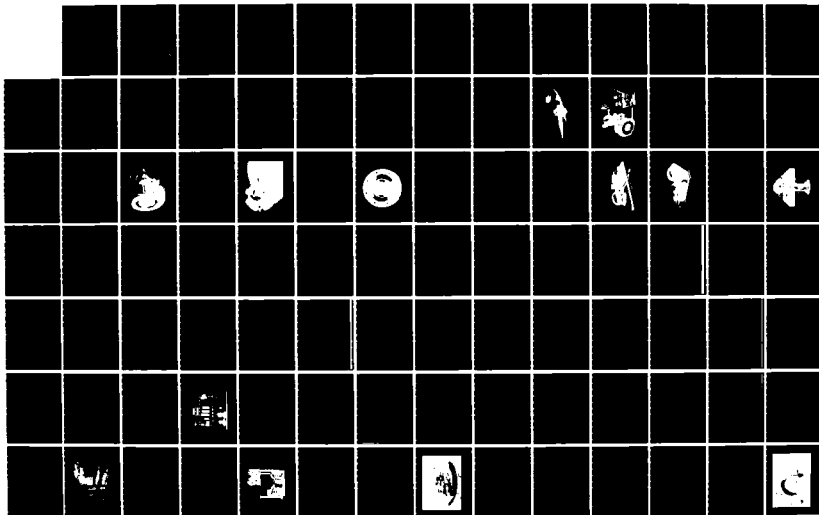
AD-A165 223

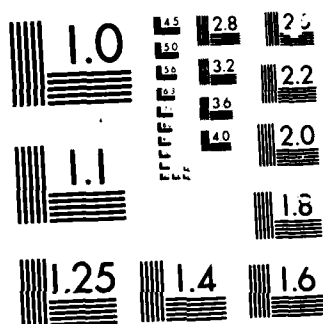
A NEUTRAL PLASMA SOURCE FOR ACTIVE SPACECRAFT CHARGE  
CONTROL(U) JET PROPULSION LAB PASADENA CA  
W D DEININGER ET AL. AUG 85 JPL-D-2734 AFGL-TR-85-0313  
NAS7-918 F/G 22/2

1/2

UNCLASSIFIED

NL





MICROCOPY RESOLUTION TEST CHART

12

AFGL-TR-85-0313

A NEUTRAL PLASMA SOURCE FOR ACTIVE SPACECRAFT CHARGE CONTROL

W. D. Deininger  
G. Aston  
L. C. Pless

Jet Propulsion Laboratory  
California Institute of Technology  
Pasadena, California 91109

August 1985

Final Report  
July 1983 - August 1985

APPROVED FOR PUBLIC RELEASE; DISTRIBUTION UNLIMITED

DTIC  
SELECTED  
MAR 14 1986  
B

AIR FORCE GEOPHYSICS LABORATORY  
AIR FORCE SYSTEMS COMMAND  
UNITED STATES AIR FORCE  
HANSCOM AIR FORCE BASE, MASSACHUSETTS 01731

AD-A165 223

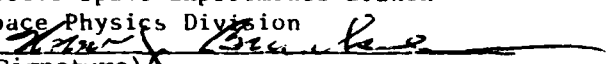
DTIC FILE COPY

86 3 1 021

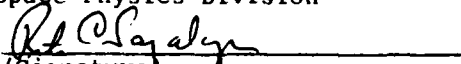
"This technical report has been reviewed and is approved for publication"

FOR THE COMMANDER

WILLIAM J. BURKE, Chief  
Active Space Experiments Branch  
Space Physics Division

  
(Signature)

RITA C. SAGALYN, Director  
Space Physics Division

  
(Signature)

This document has been reviewed by the ESD Public Affairs Office (PA) and is releasable to the National Technical Information Service (NTIS)

Qualified requestors may obtain additional copies from the Defense Technical Information Center. All others should apply to the National Technical Information Service.

If your address has changed, or if you wish to be removed from the mailing list, or if the addressee is no longer employed by your organization, please notify AFGL/DAA, Hanscom AFB, MA 01731. This will assist us in maintaining a current mailing list.

Unclassified

SECURITY CLASSIFICATION OF THIS PAGE

## REPORT DOCUMENTATION PAGE

1a. REPORT SECURITY CLASSIFICATION Unclassified			1b. RESTRICTIVE MARKINGS 4D-416.5 223		
2a. SECURITY CLASSIFICATION AUTHORITY			3. DISTRIBUTION/AVAILABILITY OF REPORT APPROVED FOR PUBLIC RELEASE; DISTRIBUTION UNLIMITED		
2b. DECLASSIFICATION/DOWNGRADING SCHEDULE					
4. PERFORMING ORGANIZATION REPORT NUMBER(S) JPL D-2734			5. MONITORING ORGANIZATION REPORT NUMBER(S) AFGL-TR-85-0313		
6a. NAME OF PERFORMING ORGANIZATION Jet Propulsion Laboratory California Institute of Technology		6b. OFFICE SYMBOL (If applicable)	7a. NAME OF MONITORING ORGANIZATION Air Force Geophysics Laboratory		
6c. ADDRESS (City, State and ZIP Code) Pasadena, California 91109			7b. ADDRESS (City, State and ZIP Code) Hanscom AFB Massachusetts 01731		
8a. NAME OF FUNDING/SPONSORING ORGANIZATION		8b. OFFICE SYMBOL (If applicable)	9. PROCUREMENT INSTRUMENT IDENTIFICATION NUMBER NAS 7-918 Task Order RE-182 Amendment No. 325		
8c. ADDRESS (City, State and ZIP Code)			10. SOURCE OF FUNDING NOS.		
			PROGRAM ELEMENT NO.	PROJECT NO.	TASK NO.
			63410F	2822	01
11. TITLE (Include Security Classification) A Neutral Plasma Source for Active Spacecraft Charge Control			WORK UNIT NO. AA		
12. PERSONAL AUTHOR(S) W. D. Deininger, G. Aston, L.C. Pless					
13a. TYPE OF REPORT Final Report		13b. TIME COVERED FROM July 1982 TO Aug 85		14. DATE OF REPORT (Yr., Mo., Day) 1985 August	
15. PAGE COUNT 136					
16. SUPPLEMENTARY NOTATION					
17. COSATI CODES			18. SUBJECT TERMS (Continue on reverse if necessary and identify by block number)		
FIELD	GROUP	SUB GR.	Neutral plasma		
			Krypton gas		
			Active spacecraft charge control		
19. ABSTRACT (Continue on reverse if necessary and identify by block number) The control of spacecraft charging is important since many satellite operating anomalies and systems malfunctions have been attributed to charging related phenomena. Overall spacecraft frame charging and differential surface charging can manifest themselves in many ways including electrostatic discharge, logic circuit upsets, space plasma measurement complications, enhancement of surface contamination and sputter erosion of surfaces. A prototype plasma source spacecraft discharge device has been developed at JPL to reduce overall and differential spacecraft surface charging and its effects. The plasma source is based on a hollow cathode discharge where the plasma generation process is contained completely within the cathode. The system operates on krypton gas and has cold start times of less than 4 seconds. A particle current control electrode just downstream of the cathode orifice can be used to enhance or inhibit electron flow from the cathode. The required inputs are power, telemetry line downlink, gas system latching valve open/close and control inputs from spacecraft potential monitors. A spacecraft discharge, net charge sensing circuit provides the ability to measure the polarity, magnitude, pulse shape. (Over)					
20. DISTRIBUTION/AVAILABILITY OF ABSTRACT UNCLASSIFIED/UNLIMITED <input type="checkbox"/> SAME AS RPT <input type="checkbox"/> DTIC USERS <input type="checkbox"/>			21. ABSTRACT SECURITY CLASSIFICATION Unclassified		
22a. NAME OF RESPONSIBLE INDIVIDUAL Dana Rush, Capt, USAF			22b. TELEPHONE NUMBER (Include Area Code)		22c. OFFICE SYMBOL AFGL/PHE

DD FORM 1473, 83 APR

EDITION OF 1 JAN 73 IS OBSOLETE.

Unclassified

SECURITY CLASSIFICATION OF THIS PAGE

Unclassified

SECURITY CLASSIFICATION OF THIS PAGE

Cont of Block 19:

and time duration of a discharge event.

All system requirements have been met or exceeded. In ground simulation tests, the plasma source successfully discharged capacitively biased plates, from as high as + 2500V, to ground potential. Actively biased plates could be discharged and clamped at +5V with respect to ground.

Unclassified

SECURITY CLASSIFICATION OF THIS PAGE

## ACKNOWLEDGEMENTS

The authors wish to thank Robert L. Toomath for assistance in the electronics layout and fabrication, Allison G. Owens for assistance in the mechanical layout and fabrication and Col. W. T. McLyman for electronics design support.

The research described in this report was performed at the Jet Propulsion Laboratory by Members of the Electric Propulsion and Plasma Technology Group under contract to the Air Force Geophysics Laboratory, NAS7-918, Task Order Number RE-182, Amendment Number 325.

Approved for	✓
NE	
PM	
Un	
3	
Dis	
A-1	



## CONTENTS

	<u>Page</u>
1. INTRODUCTION . . . . .	1-1
2. PLASMA SOURCE DEVELOPMENT . . . . .	2-1
2.1 BASIC CONSIDERATIONS . . . . .	2-1
2.2 PLASMA GENERATION REQUIREMENTS . . . . .	2-2
2.3 DESIGN AND OPERATING CHARACTERISTICS . . . . .	2-4
2.4 PRESSURE AND GAS FLOW REQUIREMENTS . . . . .	2-10
3. FLIGHT PLASMA SOURCE SYSTEM . . . . .	3-1
3.1 SUPPORT VESSEL AND HOLLOW CATHODE . . . . .	3-1
3.1.1 Cathode Emitter Tube Handling Procedure . . . . .	3-8
3.2 GAS SYSTEM . . . . .	3-8
3.3 POWER PROCESSORS . . . . .	3-14
3.3.1 Primary Converter Design and Operation . . . . .	3-14
3.3.1.1 START Converter . . . . .	3-22
3.3.1.2 RUN Converter . . . . .	3-24
3.3.1.3 KEEPER Converter . . . . .	3-25
3.3.2 Support Function Circuitry . . . . .	3-26
3.3.2.1 Housekeeping Power Processor . . . . .	3-26
3.3.2.2 Commands . . . . .	3-30
3.3.2.2.1 Command Buffer . . . . .	3-30
3.3.2.2.2 Command Isolator . . . . .	3-31
3.3.2.2.3 Ground Test Controller . . . . .	3-32
3.3.2.3 Telemetry . . . . .	3-32
3.3.2.3.1 Operations Monitor Telemetry . . . . .	3-32



## CONTENTS (Continued)

	<u>Page</u>
3.3.2.3.2 Output Monitor Telemetry . . . . .	3-37
3.3.3 Power Processor Boxes . . . . .	3-38
3.4 OVERALL PROTOTYPE FLIGHT SYSTEM . . . . .	3-43
4. MECHANICAL AND THERMAL TESTING . . . . .	4-1
4.1 GAS SYSTEM MECHANICAL TESTING . . . . .	4-1
4.2 CATHODE AND VESSEL MECHANICAL TESTING . . . . .	4-7
4.3 POWER PROCESSOR MECHANICAL TESTING . . . . .	4-7
4.4 POWER PROCESSOR THERMAL CYCLING TESTS . . . . .	4-14
5. PLASMA SOURCE OPERATION . . . . .	5-1
5.1 PLASMA SOURCE START-UP . . . . .	5-1
5.2 SYSTEM FUNCTIONAL CHECKOUT . . . . .	5-4
5.3 SYSTEM OPERATIONAL CHARACTERISTICS . . . . .	5-6
5.3.1 Battery Voltage Telemetry . . . . .	5-6
5.3.2 Box Temperature Telemetry . . . . .	5-6
5.3.3 Gas Pressure Telemetry . . . . .	5-9
5.3.4 Cathode Current Telemetry . . . . .	5-9
5.3.5 Cathode Voltage Telemetry . . . . .	5-9
5.3.6 Keeper Current Telemetry . . . . .	5-12
5.3.7 Keeper Voltage Telemetry . . . . .	5-12
5.3.8 Keeper Polarity Telemetry . . . . .	5-16
5.3.9 Amplified Net Current Telemetry . . . . .	5-16
5.3.10 Amplified Net Current Polarity Telemetry . . . . .	5-20
5.3.11 Integrated Net Current Telemetry . . . . .	5-20

## CONTENTS (Continued)

	<u>Page</u>
5.3.12 Integrated Net Current Polarity Telemetry . . . . .	5-22
5.4 PLASMA SOURCE SYSTEM TESTING . . . . .	5-22
5.4.1 Operational Characteristics . . . . .	5-23
5.4.2 Functional Characteristics . . . . .	5-25
6. CONCLUSIONS . . . . .	6-1
7. REFERENCES . . . . .	7-1

# LIST OF ILLUSTRATIONS

<u>Figure</u>	<u>Page</u>
2-1. General Schematic of Plasma Source System. . . . .	2-5
2-2. Flight Version of Cathode Emitter Tube Assembly . . . . .	2-6
2-3. Prototype Plasma Source System in the JPL Test Configuration . . . . .	2-7
2-4. Typical Plasma Source Starting Characteristics . . . . .	2-9
2-5. Plasma Source Gas Flow Requirements As a Function of Gas Molecular Weight . . . . .	2-11
3-1. Plasma Source Vessel . . . . .	3-2
3-2. Schematic of Plasma Source Vessel. . . . .	3-3
3-3. View of Keeper Electrode Assembly and Cathode Barrel Before Final Fabrication of The Vessel. . . . .	3-4
3-4. Downstream End of Support Vessel . . . . .	3-6
3-5. Flight Cathode Emitter Tip . . . . .	3-7
3-6. Mounted Flight Gas System . . . . .	3-10
3-7. Another View of the Flight Gas System . . . . .	3-11
3-8. Support Vessel and Gas System Mounted on JPL Test Hardware .	3-13
3-9. Gas System Filling Setup . . . . .	3-15
3-10. Block Diagram of Power Processor . . . . .	3-16
3-11. Plasma Source Shutoff Characteristics. . . . .	3-19
3-12. Plasma Source Pulse Width Modulator/Output Stage . . . . .	3-21
3-13. Detailed Schematic of the Start Converter (JPL Drawing No. 10111300) . . . . .	3-23
3-14. Detailed Schematic of the RUN Converter (JPL Drawing No. 10111303) . . . . .	3-27
3-15. Detailed Schematic of the Keeper Converter (JPL Drawing No. 10111302) . . . . .	3-28
3-16. Keeper Polarity Feedback Signal Extraction . . . . .	3-29

# LIST OF ILLUSTRATIONS (Continued)

<u>Figure</u>	<u>Page</u>
3-17. Detailed Schematic of the Housekeeping Converter (JPL Drawing No. 10111301) . . . . .	3-33
3-18. Detailed Schematic of the Control Buffer (JPL Drawing No. 10111305) . . . . .	3-34
3-19. Detailed Schematic of the Control Isolator . . . . .	3-35
3-20. Plasma Source Ground Test Controller . . . . .	3-36
3-21. Detailed Schematic of the Ground Test Controller (JPL Drawing No. 10111304) . . . . .	3-39
3-22. Detailed Schematic of the Plasma Source Operations Monitoring Telemetry (JPL Drawing No. 10111307) . . . . .	3-40
3-23. Detailed Schematic of the Plasma Source Net Current Monitoring Telemetry (JPL Drawing No. 10111306). . . . .	3-41
3-24. Front Cover and Contents of Power Processor Box A. . . . .	3-42
3-25. Front Cover and Contents of Power Processor Box B. . . . .	3-44
3-26. Prototype Plasma Source System in JPL Test Configuration . .	3-47
4-1. Axis Orientations for Gas System Mechanical Testing. . . . .	4-2
4-2. Gas System Mounted for Shock and Vibration Testing Along Z Axis . . . . .	4-3
4-3. Shock Test Pulse Applied Along Z-Axis of Gas System . . . . .	4-4
4-4. Vibration Test Programmed Reference Spectrum . . . . .	4-5
4-5. Typical Vibration Test Response Signals for the Control and Monitor Accelerometers During Gas System Mechanical Testing. . . . .	4-6
4-6. Axis Orientations for Support Vessel Mechanical Testing. . .	4-8
4-7. Support Vessel Mounted for Shock and Vibration Testing Along the X-Axis . . . . .	4-9
4-8. Typical Response Signal of the Control Accelerometer During a Shock Pulse . . . . .	4-10

# LIST OF ILLUSTRATIONS (Continued)

<u>Figure</u>	<u>Page</u>
4-9. Typical Vibration Test Response Signals for the Control and Monitor Accelerometers During Support Vessel Mechanical Testing . . . . .	4-11
4-10. Axis Orientations for Electronics Box Mechanical Testing . .	4-12
4-11. Box A Mounted for Shock and Vibration Testing Along the Z Axis . . . . .	4-13
4-12. Shock Pulse Response Signal for Box a Along the Z Axis . . .	4-15
4-13. Typical Vibration Test Response Signals for the Control and Monitor Accelerometers During Power Processor Mechanical Testing . . . . .	4-16
5-1. Battery Potential Telemetry Output Calibration Curve . . . .	5-7
5-2. Box Temperature Telemetry Output Calibration Curve . . . . .	5-8
5-3. Gas Pressure Telemetry Output Versus Real Pressure . . . . .	5-10
5-4. Cathode Current Telemetry Output Calibration Curve . . . . .	5-11
5-5. Cathode Voltage Telemetry Output Calibration Curve, Low Sensitivity . . . . .	5-13
5-6. Cathode Voltage Telemetry Output Calibration Curve, High Sensitivity . . . . .	5-14
5-7. Keeper Current Telemetry Output Calibration Curve. . . . .	5-15
5-8. Keeper Potential Telemetry Output Calibration Curves . . . .	5-17
5-9. Keeper Polarity Telemetry . . . . .	5-18
5-10. Amplified Net Current Telemetry Output Calibration Curve . .	5-19
5-11. Integrated Net Current Telemetry Output Calibration Curve. .	5-21
5-12. Plasma Source ON/OFF Sequence (T/M Outputs) . . . . .	5-24
5-13. Plasma Source Operational States (T/M Outputs) . . . . .	5-27
5-14. Typical Net Current Discharge Pulse . . . . .	5-30
5-15. Typical Plate Discharge Pulse and the Plate Potential During the Discharge Pulse . . . . .	5-31

LIST OF ILLUSTRATIONS (Continued)

<u>Figure</u>	<u>Page</u>
5-16. Current Collection By a Positively Biased Plate During Plasma Source Operation (T/M Outputs) . . . . .	5-32
5-17. Collected Current As a Function of Plate Potential for Various Plasma Source Operating Modes . . . . .	5-33
5-18. Current Collection by a Negatively Biased Plate During Plasma Source Operation . . . . .	5-34

# LIST OF TABLES

<u>Table</u>	<u>Page</u>
2-1. Functional Design Requirements for the Prototype Plasma Source . . . . .	2-3
3-1. Guidelines for Handling Hollow Cathode Emitter Tubes . . . .	3-9
3-2. Gas System Characteristics . . . . .	3-12
3-3. Characteristics of the Three Primary DC-DC Converters . . .	3-17
3-4. Plasma Source Command Capability . . . . .	3-31
3-5. Analog Telemetry Outputs . . . . .	3-37
3-6. Disassembly of Box A . . . . .	3-43
3-7. Disassembly of Box B . . . . .	3-45
4-1. Thermal Cycling Test Temperature Characteristics . . . . .	4-17
5-1. Starting and Operating Procedure for Plasma Source . . . . .	5-2
5-2. Plasma Source Checkout Resistive Load Characteristics . . .	5-5
5-3. Integrator Saturation Times Versus Plasma Source Mode for Various Leakage Currents . . . . .	5-22
5-4. Plasma Source Operational States . . . . .	5-26
5-5. Sounding Rocket Capacitance Versus Debye Length . . . . .	5-29
6-1 Plasma Source Functional Requirements and Characteristics .	6-2

## SECTION 1

### INTRODUCTION

The tendency of spacecraft and spacecraft surfaces to charge has been noted since the beginning of satellite flight. Spacecraft charging appears to be particularly severe at geosynchronous orbit. Spacecraft frame potentials of thousands of volts negative with respect to the ambient space plasma have been observed during eclipse on the ATS-5 and ATS-6 spacecraft<sup>1-6</sup> and the SCATHA<sup>1,7,8</sup> satellite. The largest potential observed to date was -19 kV on ATS-6 during eclipse, but potentials as high as -2.2 kV have been seen in sunlight.<sup>5,9</sup> These potentials result from a natural balance of the charged particle fluxes to the spacecraft surfaces from the ambient electron and ion population following a geomagnetic substorm.<sup>1,10</sup> Spacecraft potentials are generally negative since electrons have higher mobilities as compared to ions. Overall spacecraft frame charging enhances surface contamination which can cause the degradation of thermal and optical surfaces. In addition, charging interferes with science measurements of the ambient space environment.

Of more concern than overall spacecraft charging is differential charging of adjacent surfaces, or differential charging resulting from charge deposition in dielectrics. Differential charging and its subsequent electrostatic discharge (ESD) is believed to be responsible for much of the anomalous behavior seen on various satellites.<sup>9,11-16</sup> The transient electrical impulses produced as a result of ESD can couple into the spacecraft electronics and cause problems ranging from logic upsets to complete system failures. In addition, ESD can cause mechanical damage to spacecraft surfaces and enhance surface contamination.



As a result of the connection between anomalous satellite behavior, differential charging and ESD, considerable effort has gone into developing methods for preventing spacecraft charging using both passive and active means. Passive means include the use of conductive materials on spacecraft surfaces, use of proper grounding techniques and filtering of electronics.<sup>17</sup> Active spacecraft charge control encompasses the use of a wide range of charged particle emitters, including electron, ion and plasma emitters. All active charge control devices have been successful, to some degree, in discharging overall and differentially charged spacecraft. However, only devices emitting a neutral plasma have been found to maintain spacecraft potentials near plasma ground and significantly suppress differential charging.<sup>2-7,17</sup>

This report details the development of a unique hollow cathode, neutral plasma source for use in controlling spacecraft charging. As originally envisioned, this device was to be part of the Satellite Active Automatic Discharge System (SAADS) on the Air Force Geophysics Laboratory (AFGL) Beam Emission Rocket Test-1 (BERT-1) sounding rocket. The Jet Propulsion Laboratory (JPL) was charged with the responsibility of developing the plasma source device within the AFGL BERT-1/SAADS program. AFGL retained responsibility for requirements definition, qualification testing, sounding rocket integration, flight operations and data reduction. Launch window constraints coupled with the need for AFGL to rebuild an electrostatic analyzer prevented final integration of the JPL plasma source into the BERT-1 sounding rocket.

The plasma source spacecraft discharge device as developed during this program, is capable of turning on in less than five seconds and has demonstrated the ability to prevent charge buildup and discharge charged surfaces to ground potential during ground simulation tests. The general operating principle of the hollow cathode plasma source is described first, including the specific details of hollow cathode operation. A detailed description of the prototype flight plasma source system is given next including a mechanical and functional description of the support vessel and hollow cathode, power processor and gas handling system. The environmental testing is then described followed by a detailed discussion of plasma source operation and some concluding remarks.

## SECTION 2

### PLASMA SOURCE DEVELOPMENT

This section discusses the design rational, operating principles and performance characteristics of the plasma source spacecraft charge control device.

#### 2.1 BASIC CONSIDERATIONS

A charged spacecraft, or spacecraft surface cannot generally bleed it's charge back to the surrounding low density space plasma since the electrical conductivity of the intervening plasma sheath region between the spacecraft and space plasma is too low. In order to reduce the potential of the spacecraft, it is necessary to artificially increase the electrical conductivity between the spacecraft and surrounding space plasma. An effective way of doing this is to form a relatively high conductivity plasma bridge to allow the passage of positively and negatively charged particles through the sheath. The plasma bridge provides an additional source of charged particles for current balance to reduce and prevent spacecraft-surface potential buildups. This process may be thought of conceptually by visualizing the spacecraft and surrounding space plasma as the charged plates of a capacitor and the sheath as the medium between the plates. The plasma bridge acts as a shorting strip across the capacitor. The plasma bridge must be established in a controlled way with an adequate particle flux and spatial extent to ensure that the spacecraft, or portion thereof, is returned to zero space potential without experiencing an uncontrolled and potentially damaging arc discharge (ESD).

## 2.2 PLASMA GENERATION REQUIREMENTS

There are many ways that one can create a plasma and even more devices that utilize these various production methods for applications as diverse as fluorescent lighting to controlled fusion nuclear reactors. For the sounding rocket plasma source application the specific starting and operating requirements are listed in Table 2-1. A precedent has been established in the plasma generation technique used for active spacecraft charge control by the successful charge control experiments on the ATS-6 and SCATHA satellites which used small ion engines and hollow cathode plasma bridge ion beam neutralizers.<sup>3-7</sup> During tests with these satellites it was observed that the hollow cathode plasma bridge neutralizer was sufficient to control satellite charging under a variety of space plasma environments. These results are consistent with previous experiments where hollow cathode plasma bridge neutralizers were used to neutralize the positive ion beam emerging from an ion engine spacecraft propulsion system.<sup>18-20</sup> For that application, the hollow cathode created a plasma bridge for electron flow between itself and the ion beam edge which was generally several centimeters away.

A hollow cathode discharge typically produces plasma densities on the order of  $10^{20}$ - $10^{21}$   $m^{-3}$  just downstream of the cathode orifice. Electrons in this plasma have an average temperature of about 1.0 eV while ions have the cathode thermal temperature of approximately 0.1 eV. The much higher electron speed means that, in the plasma bridge coupling process, the electrons are carrying most of the current. Furthermore, the low thermal ion velocity encourages plasma flow by ambipolar diffusion which ensures adequate space charge coupling of the ions to the emitted hollow cathode electrons so that a significant ion population is always present in the plasma bridge.

Table 2-1. Functional Design Requirements for the Prototype Plasma Source

Parameter	Requirement
Startup Time	<5 s
Working Gas	Krypton
Startup Energy	2500 W-s
Run Power	200 W
Particle Currents:	
Extracted Electron	>20 mA
Extracted Ion	>20 $\mu$ A
Electron Leakage	<2 mA
Mass	<12.25 kg
Lifetime:	
Total	>450 s
Duty Cycle (Max.)	0.3
Starts	>36

It was felt that the functional requirements of the plasma source could be best met by designing the plasma source around a hollow cathode plasma generator. However, typical ion engine hollow cathode designs require several minutes to turn on and achieve stable operation. As seen in Table 2-1, long startup times were not acceptable for the proposed sounding rocket application. In addition, a further requirement not listed in Table 2-1, was that the plasma source hollow cathode not be subject to failure after exposure to air and moisture between ground tests. This latter requirement was to obviate the necessity for keeping the plasma source under carefully controlled vacuum conditions before and during the launch. Controlled vacuum enclosures were required to prevent contamination of the rare earth oxide hollow cathodes used in ion engines in the past.<sup>6,7,18-21</sup>

### 2.3 DESIGN AND OPERATING CHARACTERISTICS

In order to satisfy the rapid start requirement of less than 5 s as well as provide resistance to contamination, a hollow cathode design was selected for the plasma source which had previously demonstrated these desirable features.<sup>22</sup> A schematic of the plasma source, delineating the basic features of the hollow cathode, containment vessel, control electrode and the power processor is shown in Fig. 2-1. Figure 2-2 shows the hollow cathode emitter tube assembly and Fig. 2-3 shows the plasma source fully assembled in the JPL test configuration. The Field Enhanced Refractory Metal (FERM) hollow cathode used with the plasma source is significantly different from most other cathode designs in that the plasma generation process is contained completely within the hollow cathode barrel. No external sustaining electrodes are needed. The hollow cathode is started by applying 300-400 volts between the central emitter tube and surrounding cathode barrel, as shown in Figure 2-1. In this arrangement, the cathode barrel acts as an anode and the working gas, which is flowing through the cathode, breaks down resulting in a glow discharge to the central cathode emitter tube. Ion bombardment of the emitter tube rapidly heats the tube end to thermionic electron emitting temperatures. The much larger heat capacity of the cathode barrel prevents this component from heating significantly during the starting process. When the tube reaches thermionic emission temperatures, the cathode transitions from a glow to an arc discharge, resulting in a low coupling voltage between the emitter tube and surrounding cathode barrel. Once this arc is established, the cathode is said to be on and is a stable, high density plasma source. The entire starting sequence takes less than five seconds.

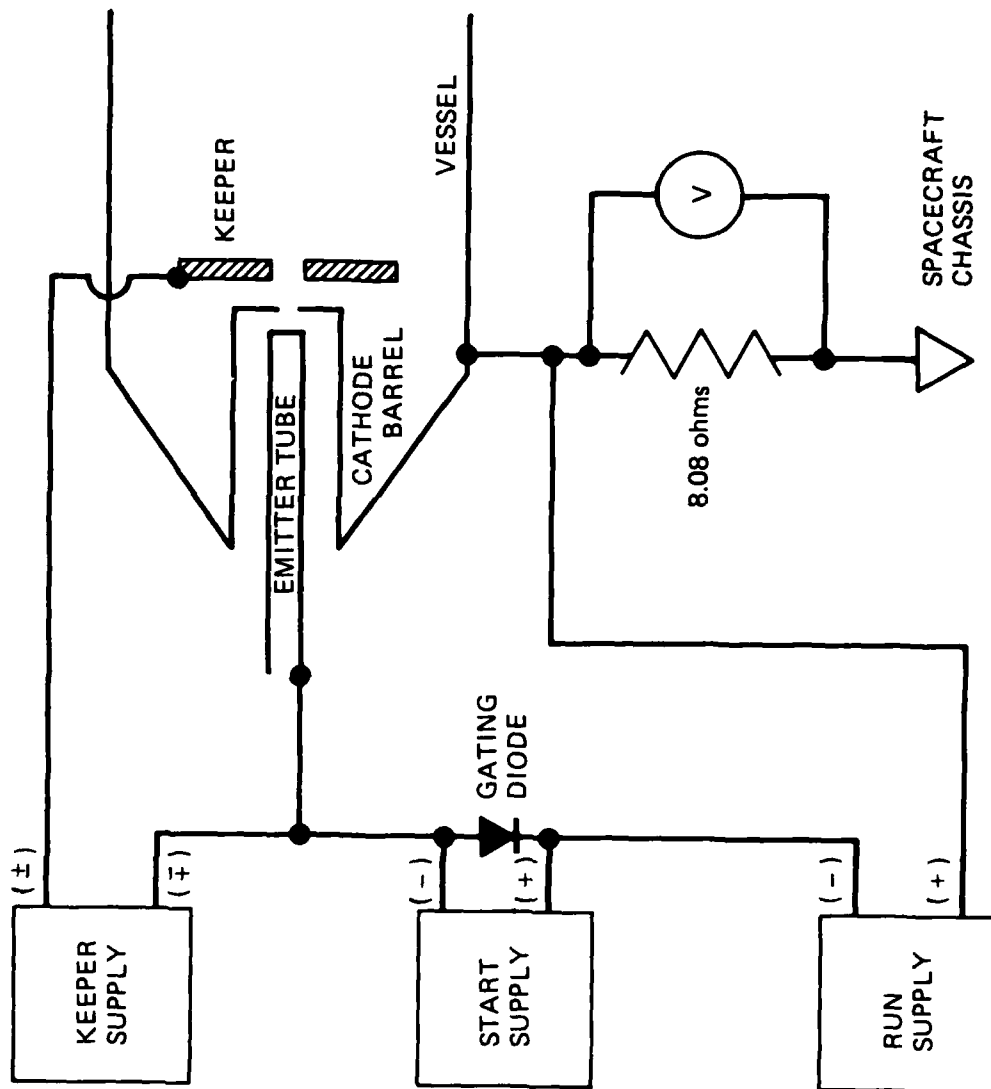


Figure 2-1. General Schematic of Plasma Source System



Figure 2-2. Flight Version of Cathode Emitter Tube Assembly



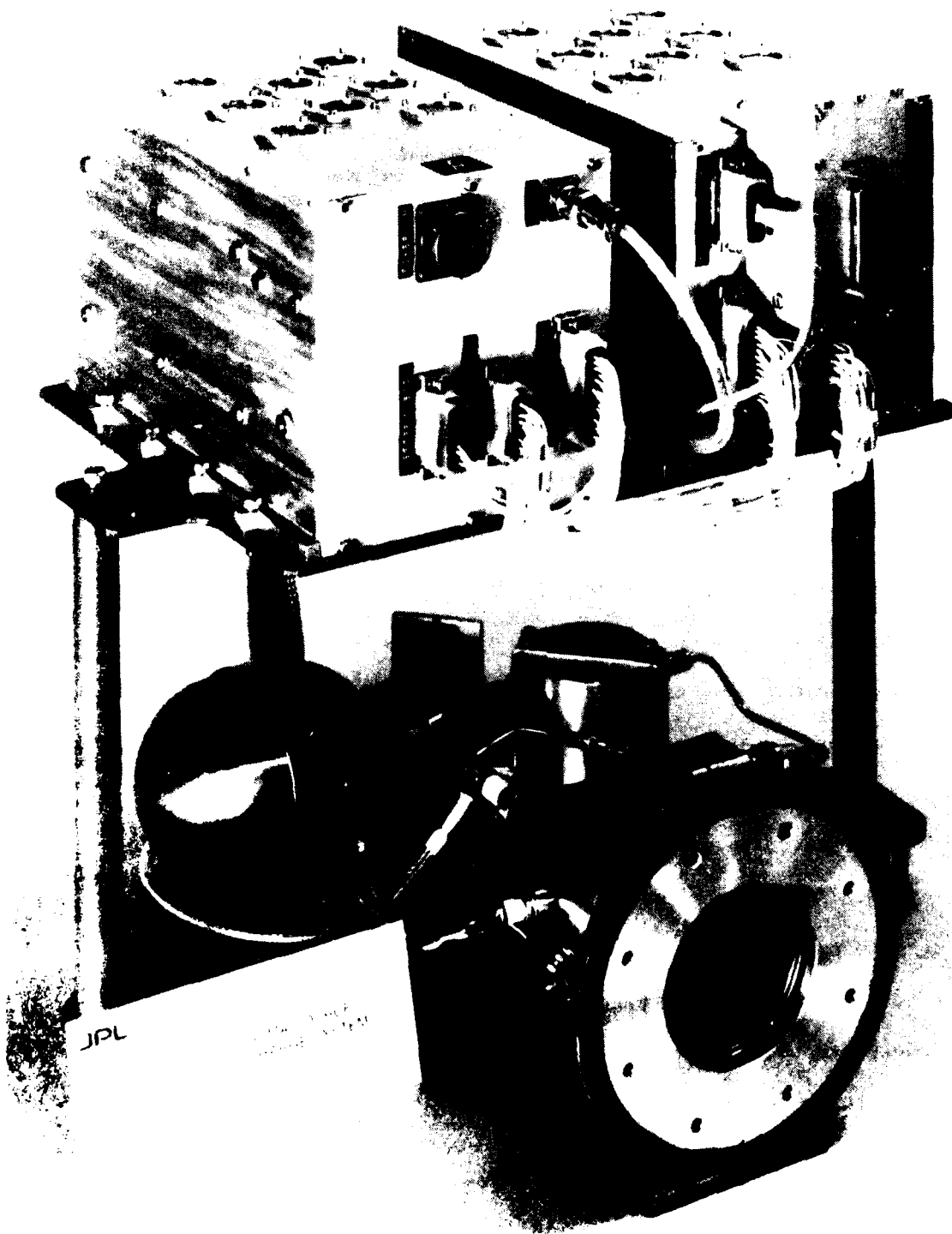


Figure 1. Prototype Plasma Source System in the JPL Test Configuration

Plasma flows with either predominately electron or ion currents, may be extracted through the cathode orifice by applying either a positive or negative bias, respectively, to the external keeper electrode shown in Figure 2-1. Ambipolar diffusion ensures that, for the few tens of volts keeper electrode bias, a plasma will be drawn from the cathode.

Typical volt-ampere starting characteristics for the plasma source hollow cathode are shown in Fig. 2-4 (a,b). The power consumed as a function of time is shown in Fig. 2-4c where it can be seen that the starting energy (watt-secs) and running power level are well within the design specifications listed in Table 2-1. The most critical parameter controlling the turn on time and hollow cathode power consumption is the heat capacity of the end portion of the emitter tube where the plasma discharge occurs. It was found from previous studies of the FERM cathode<sup>22</sup> and during this development program that only the last 2-3 mm of the emitter tube emitted thermionic electrons and participated in the plasma discharge. As a result, the emitter tube tip was optimized for minimum heat capacity while providing good mechanical strength. This optimization process resulted in the particular emitter tube design shown in Fig. 2-2 which has a lifetime of hundreds of start and run cycles.

No rare earth oxide impregnates are used in the FERM cathode emitter tube to lower its electron work function, thus eliminating the poisoning problem which often occurs with low work function impregnates upon exposure to air and moisture. The pure tantalum emitter tube of the FERM cathode can be exposed to humid air after use and, then, placed under vacuum again and restarted with no significant change in it's start or run characteristics.

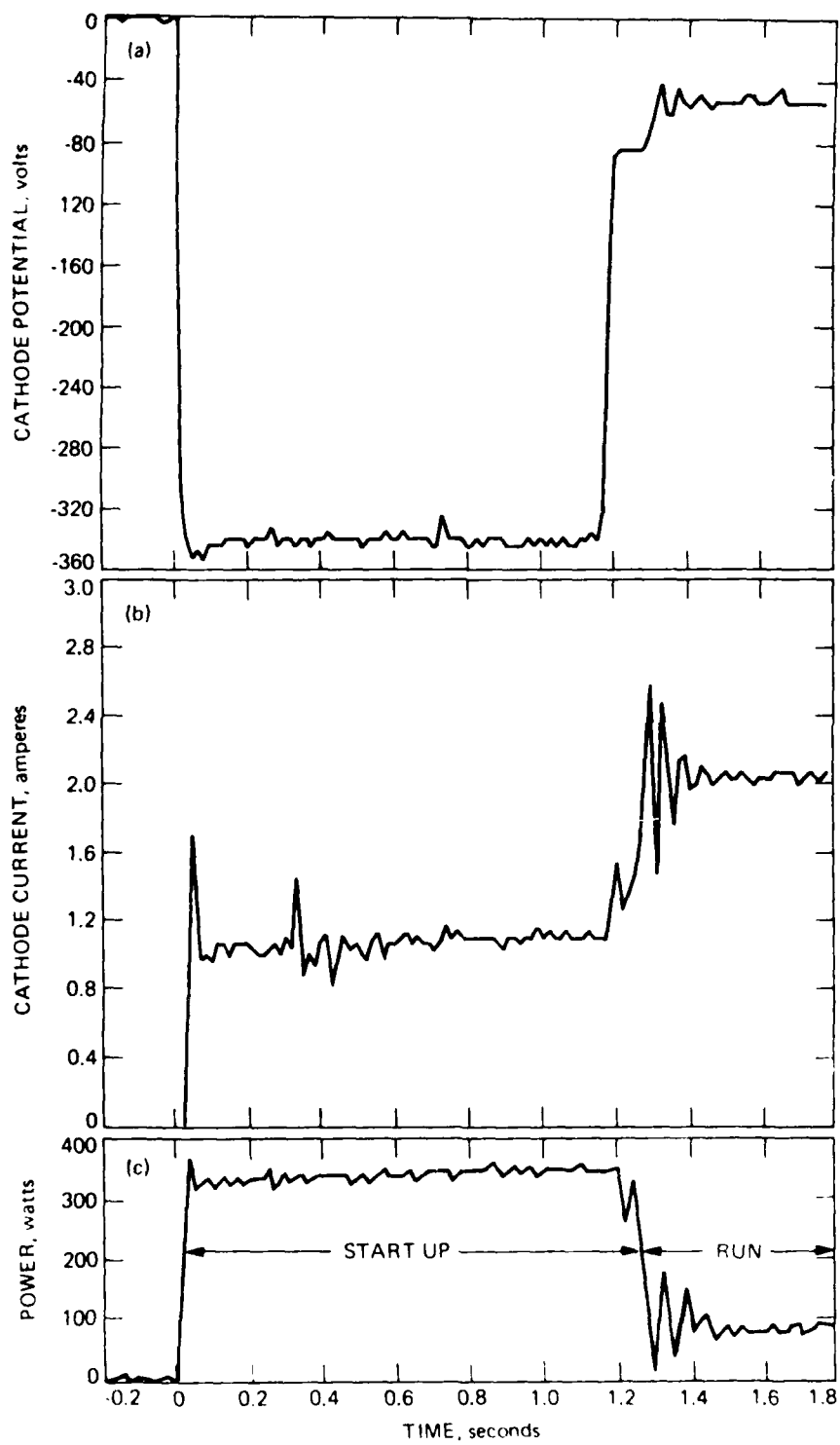


Figure 2-4. Typical Plasma Source Starting Characteristics

## 2.4 PRESSURE AND GAS FLOW REQUIREMENTS

An important parameter in successfully starting the plasma source, was ensuring that the hollow cathode internal gas stagnation pressure was in the proper range, given by the Paschen break down curve, for a minimum potential glow discharge to occur. For the plasma source cathode barrel and emitter tube geometry, low Paschen break down voltages are realized, for most gases, with a pressure distance product of about 1.0 Torr-cm.<sup>23</sup> Various tests were performed to determine the emitter tube to cathode orifice plate separation that gave the most reliable cathode startup and the lowest run power requirements. Eventually, a separation distance of 4.8 mm was selected. Consequently, the stagnation pressure within the cathode for most reliable startup was about 2.0 Torr. The plasma source has been operated on krypton, argon and xenon. Stagnation pressure measurements were taken (with the cathode off) at a variety of flow rates for each gas tested. Cross plotting these data for the optimum cathode internal pressure of 2.0 Torr gives the required gas flow rate as a function of the molecular weight of the flowing gas as shown in Fig. 2-5. This curve is for the particular cathode orifice diameter of 1.00 mm and orifice plate thickness of 1.83 mm used in the plasma source cathode developed under this program.

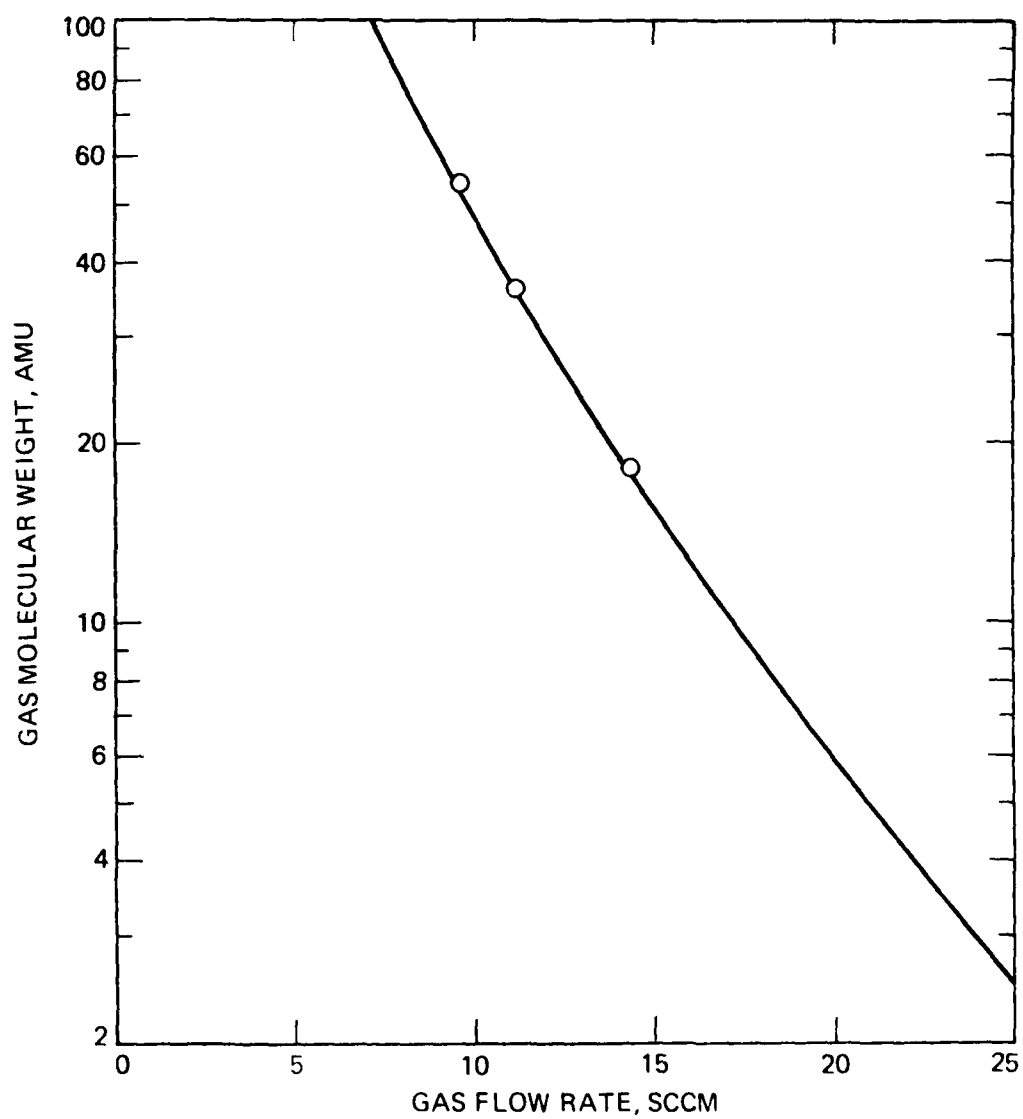


Figure 2-5. Plasma Source Gas Flow Requirements as a Function of Gas Molecular Weight

## SECTION 3

### FLIGHT PLASMA SOURCE SYSTEM

A detailed description of each flight subsystem (hollow cathode and vessel, gas system and power processor) is given, followed by a description of the overall plasma source system.

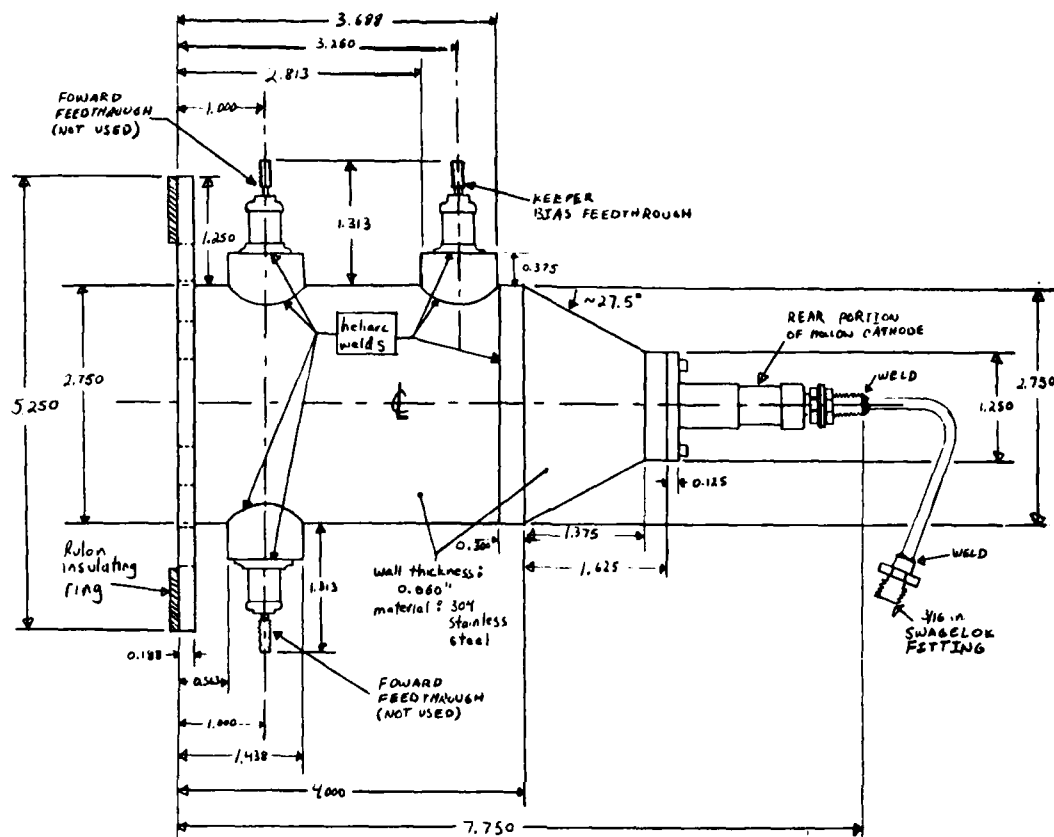
#### 3.1 SUPPORT VESSEL AND HOLLOW CATHODE

The flight plasma source vessel is shown in Fig. 3-1 and schematically in Fig. 3-2. This vessel is fabricated from 304 stainless steel and has a wall thickness of approximately 0.15 cm. It's overall length is approximately 20.0 cm with a maximum width of approximately 14.6 cm. The mounting ring has a thickness of 0.48 cm and has an outer diameter of 13.3 cm. The mounting ring, feedthroughs and cone at the rear of the vessel are heliarc-welded in place. The three feedthroughs on the support vessel body are commercially available high-vacuum, high-voltage feedthroughs and are brazed to the feedthrough ports. The two forward feedthroughs were for a plasma probing system and are not used. A Rulon insulating ring can be seen on the downstream end of the vessel.

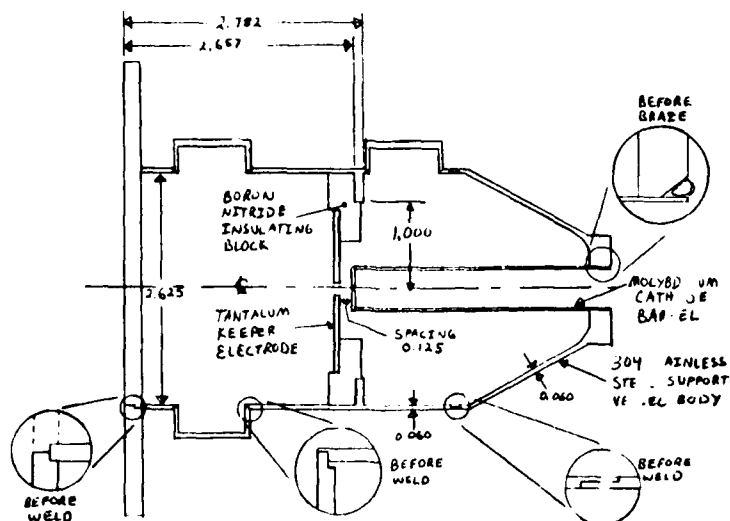
The back side of the keeper electrode assembly and the cathode barrel are shown in Fig. 3-3 before the rear cone was welded to the front portion of the flight support vessel. The keeper bias wire runs from the feedthrough to a nut attached to the keeper electrode via a keeper tie-down bolt. This wire is sheathed in ceramic insulators. All four nuts on the keeper tie-down bolts are spot-welded in place to prevent them from backing off. The keeper electrode is mounted in an insulating, boron nitride block and is a 4.76 cm diameter, 0.1 cm thick tantalum plate with a 0.32 cm center



Figure 3-1. Plasma Source Vessel



SIDE VIEW OF SUPPORT VESSEL



SUPPORT VESSEL INTERNAL DETAIL

Figure 3-2. Schematic of Plasma Source Vessel





Figure 3-3. View of Keeper Electrode Assembly and Cathode Barrel Before  
Final Fabrication of the Vessel

hole. The rear cone angle is approximately 27.5 degrees. The hollow cathode barrel is a 7.6 cm long, 1.3 cm outer diameter molybdenum tube which is high temperature brazed to the flange machined onto the small end of the support vessel cone. The brazing alloy used was Wesgo-type Palaro, which has a nominal composition of 92 percent Au and 8 percent Pd. An 80 percent dense 0.183 cm thick, tungsten plate is welded to the end of the molybdenum tube and contains a 0.1 cm orifice. The orifice serves as the exit for the low energy, hollow cathode plasma. Rulon insulating bushings can be seen on the back surface of the mounting flange.

The downstream side of the keeper electrode and support vessel are shown in Fig. 3-4. All bolts used to mount the keeper electrode and boron nitride insulator ring are wired together to prevent them from backing out when subjected to vibration testing and the launch loads. The cathode orifice is back-lit so it is easily recognized.

The emitter tube assembly shown in Fig. 2-2, consists of a commercially available vacuum, high-voltage feedthrough welded to a 0.7 cm thick, 3.2 cm diameter stainless-steel mounting flange. A 0.32 cm stainless-steel tube is welded to the threaded end of the feedthrough which joins a 0.48 cm stainless-steel tube inside the feedthrough. A 3.0 cm long, tapered, tantalum emitter tube is threaded onto the other end of the 0.48 cm stainless-steel tube. The 0.48 cm diameter tube and the first 0.5 cm of the Ta emitter tube are covered by a mullite insulator. The 0.32 cm tube is bent to avoid contact with the components of the gas handling system.

A schematic of the flight cathode emitter tip is shown in Fig. 3-5. Three separate copies of this emitter tip were shipped to AFGL with the plasma source system, along with detailed accounts of each emitters complete run history. The specific parameters for each tip are given in Fig. 3-5.

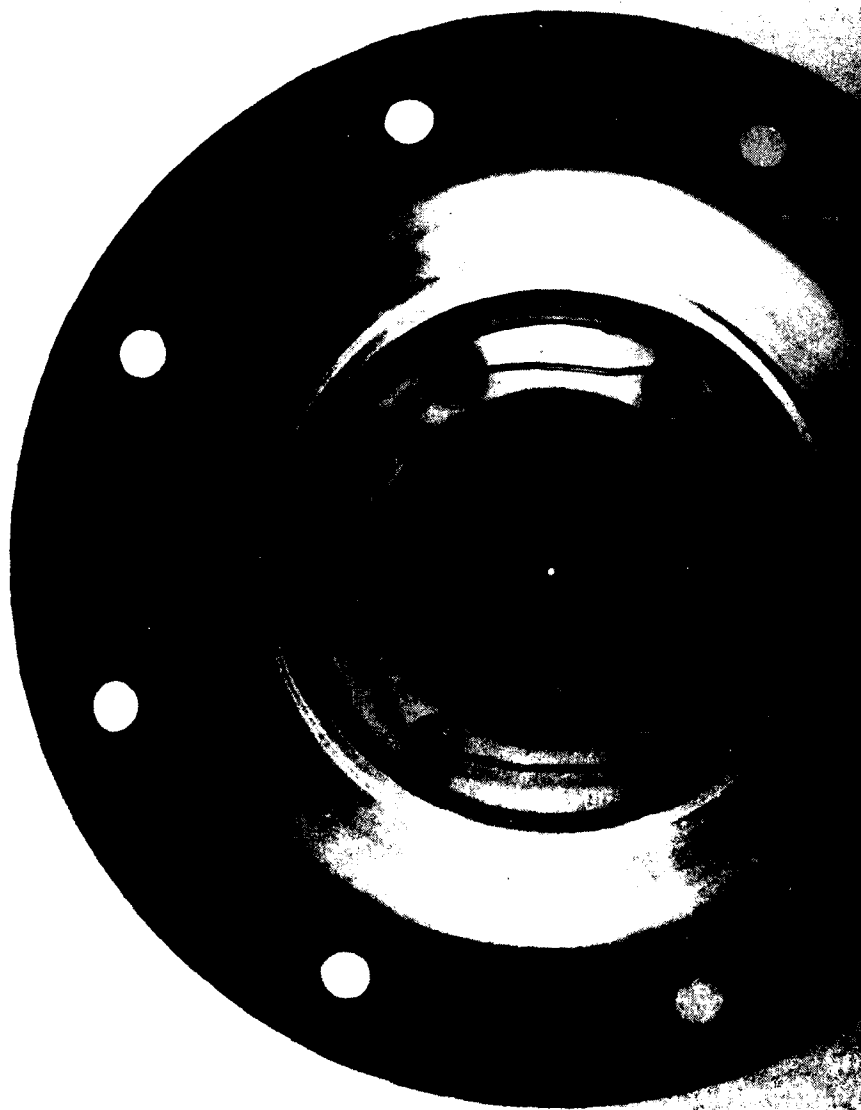
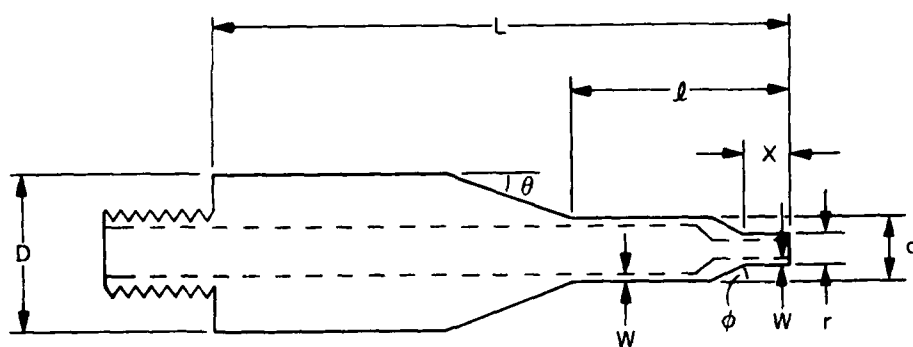


Figure 3-4. Downstream End of Support Vessel



TIP	PARAMETERS <sup>#</sup>									
	$\theta$	$\phi$	L	$\ell$	W	X	$S^*$	D	d	r
I	11	30	4.285	1.113	0.030	0.452	0.264	0.635	0.318	0.224
K	11	30	4.285	1.113	0.030	0.434	0.284	0.635	0.318	0.224
M	11	30	4.285	1.113	0.030	0.452	0.259	0.635	0.318	0.224

<sup>#</sup> ANGLES IN DEGREES, OTHER PARAMETERS IN CENTIMETERS.

<sup>\*</sup> SPACING BETWEEN END OF EMITTER TUBE TIP AND BACKSIDE OF CATHODE ORIFICE PLATE.

Figure 3-5. Flight Cathode Emitter Tip

Cathode emitter tip M was installed in the plasma source at delivery. This tip design appears to provide fast, reliable cathode starts with cold cathode starting times of approximately 3 to 4 seconds, and was the result of an extensive cathode optimization program.

### 3.1.1 Cathode Emitter Tube Handling Procedure

Hollow cathode emitter tube handling guidelines are given in Table 3-1. These guidelines are necessary since handling and exposing the cathode to the ambient environment have, on occasion, resulted in an initial start time in excess of 5 secs. during its next use. After exposure to the ambient environment, a cathode emitter tube can be reconditioned by starting and running it in an arc discharge for at least 5s to ensure that it is clean. Additional testing would be required to pin down and categorize exposure hazards.

### 3.2 GAS SYSTEM

The gas system is shown in Figs. 3-6 and 3-7 mounted on the magnesium BERT-1 flight deck plate. It consists of a reservoir, fill-fitting and pressure transducer, latching valve, pressure regulator, flow-metering valve and the interconnecting cabling and tubing. The working gas is krypton. Table 3-2 summarizes the main characteristics of the gas system. The components in this assembly were provided to JPL by AFGL and aside from the flow metering valve were spare parts from the SPIBS instrument.<sup>21</sup> Mounting of the gas system is accomplished with stainless-steel straps around the reservoir and over the regulator with the flow metering valve mounted on an aluminum bracket. The pressure regulator outlet is connected to the metering valve inlet via 0.32-cm outside-diameter, stainless-steel tubing and swagelok

Table 3-1. Guidelines for Handling Hollow Cathode Emitter Tubes

---

A. After Operation:

1. Cool for 15 minutes with the gas flow on before venting the vacuum facility up to atmosphere.
2. Vacuum tank should have a dust filter on the vent port.
3. The cover should be placed over the plasma source opening after venting up the vacuum system.

B. After removal from cathode barrel (also applies to spares):

1. Never touch the emitter tube tips.
  2. When handling the emitter tubes, wear white cotton gloves.
  3. When removing the emitter assembly, hold vessel so plasma source opening is up; this will prevent the Mullite insulator from slipping off and falling.
- 

fittings. The metering valve outlet is connected to the hollow cathode gas inlet via 0.48-cm outside-diameter Tygon tubing and swagelok fittings. The gas system and support vessel are shown tied together in the JPL test configuration in Fig. 3-8.

Specific details on the reservoir, latching valve, pressure regulator and pressure transducer can be found elsewhere.<sup>21</sup> The model VCD-1000/ A-60-A flow metering valve was manufactured by Porter Instrument Company. The valve utilizes a controller diaphragm and preset pressure differential to control flow. The maximum inlet pressure is 250 psig with a maximum operating temperature of 110°C. The flow range for Helium gas at an input pressure of 50 psig is 6.0 to 60.0 sccm. However, the gas system for the plasma source provided a krypton inlet pressure of 5 psia to the flow metering valve, resulting in a flow range of 0.5 to 9.5 sccm.



Figure 3-6. Mounted Flight Gas System

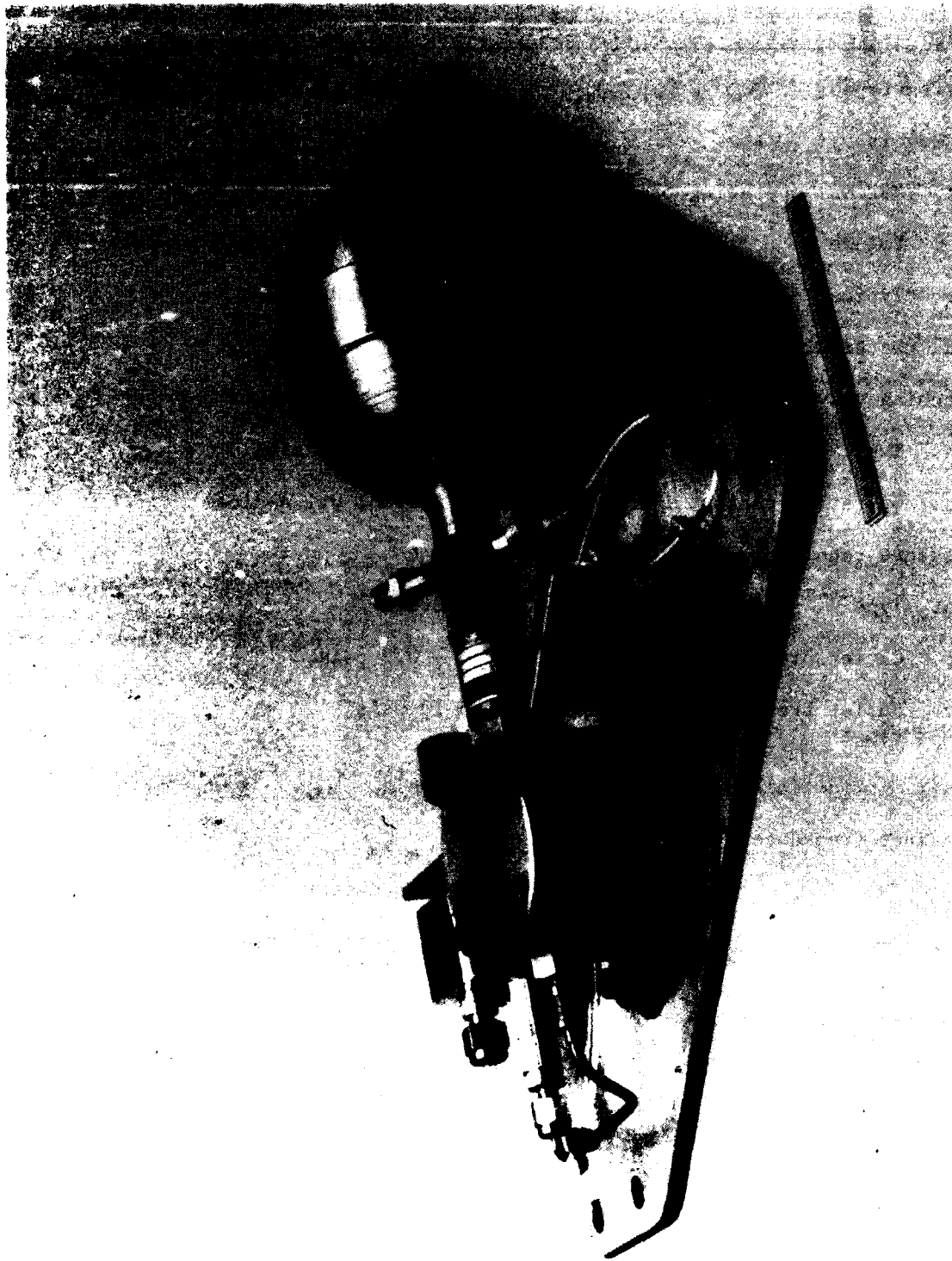


Figure 3-7. Another View of the Flight Gas System



Table 3-2. Gas System Characteristics

Parameter	Value
System type	Regulated, high pressure
Reservoir	
a. Maximum operating pressure	1000 psi
b. Volume	0.5 liter
c. Typical capacity (Kr)	50 standard liters
d. Material	Steel
Latching valve	
a. Type	Solenoid-latching
b. Operating current (100 ns)	1 A-open; 0.1 A-close
Pressure regulator	
a. Type	Aneroid
b. Outlet pressure	5 $\pm$ 0.3 psia
c. Outlet pressure adjustable range	5-10 psia
d. Minimum inlet pressure	20 psia
Pressure transducer	
a. Type	Semiconductor
b. Mounting	Built into a screw and attached to fill fitting
Flow metering valve	
a. Type	diaphragm
b. Flow metering range	6.0-60.0 sccm with 50 psig inlet pressure (for He)
c. Maximum inlet pressure	250 psig

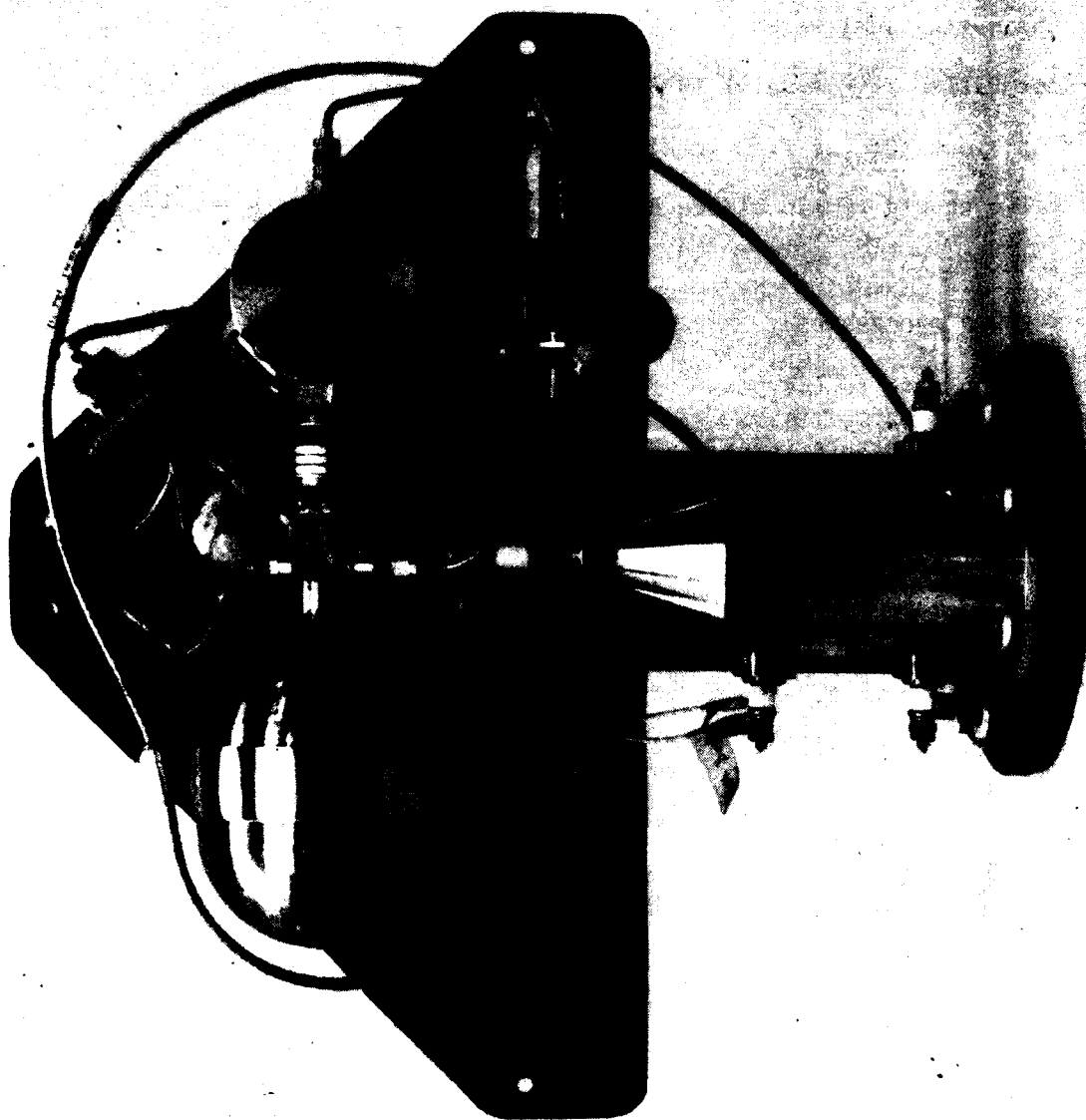


Figure 3-8. Support Vessel and Gas System Mounted on JPL Test Bed

The gas reservoir can be pressurized to as high as 1000 psi with krypton gas. The reservoir should be pumped down to the  $10^{-5}$  torr range before back-filling with pure-grade (99.95%) krypton gas. A reservoir filling setup similar to the one outlined in Fig. 3-9 should be used. A special swagelok fitting on the schrader fill-post keeps the schrader needle depressed and contains the o-ring seal which prevents gas leaks through the threads along the schrader fill-port. A valve (V3) is required beyond the special swagelok fitting to prevent the gas from leaking back out of the reservoir. The latching valve should remain closed during the reservoir filling procedure.

### 3.3 POWER PROCESSORS

The plasma source power processor consists of three source operating DC-DC converters (START, RUN and KEEPER), a low voltage DC-DC converter which provides the converter control voltages, and the associated command and telemetry circuitry. A block diagram of the overall power processor is shown in Fig. 3-10. The flight power processor has been used to start the plasma source several thousand times and operate it for a total time in excess of fortyfive (45) hours. A modular fabrication approach was used in constructing the flight power processors to allow for easy debugging, repair and/or replacement.

#### 3.3.1 Primary Converter Design and Operation

The operating characteristics for the three primary converters are given in Table 3-3. Current regulated, DC-DC converters are used since the loads are plasma discharges and the converters must limit their output currents. The plasma source is started by activating both the START and RUN converters, which are connected in series, after the gas flow has begun. Each converter contains an independent control loop, but they share a common current

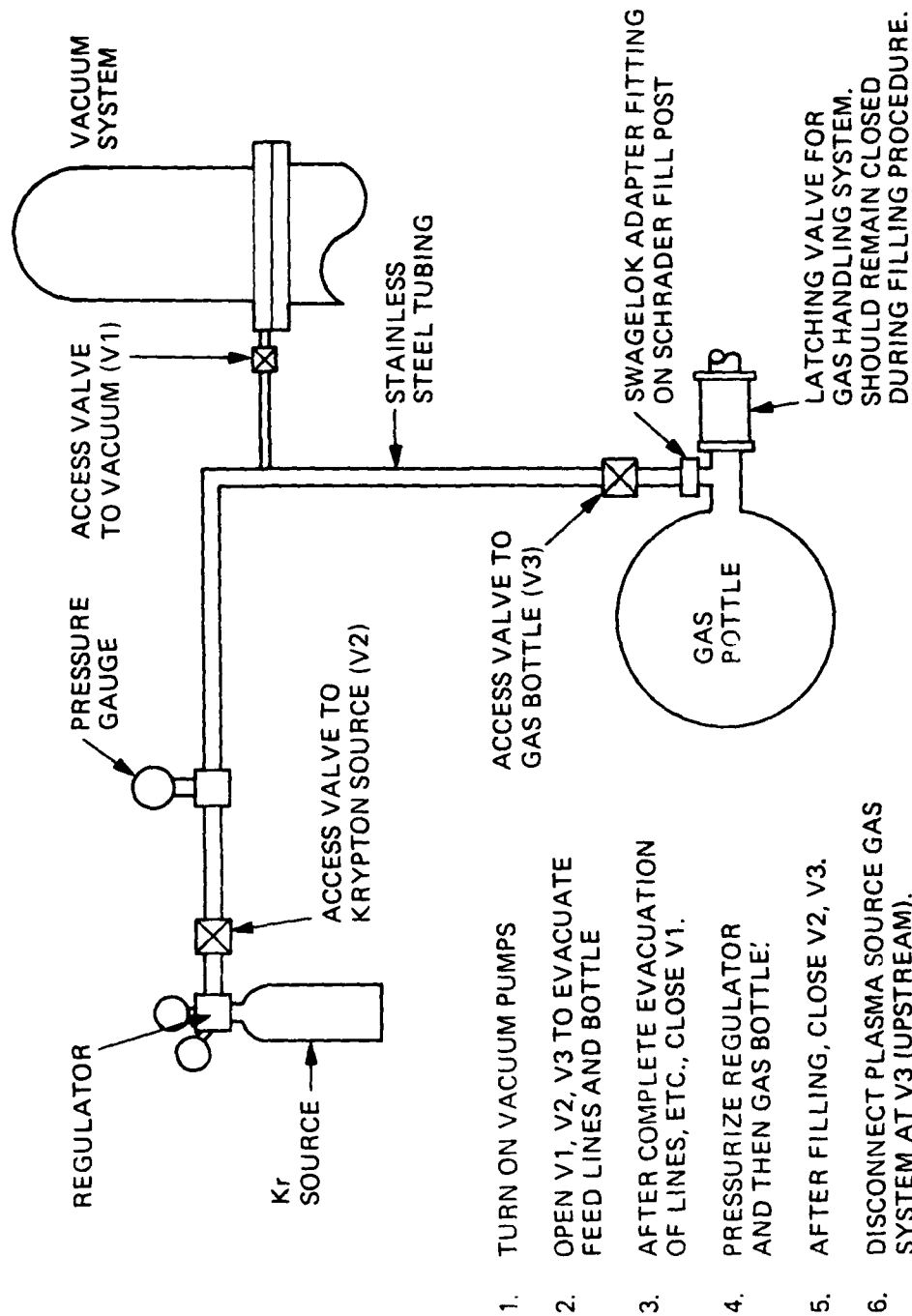


Figure 3-9. Gas System Filling Setup

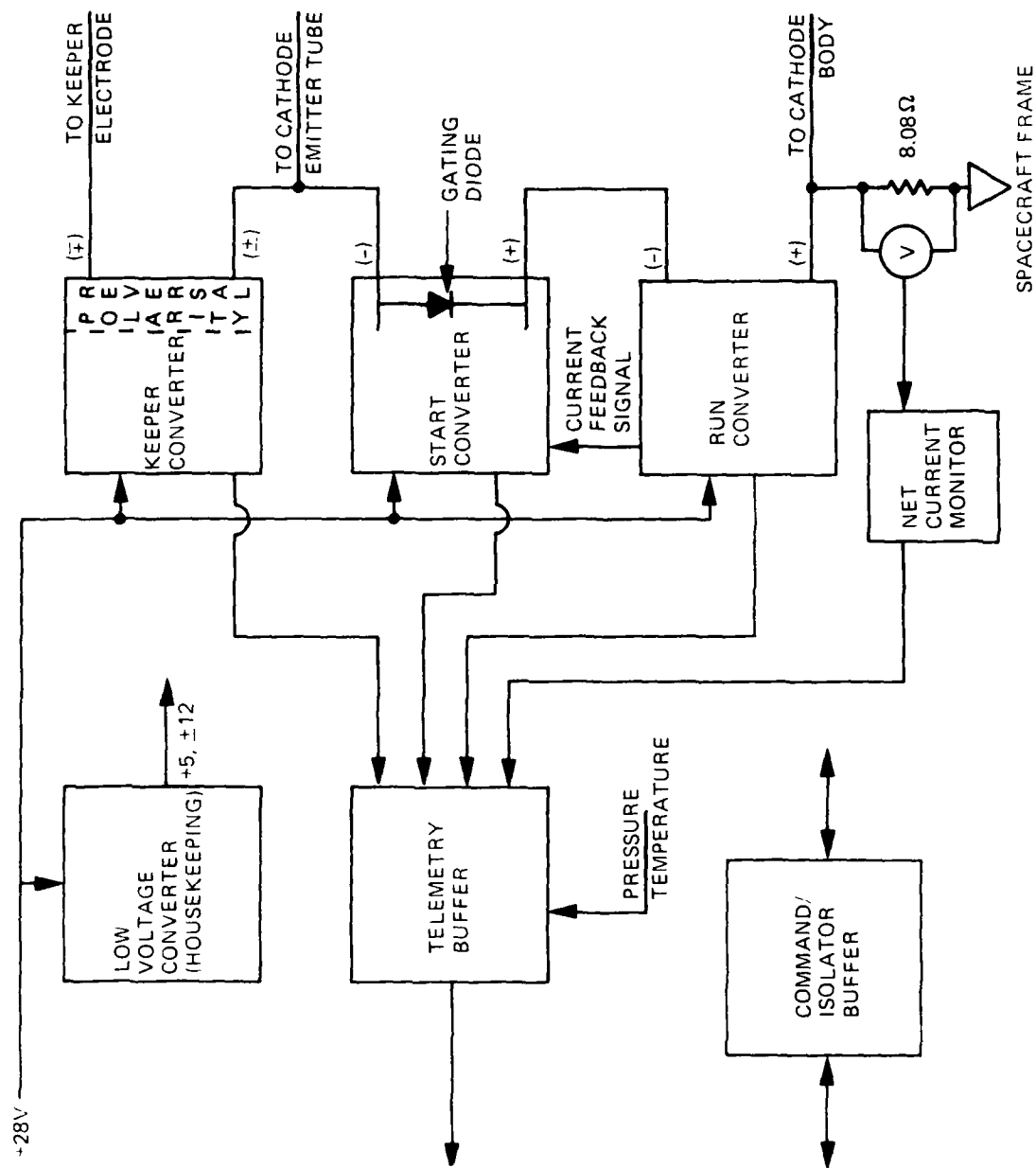


Figure 3-10. Block Diagram of Power Processor

Table 3-3. Characteristics of the Three Primary DC-DC Converters

Converter	Output Potential (V)	Current Characteristics (A)
START*	100-300	1.0
RUN	15-60	2.0
KEEPER	10-60	0.3-2.0

\*30 seconds maximum operating time with a 0.16 duty cycle.

transducer/isolator. The open circuit voltage of the RUN converter is about 90 volts, and that of the START converter is about 300 volts. The sum of the output voltages of these two converters is sufficient to initiate a glow discharge in the hollow cathode. When this occurs, the start converter limits the glow discharge current to one ampere. Since the RUN supply set point is two amperes, the RUN converter is switching at the maximum pulse width providing about 78 volts at one ampere. As the cathode emitter tube temperature rises (due to heating from ion bombardment) the cathode terminal voltage drops. The START converter maintains the current at about one ampere until cathode heating results in thermionic emission of electrons and the cathode transfers to the arc discharge mode. At this point, the cathode terminal voltage drops below the RUN converter output voltage at one ampere allowing the RUN converter to conduct more current. This allows the cathode plasma voltage to drop along a negative resistance characteristic and forces the START converter to shut down since the cathode current is higher than the START converter set point. At a cathode current of about 1.2 amperes, the START converter is forced completely off. At this point, the gating diode in the START converter provides a bypass path for the current around the START

converter. The negative resistance characteristic of the arc discharge causes the cathode current to rapidly increase to two amperes, which is the control set point for the RUN converter. The system is now on with the RUN supply providing 2 A at the cathode arc-discharge operating potential, typically 40-50 V and the START supply is off. The system is a stable, high density plasma source in this mode. The entire starting process takes less than 5 seconds. Typical start characteristics for the plasma source are shown in Fig. 2-4. The efficiency of these supplies, during both the start and run modes, is approximately 80 percent. Typical turn-off characteristics for the plasma source are shown in Fig. 3-11. Cathode shut down times are generally on the order of 2.0 ms.

As noted earlier, the primary converters are current regulated supplies. As a result, the feedback voltage signal for the converters must be derived from a plasma source current that is at a different potential from that of the control loop. This is accomplished by sensing the cathode discharge current with a shunt and using a voltage isolator. The isolator is a magnetically coupled circuit, which has internally isolated power supply for the input circuit, which is referenced to the potential to be isolated. This isolator also provides gain at the input so that relatively high-level signals can be transmitted through the isolation transformer.

The KEEPER converter is a constant current converter with a reversible output polarity. The KEEPER converter output voltage is referenced to the cathode emitter tube potential (Fig. 3-10). This converter is used to bias the keeper electrode to preferentially extract either positive or negative particles from the cathode plasma. In the electron collection mode (keeper-positive), the KEEPER has three operating set points. The set points are defined in terms of electron current collected by the keeper electrode, and

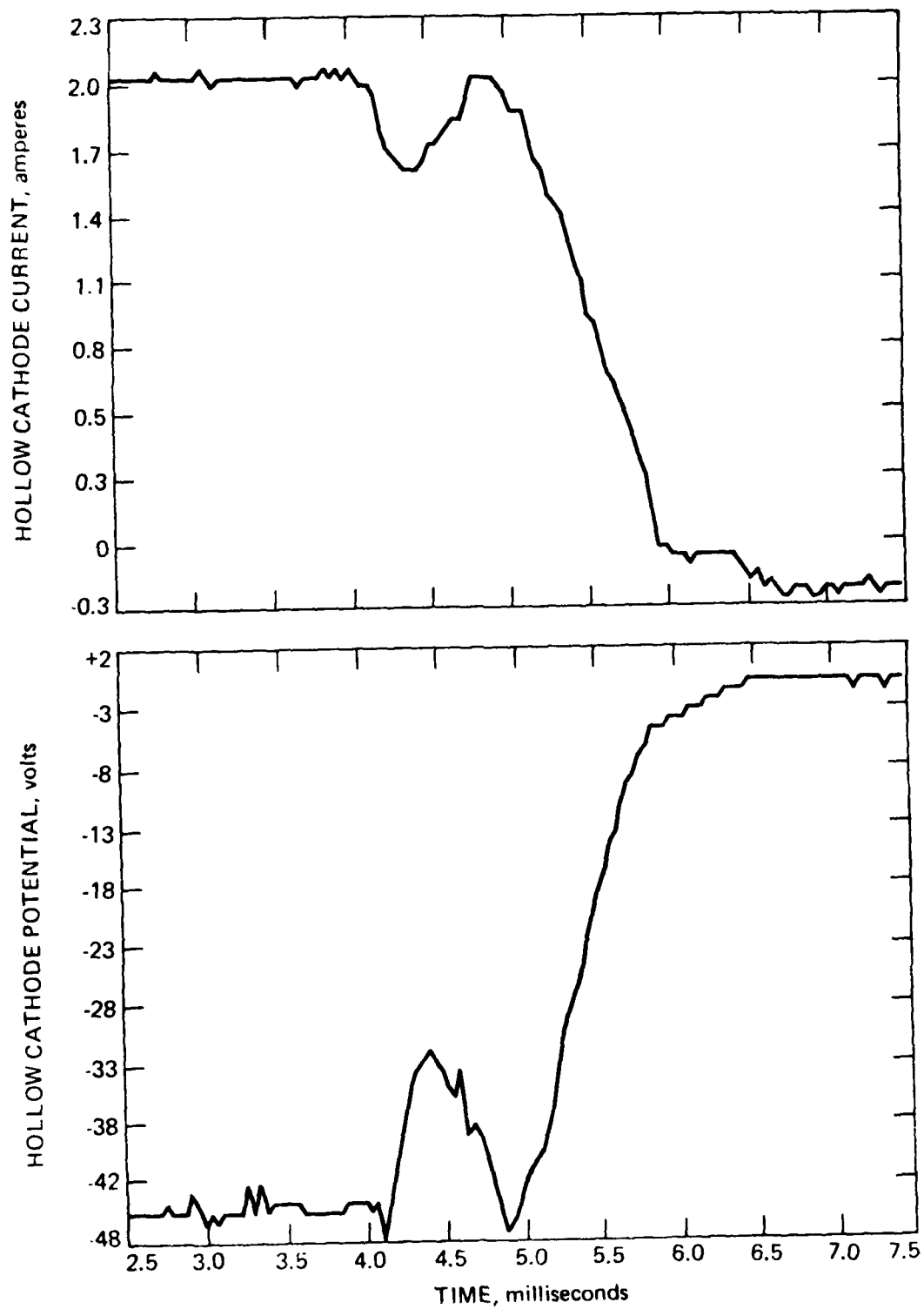


Figure 3-11. Plasma Source Shutoff Characteristics



are: 0.3 A, 1.2 A and 2.0 A, at potentials of 30 to 50 V. There is only one set point with the keeper electrode biased negatively corresponding to collected ion currents of tens of microamperes. When biased negatively, the keeper also acts to inhibit electron flow from the cathode. Since the collected ion current is well below the first KEEPER set point, when biased negatively, the converter output potential remains at its maximum (open circuit) value of approximately 88 volts.

The three primary converters each have a pulsed width modulator/output stage like the one shown in the block diagram of Fig. 3-12. The error amplifier amplifies the difference between the amplified and isolated current signal based on the current reference signal. The amplified difference controls the duty cycle of the pulse width modulator (PWM) which is a Motorola MC3420. The two main reasons for the selection of this PWM are:

- (1) Internal gating that prevents double pulsing of one-half of the output transformer primary. This eliminates one possible cause of output transformer saturation and the resulting transistor failures.
- (2) A controllable maximum duty cycle, which can be used to prevent both output transistors from being "on" at the same time, another possible cause of transistor failures.

The internal phasing of this PWM is such that a low voltage from the error amplifier causes the maximum duty cycle output from the PWM. Conversely, a high voltage turns the PWM off.

The interface between the low-level outputs of the PWM and the relatively high level inputs required by the output stage is provided by a Silicon General SG 3627 driver circuit. This driver circuit features a high threshold level to provide noise immunity, and has both source and sink output

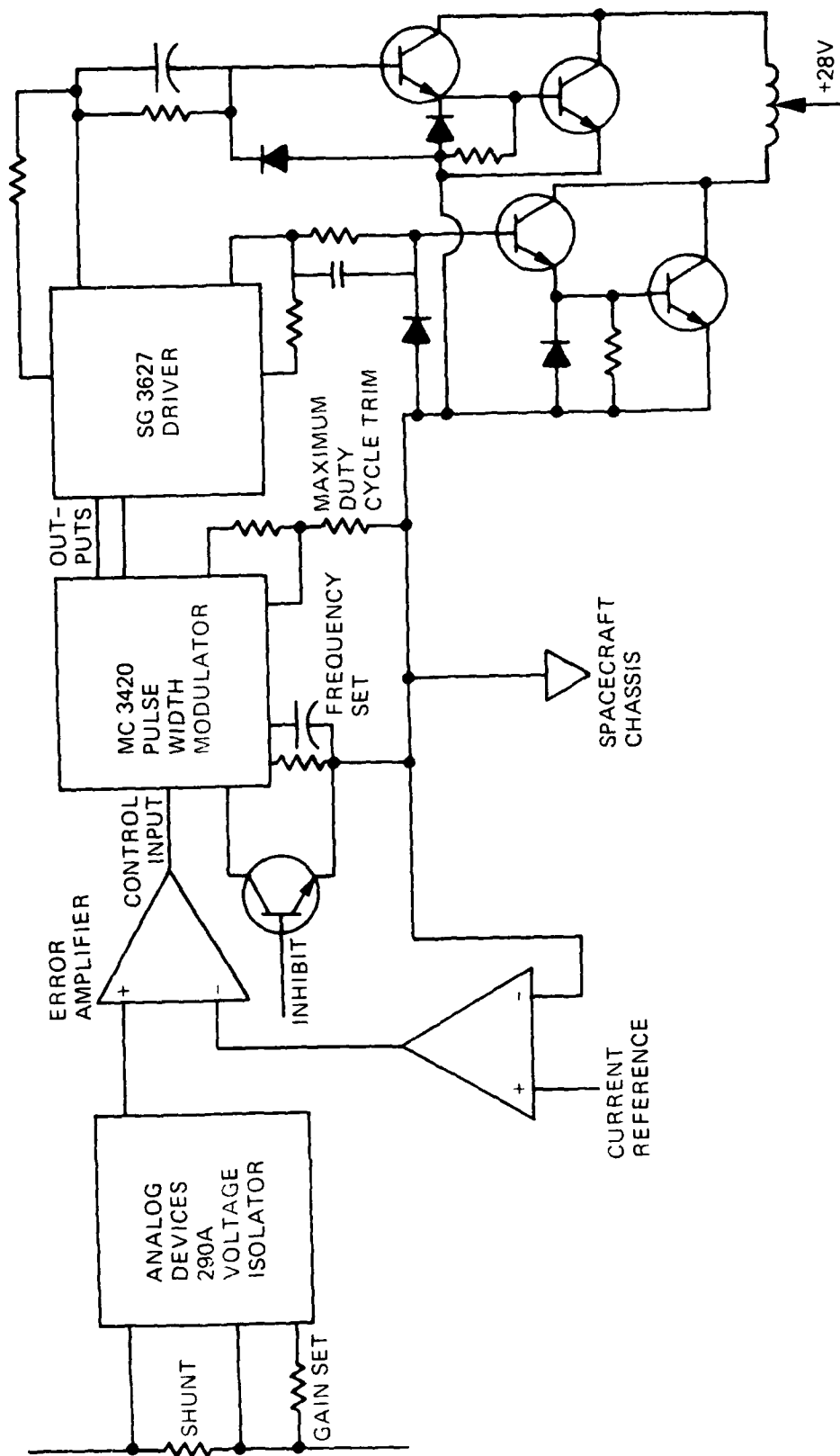


Figure 3-12. Plasma Source Pulse Width Modulator/Output Stage

transistors for rapid turn on and off of the output stage. The output stage is a standard Darlington connected set of transistors.

The three primary converters are fabricated as 2 card stacks. A 6061 aluminum base plate contains the heavy components (transformers, chokes), the heat sunk power transistors, large capacitors, isolation amplifier, bridge rectifier and the interface connector. The base plates are mounted on heat conducting slides in the power supply boxes. An epoxy circuit card is mounted to the base plate via four stainless steel standoffs and contains the majority of the small components (resistors, diodes, integrated circuits, capacitors, etc.). The two cards are conformally coated separately and then folded together such that the side of the epoxy card containing the solder joints faces the side of base plate where the power transistors are mounted.

3.3.1.1 START Converter. The START supply is a constant current, DC-DC converter with a current set point of one ampere. A detailed schematic of the START converter is shown in Fig. 3-13. The START and RUN converters use a common current feedback signal which originates in the RUN converter and is scaled at 2.5 volts/ampere. The START converter requires power inputs of +28 VDC, +12 VDC and +5 VDC. A single output in excess of 300 VDC is provided to the cathode. The output transformer has a turns ratio of 14 to 1 to act as the primary high voltage source during hollow cathode startup (the RUN converter is in series and supplies an additional 88 volts open circuit during startup). Diode CR8 is the gating diode, discussed earlier, which conducts the RUN converter current when the start converter is turned off. It should be noted that the START converter is effectively turned off when the hollow cathode potential drops to a point where the RUN converter output current is above the start converter controlling band (i.e.: the START converter pulse width modulator is forced to zero duty cycle by the current feedback signal).

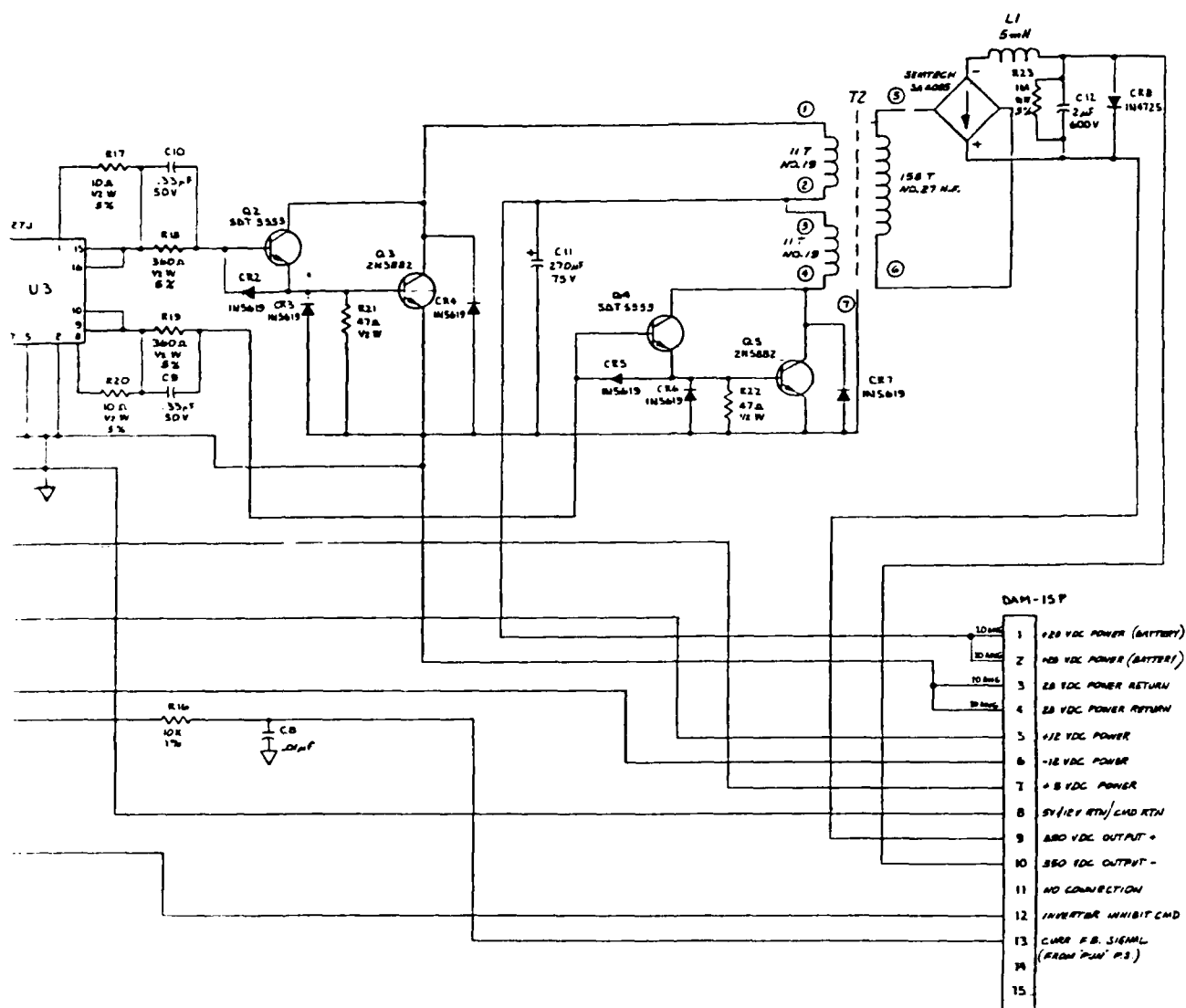
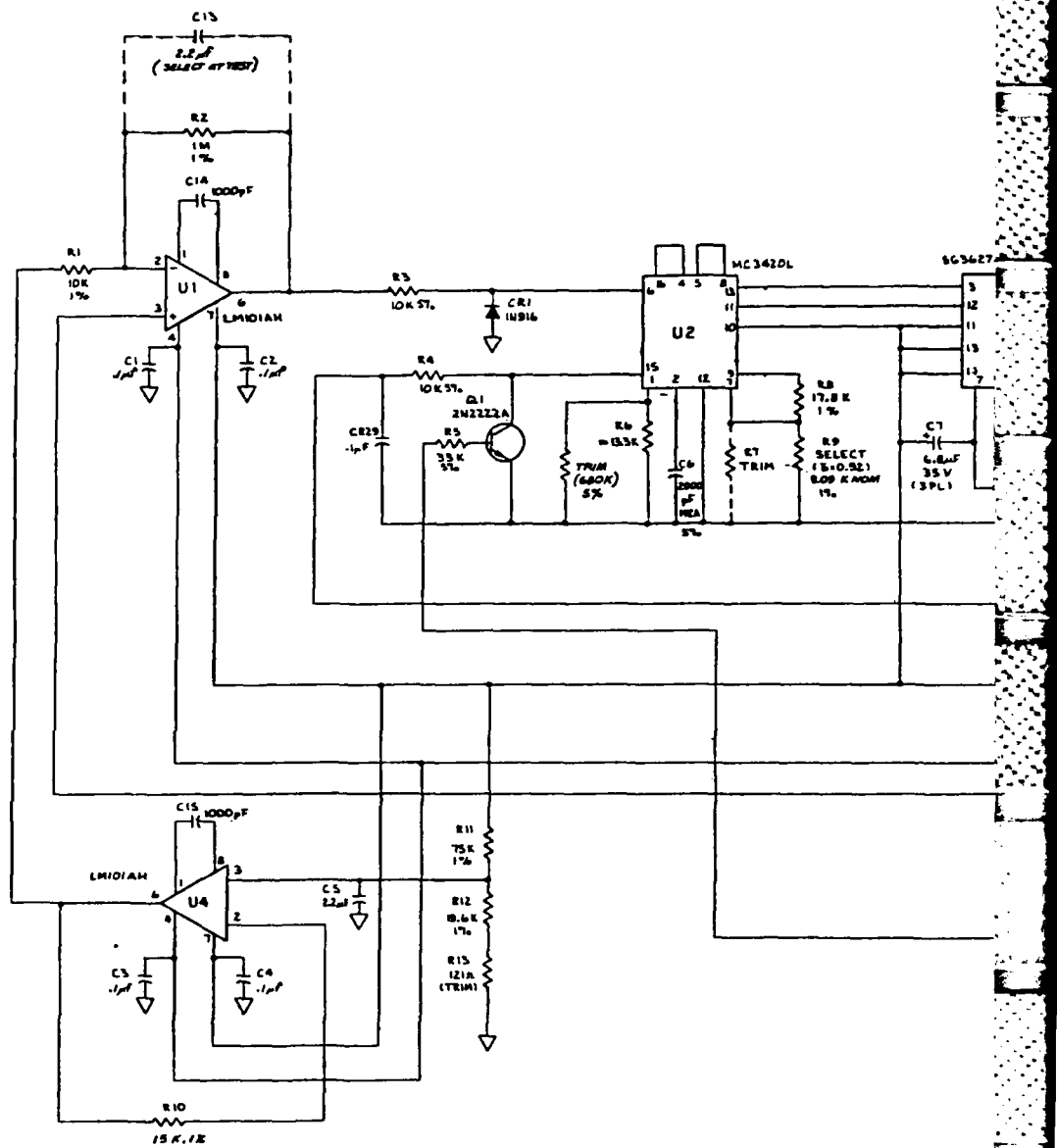


Figure 3-13. Detailed Schematic Of The Start Converter (JPL Drawing No. 10111300)



LAST REF	DES USED
U5	
R23	
CR9	
C15	
Q5	

/

The START converter has not been designed for continuous operation at full power output. The maximum "ON" time when mounted in its enclosure should be limited to 30 seconds over a period of 3 minutes for a duty cycle of 0.16. It can be tested on the bench (with fan cooling) for longer periods, but the power transistor case temperatures should be limited to 120°C.

3.3.1.2 RUN Converter. The RUN converter, shown schematically in Fig. 3-14, operates with a fixed setpoint of two amperes. The current is sensed with a 0.5  $\Omega$  shunt and then amplified so that the scale factor is 2.5 volts per ampere at the current isolator output. This output is connected to the start converter as the feedback signal and to a buffer amplifier for telemetry. The RUN converter requires power inputs of +28 VDC,  $\pm 12$  VDC and +5 VDC. A single output of up to approximately 88 V, open circuit, is provided to the cathode.

This converter also contains the cathode voltage sensing and isolation circuitry for telemetry. The potential between the cathode pin and body is connected to a divider with two output taps. A relay is used to switch the input of an isolator (whose gain is equal to 1.0) to the proper tap. The attenuation ratios are 0.01289 (388 volts full scale) and 0.0788 (63.5 volts full scale). The relay position is controlled by the  $\overline{\text{RUN}}$  function which originates in the Telemetry Buffer Module (connector pin 10). When  $\overline{\text{RUN}}$  is high (converters off or in the START mode), Q1 (see Fig. 3-14) is on which activates K1 and the isolator input is connected to the high attenuation output of the divider (388 v.f.s.). When the cathode current reaches 1.2 amperes,  $\overline{\text{RUN}}$  goes low, and the isolator input is connected to low attenuation output of the divider.

3.3.1.3 KEEPER Converter. The design of the KEEPER converter is basically the same as that of the run converter. A detailed schematic of the keeper converter is presented in Fig. 3-15. Aside from a reversible polarity the only differences are in the reference and feedback loops. The KEEPER converter requires inputs of +28 VDC, +12 VDC and +5 VDC. A single output at 60 V and one of three currents (positive bias) is provided between the cathode and keeper electrode (see Fig. 3-10).

The keeper was designed to provide three output electron current levels (2, 1 and 0.1 amperes). The references for these currents are set by a switched attenuator controlled by U4 (Fig. 3-15). When the switches in U4 are open, the reference is set for 2 amperes. Closing a pair of switches lowers the reference voltage which results in a lower output current set point. With this switching arrangement, neither a switch failure nor incorrect programming of the switches will result in a reference voltage corresponding to more than 2 amperes. The actual keeper current set points (keeper electrode biased positive) are 0.3 A, 1.2 A and 2.0 A.

The output current sense and isolator are connected after the polarity reversing relay and therefore provide a two polarity feedback signal. Since the current reference voltage is always positive, the magnitude of the feedback signal must be extracted. This is done with U2 and U3. The operation of U2 and U3 is easily understood by considering Fig. 3-16. The U2 circuit uses diode gating to provide a gain (K) of 0 for negative input voltages and a gain of -1 for positive input voltages. U3 is a summing-inverting amplifier with a gain of -5 for the input voltage and -10 for the output voltage of U2. The output voltage of U3 is always  $\geq 0$  and is equal to  $5 \times |\text{input}|$ .

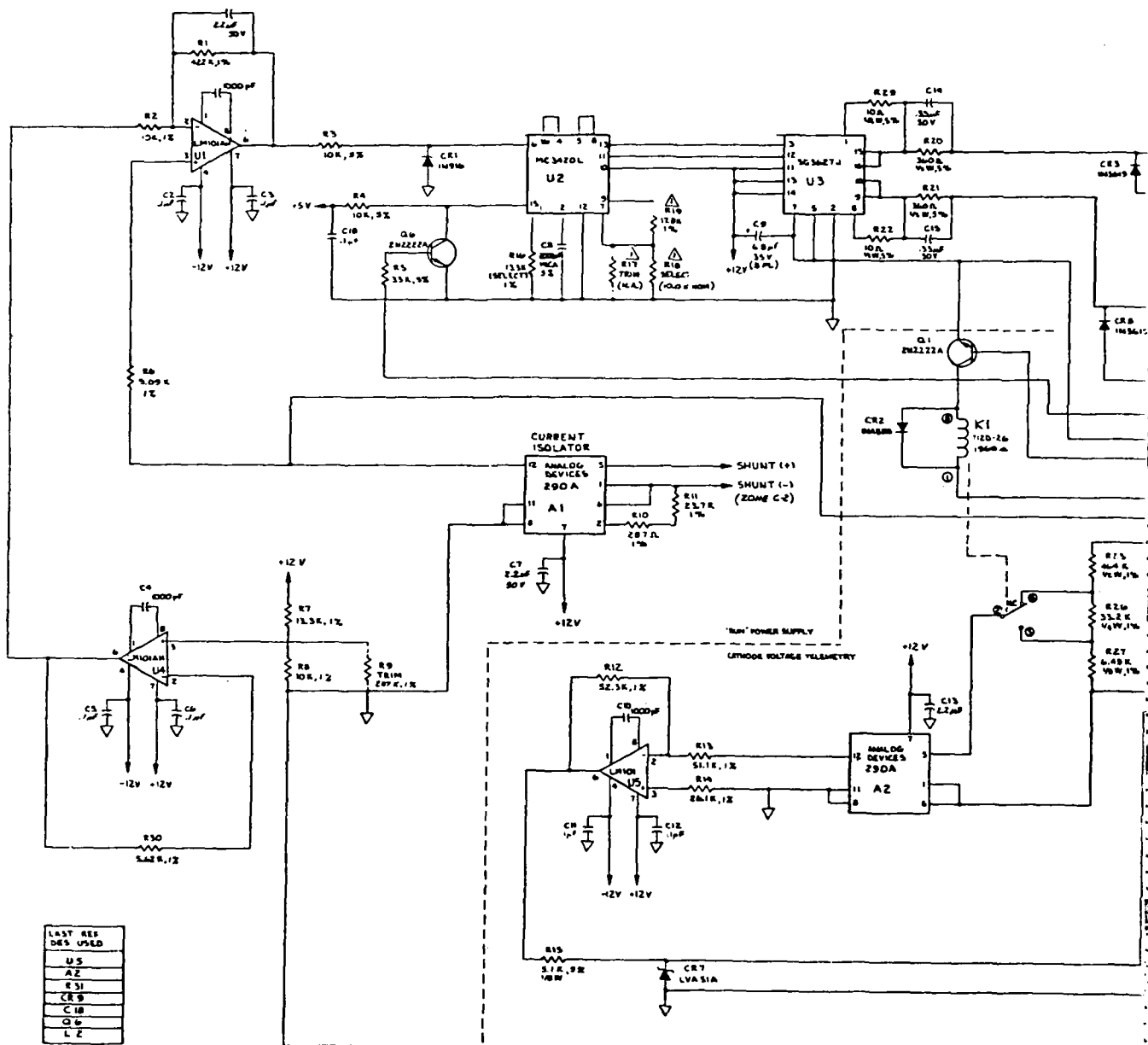
### 3.3.2 Support Function Circuitry

The support functions are those circuits which do not directly operate the plasma source but which are essential for the control and monitoring of the source. The major support circuitry is housekeeping power, command buffer and isolation, and telemetry.

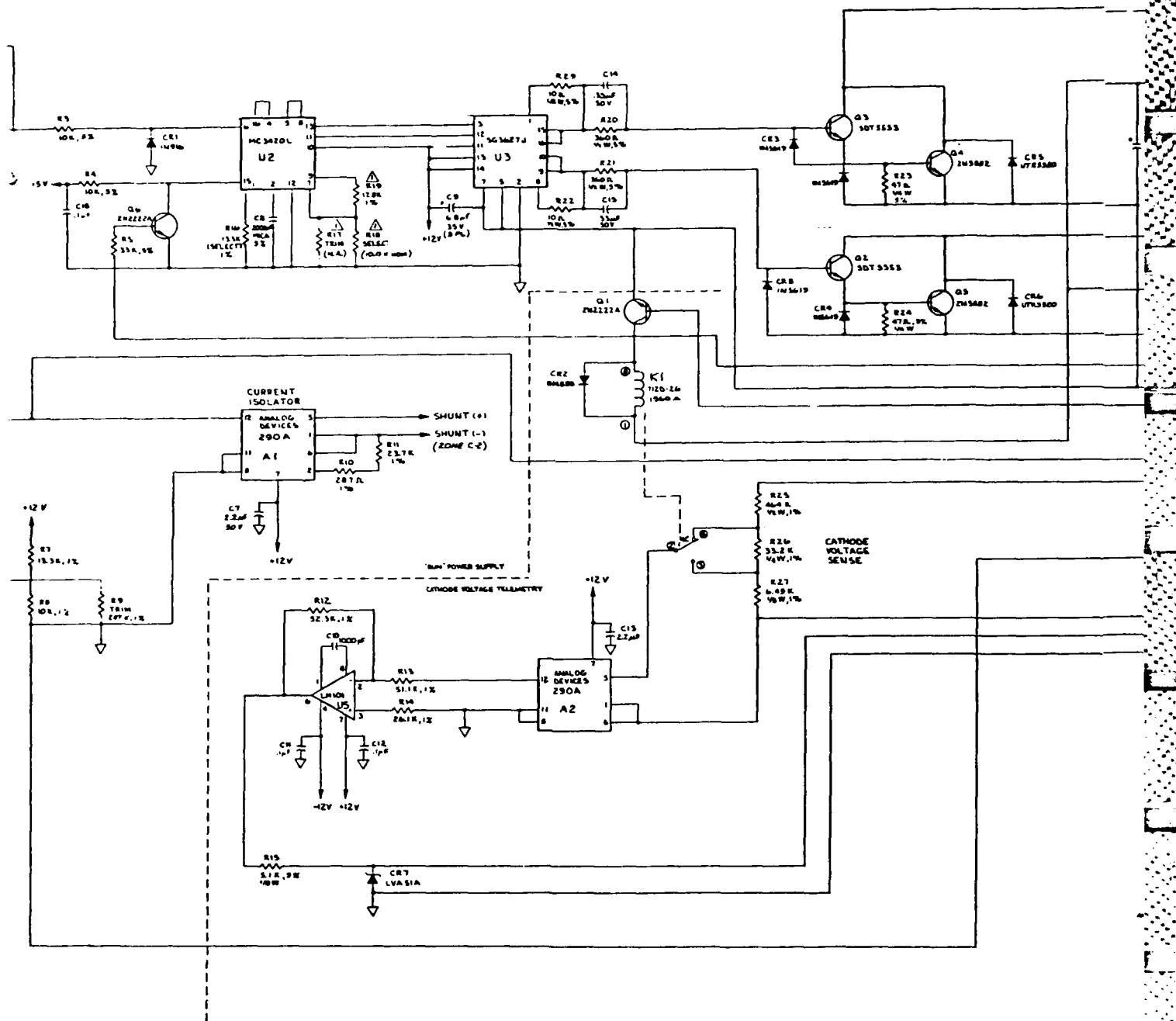
3.3.2.1 Housekeeping Power Processor. The housekeeping supply is comprised of an aluminum plate containing the transformers, chokes, large capacitors, power transistors and post mounted small components, with a small fiberglass board mounted in the center containing other post mounted small components. The housekeeping processor accepts the 28 VDC input power, processes the power and then distributes +28 VDC,  $\pm 12$  VDC and +5 VDC where needed.

A detailed schematic of the housekeeping processor is shown in Fig. 3-17. The main power switching and control circuit of the housekeeping power supply consists of a pair of field effect transistors driven by a SG 3525 switching regulator (see Fig. 3-17). A LM 350K, integrated circuit, voltage regulator is used to provide a controlled start-up voltage for the switching regulator. After the supply has started, terminals 4, 5 and 6 of transformer T1 provide 10 volts for operating the switching regulator and, through attenuators R2 and R3, the feedback voltage to close the loop around the regulator. The regulator thus controls its supply voltage to be 10 volts. When this is true, the three main secondary windings of T1 provide the proper input voltages to the 7800/7900 series linear regulators which in turn provide the desired  $\pm 12$  and +5 volt regulated outputs.





1



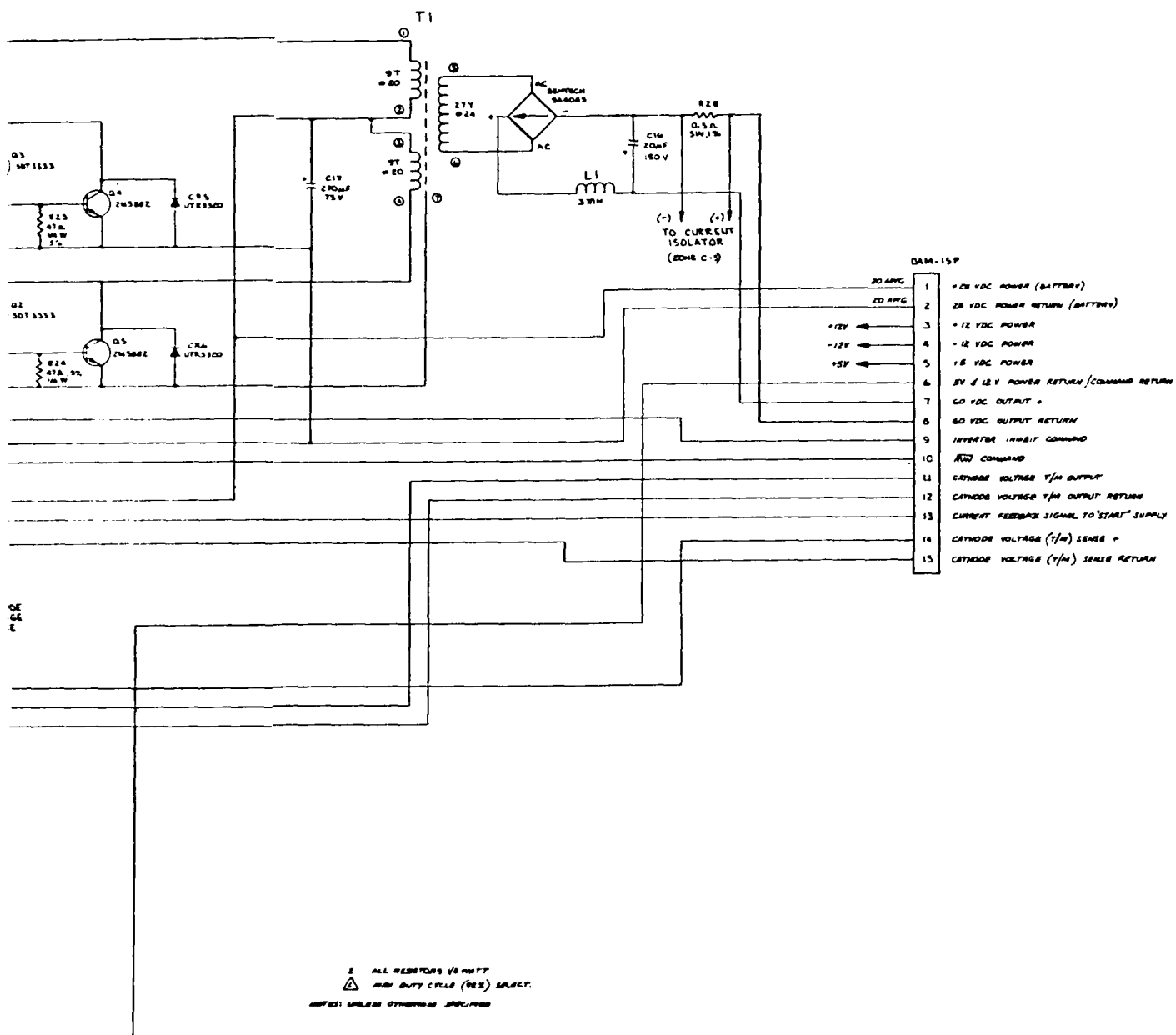
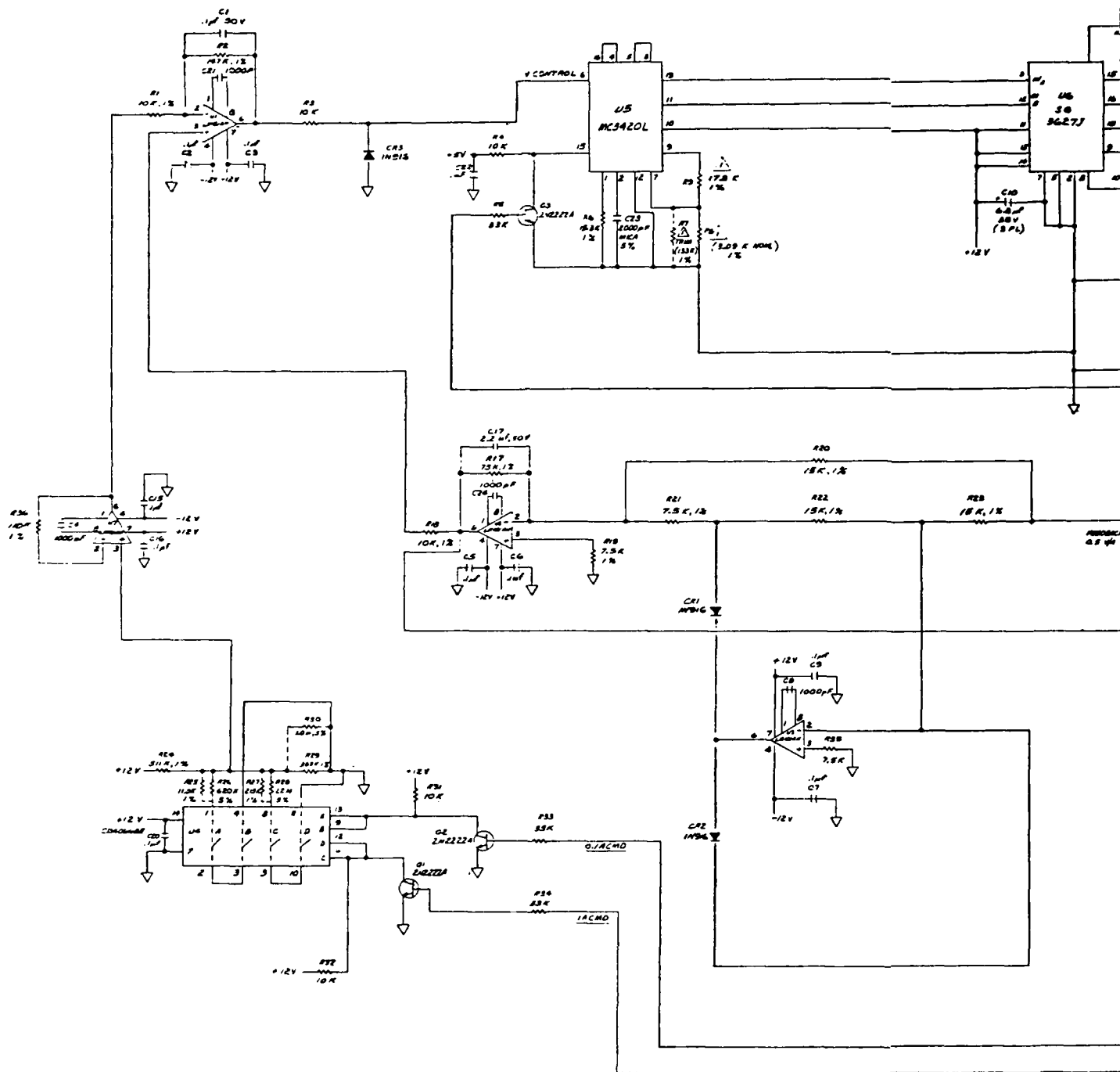
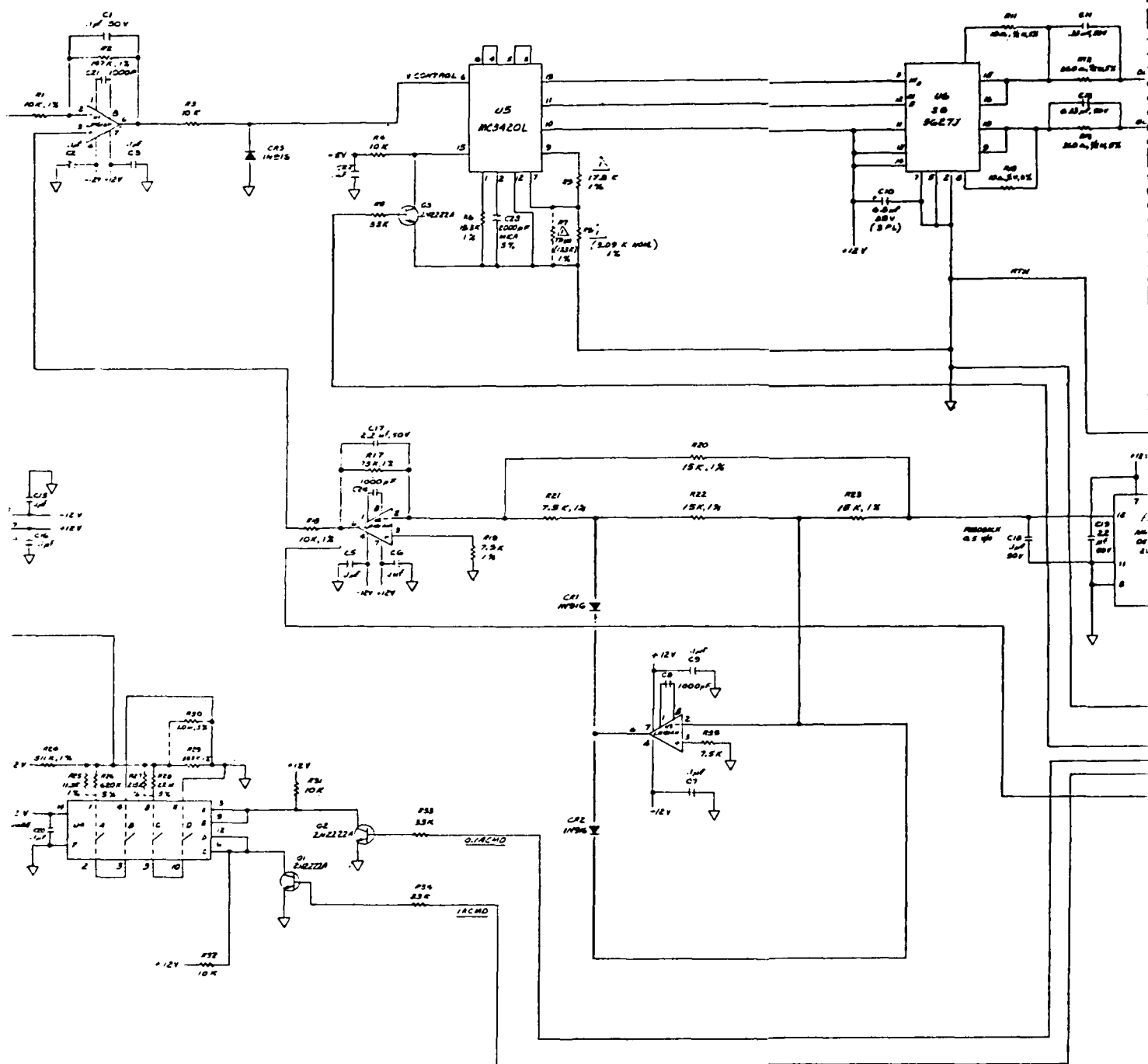


Figure 3-14. Detailed Schematic Of The  
RUN Converter (JPL  
Drawing No. 10111303)





2

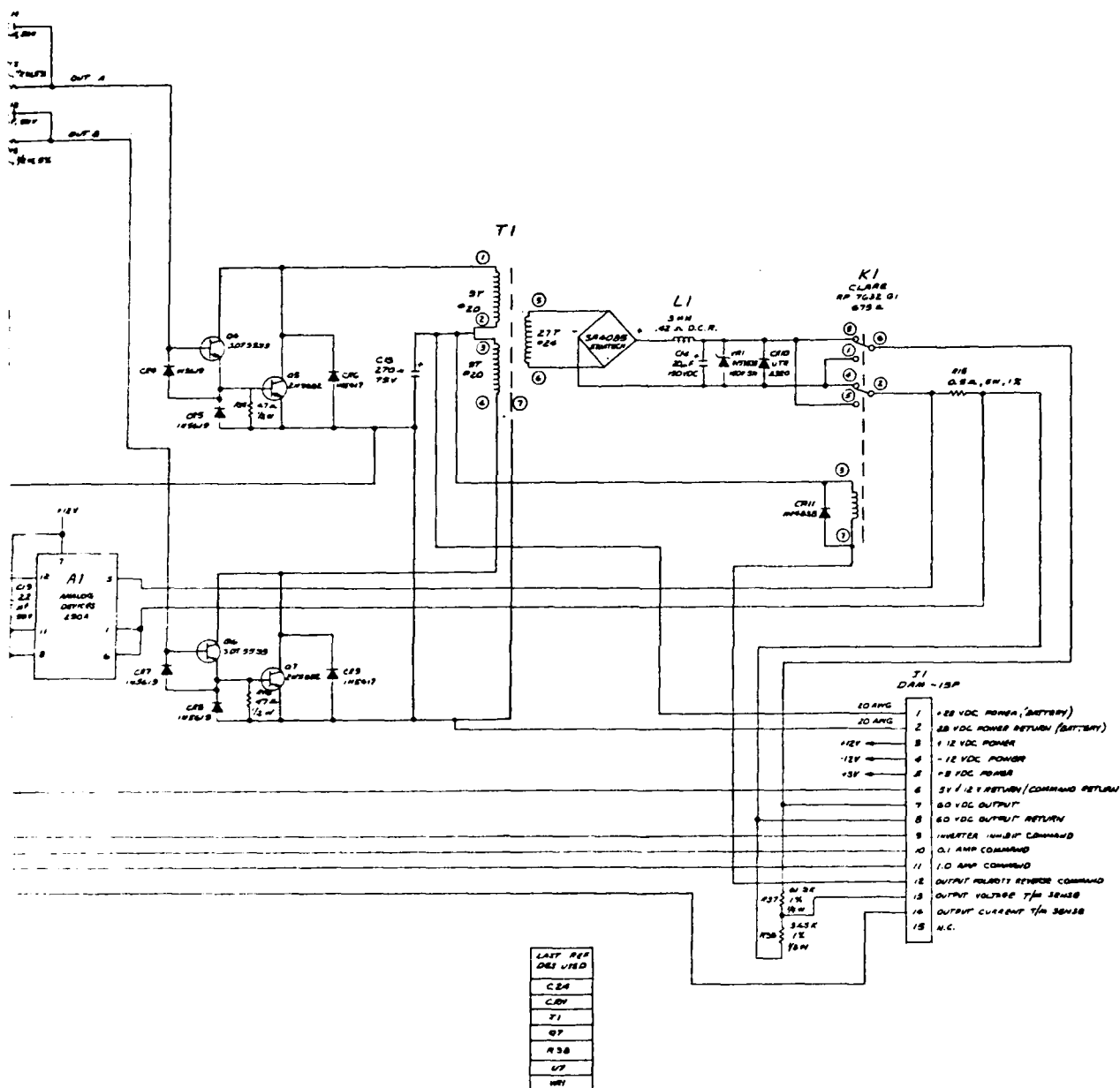
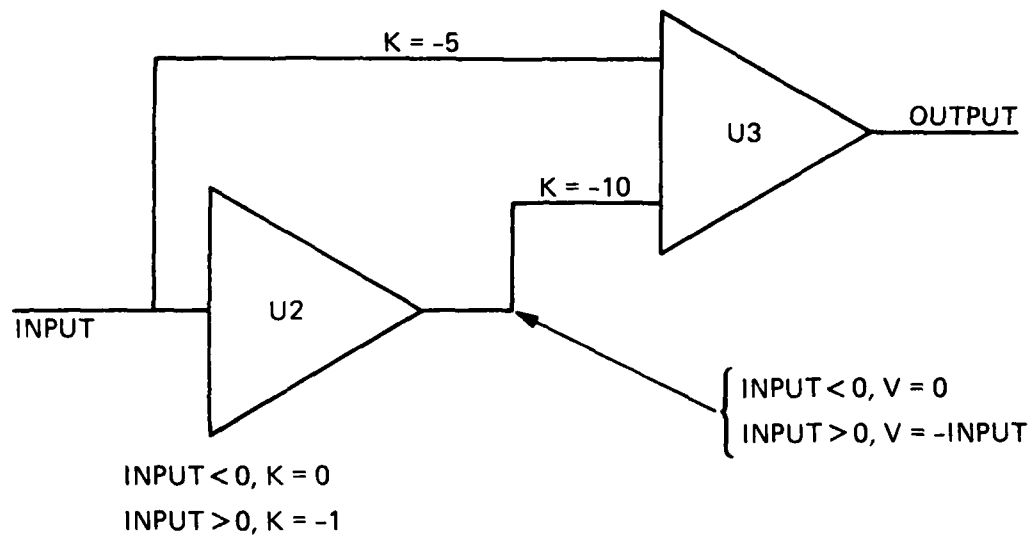


Figure 3-15. Detailed Schematic Of The Keeper Converter (JPL Drawing No. 10111302)



$\text{INPUT} < 0, \text{ OUTPUT OF U3: } (-5) \times (\text{INPUT}) > 0$   
 $\text{INPUT} > 0, \text{ OUTPUT OF U3: } [(-5) + (-1) \times (-10)] \times (\text{INPUT}) = (5) \times (\text{INPUT}) > 0$

Figure 3-16. Keeper Polarity Feedback Signal Extraction

3.3.2.2 Commands. There are six ground commands available to operate the plasma source, as indicated in Table 3-4. The commands to provide 28 VDC power to the system and to open and close the gas system latching valve are done externally to the plasma source system. A command is comprised of an 8-bit input word defining the desired source state. The command isolator/buffer provides the command interface for the source inverters. Input commands are optically isolated, stored, and then buffered. The stored commands are isolated and transmitted to the command source for display and/or verification.

3.3.2.2.1 Command Buffer. A detailed schematic of the command buffer is shown in Fig. 3-18. The command buffer stores the commands issued by the controlling source and shifts the voltage level from the TTL (5 V) to the high level (12 V) signals required by the converters. The command buffer was fabricated as a 4 card stack; a 0.3 cm thick aluminum base plate for slide mounting, and three epoxy cards containing the command buffer electronics. The connector is mounted on the base plate.

In the command buffer capacitors C2 and C3 are initially uncharged. When power is applied, these capacitors hold the clear inputs to the D-type flipflops (U6 and U7) low, which forces the flipflops to store converter "OFF" commands ( $\bar{Q}$  high). The input commands are buffered and inverted by U2 and U3. After the command pattern is set up, a strobe signal serves as a clock for the flipflops and causes the command pattern to be stored. The voltage levels are shifted by U8, U9 and U10, and, where necessary, are connected in parallel to provide higher current levels. The state of the flipflops is buffered by U4 and part of U5 to provide an indication to the controller of the stored command status.



Table 3-4. Plasma Source Command Capability

Command	Function
1. Run on/off	Activates/deactivates RUN converter
2. Start on/off	Activates/deactivates START converter
3. Keeper on/off	Activates/deactivates KEEPER converter in high current (2.0 A electrons) collection mode.
4. Keeper medium current enable	Selects the medium current (1.2 A electrons) collection mode.
5. Keeper low current enable	Selects the low current (0.3 A electrons) collection mode.
6. Keeper polarity reverse	Selects positive (electron collection) or negative (ion collection) keeper electrode bias.

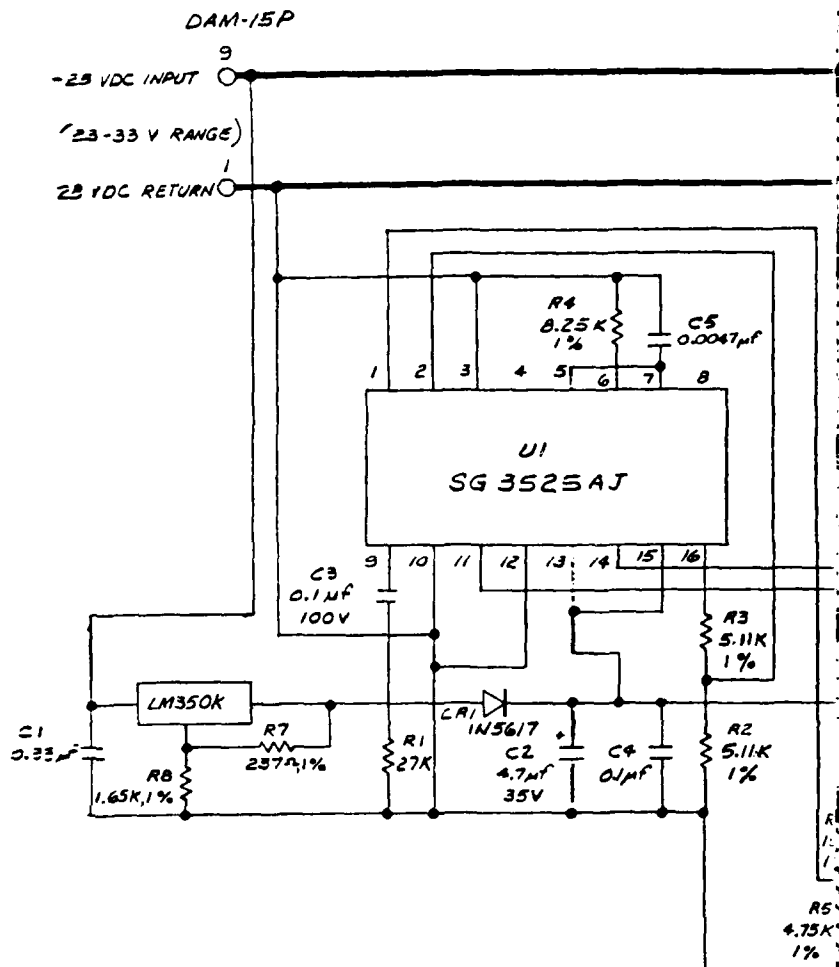
3.3.2.2.2 Command Isolator. The command isolator was added to provide optical isolation between the control point (JPL test controller or microprocessor) and the command buffer. A detailed schematic of the isolator is shown in Fig. 3-19. The command isolator consists of two sets of optical isolators which transmit signals between the controller and the command buffer while electrically isolating the two grounds.

The command isolator is mounted in a separate small box which mates directly to the commands connector on the face plate of power processor Box B, see Fig. 2-3. Two epoxy cards containing the optical isolator integrated circuits are mounted to a 0.16 cm thick aluminum plate which forms one wall of the isolator enclosure. The connectors are sandwiched between the epoxy boards. One connector is mounted in main structural part of the box machined from a solid billet of aluminum and the other is mounted on the other removable wall. The isolator circuitry box is held in place via four tie down points.

3.3.2.2.3 Ground Test Controller. The plasma source is started and operated when the control buffer receives and processes an appropriate 8-bit word. During the sounding rocket flight, the 8-bit word was to have been sent to the plasma source from the SAADS programmer. A ground test controller was built to simulate the SAADS programmer for ground testing and is shown in Fig. 3-20. The eight, two-position switches across the bottom of the front panel represent the eight individual bits of the input word. The switch labeled "RUN" represents bit 0 and the switch labeled "KEEPER BIAS" represents bit 7. The red pushbutton, labeled "SEND CMD", sends an 8-bit word, defined by the positions of the eight two-position switches, to the plasma source for processing. The two rows of LEDs define what bits are activated and provide visual display of the command as it is echoed back for verification. Bits 5 and 6 are not used. A detailed schematic of the test controller is shown in Fig. 3-21.

3.3.2.3 Telemetry. The telemetry circuits are provided to buffer, scale and clamp the analog signals which show the operating condition of the plasma source and electronics. The signals are all scaled at 0 to 5 volts and are clamped at approximately -0.5 V and +6 V. The 12 telemetry outputs are summarized in Table 3-5 and can be grouped into two types, plasma source operation monitors and plasma source output monitors.

3.3.2.3.1 Operations Monitor Telemetry. Eight of the output telemetry functions are used for source operation monitoring. These include the hollow cathode voltage and current, the keeper voltage, current and polarity, gas reservoir pressure, input battery voltage and the temperature on the RUN



LAST REF
DES USED
C22
CR12
L4
Q2
R9
T1
U1



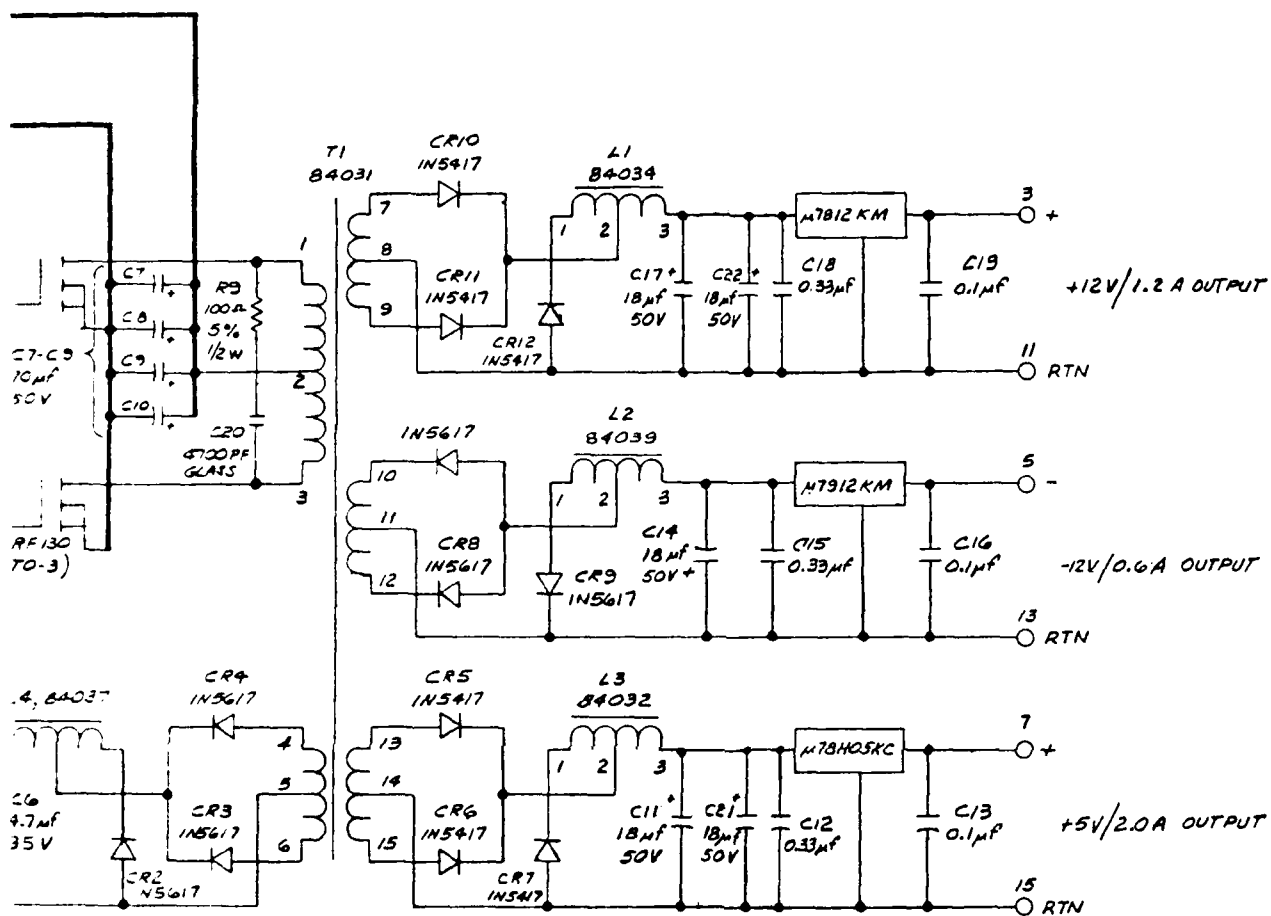
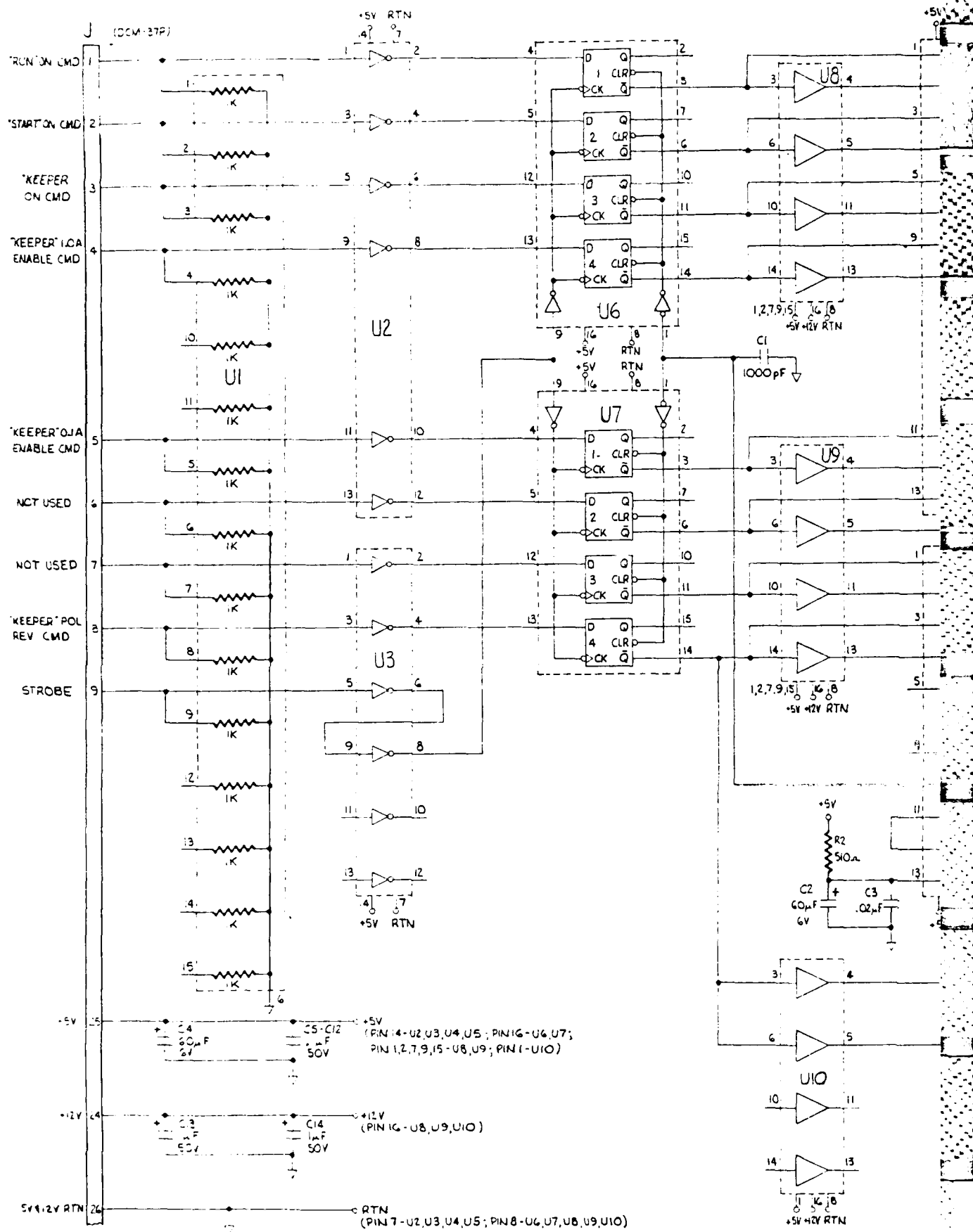
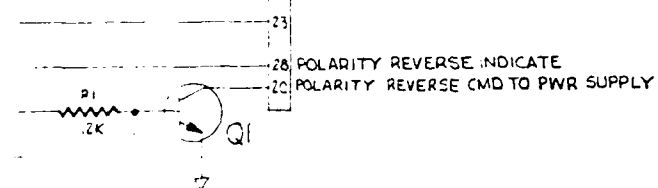
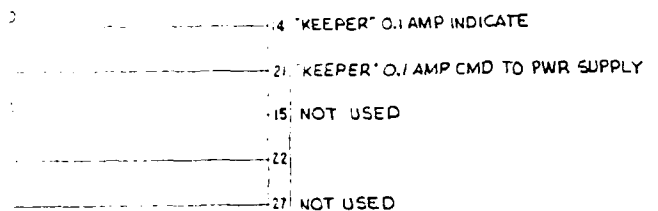
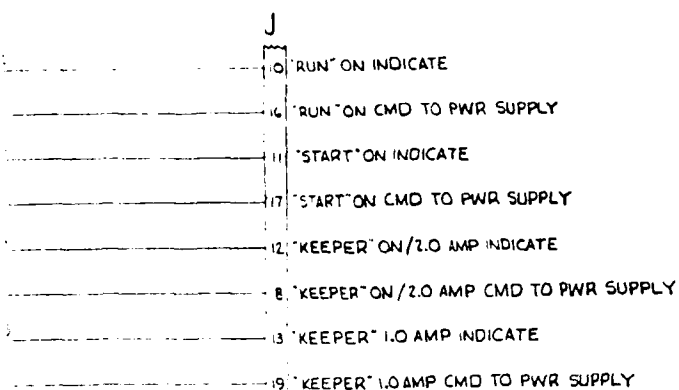


Figure 3-17. Detailed Schematic Of The Housekeeping Converter (JPL Drawing No. 10111301)

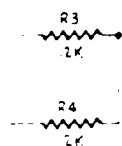
3







REF DES	TYPE / MFG
U1	916C102X2PE / SPRAGUE
U2-U5	5N7404 / TI
U6, U7	5N74175 / TI
U8-U10	CD40109B / RCA
Q1	2N2222A / TI



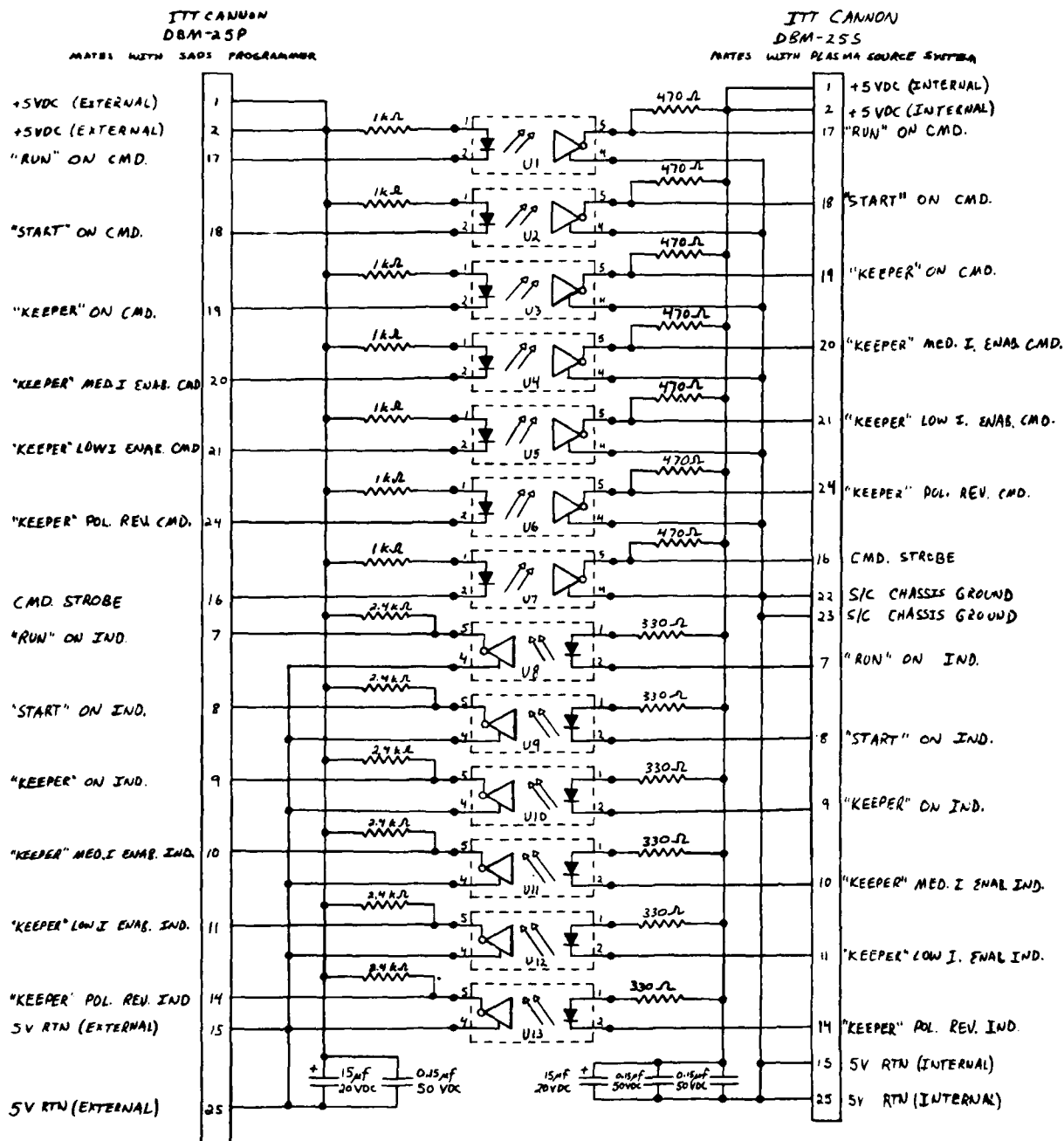
1. ALL RESISTORS ARE  $\pm 5\%$  1/8W

NOTES: UNLESS OTHERWISE SPECIFIED

Figure 3-18. Detailed Schematic of the Control Buffer (JPL Drawing No. 10111305)

3





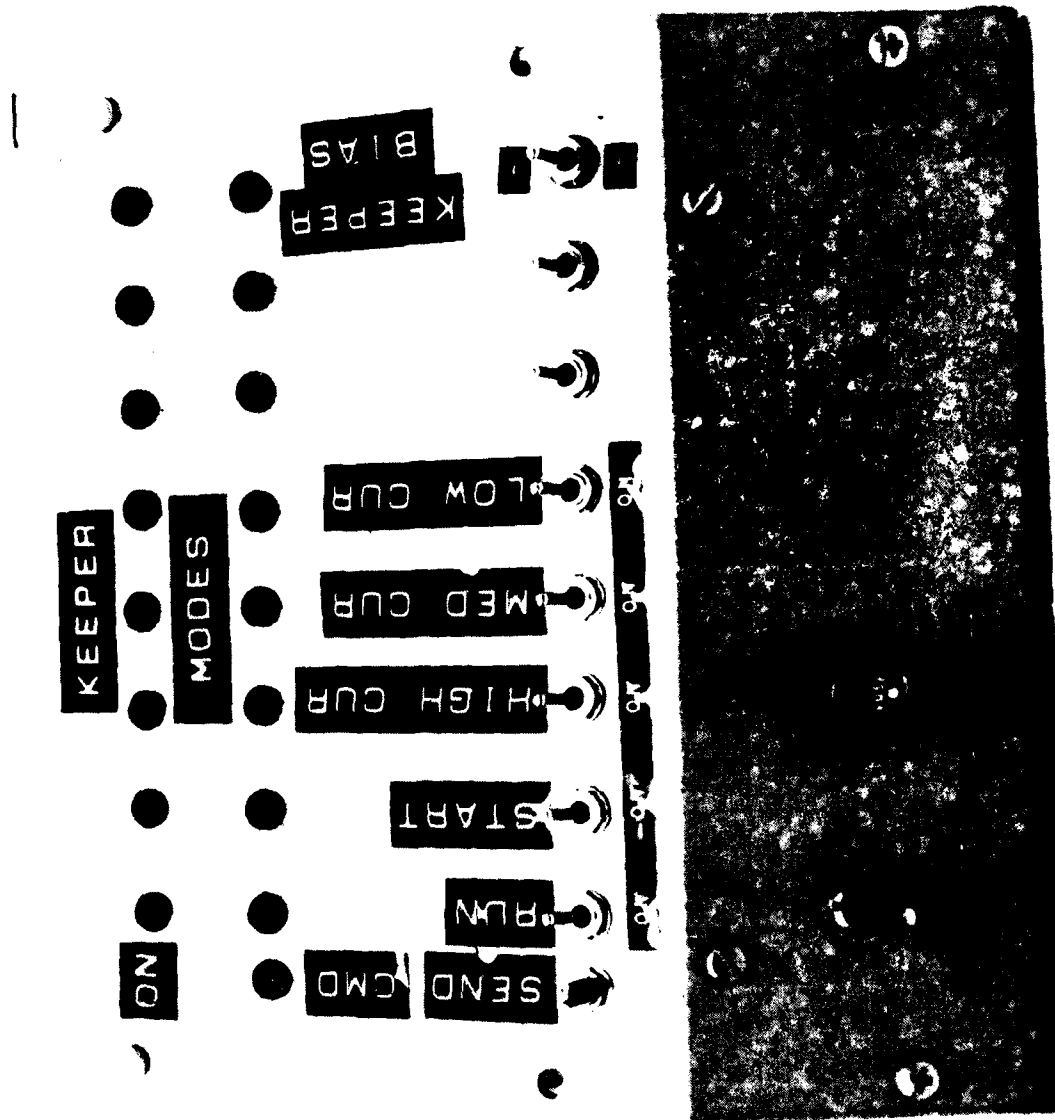


Figure 3-20. Plasma Source Ground Test Controller

Table 3-5. Analog Telemetry Outputs

Channel No.	Output Connector Pin No.	Description	Actual Value for 5 V $\pm 5\%$ Output
1	37	Hollow Cathode Voltage <sup>a</sup>	400 V
2	36	Hollow Cathode Current	2.0 A
3	35	Keeper Voltage	88 V
4	34	Keeper Current	2.3 A
5	33	Integrated Net Current <sup>b</sup>	0.44 A-s
6	32	Amplified Net Current	25 mA
8	30	Gas Reservoir Pressure	480 psia
9	27	Temperature of RUN converter <sup>c</sup> base plate	-10°C
11	24	Battery Voltage	48 V
12	23	Keeper Polarity	+
13	22	Net Curr. Integrator Polarity	See Section 5.3
14	21	Amplified Net Curr. Polarity	See Section 5.3

<sup>a</sup>In two ranges: 0-70 V, 0-400 V

<sup>b</sup>Saturates at 4.4 V output

<sup>c</sup>Inverted scale, 0.0 V  $\pm 5\%$  corresponds to 90°C

converter base plate. A detailed schematic of the source operation monitor telemetry circuitry is shown in Fig. 3-22. This circuitry includes all of the monitor functions except the cathode voltage, which can be found in Fig. 3-14, the RUN converter schematic.

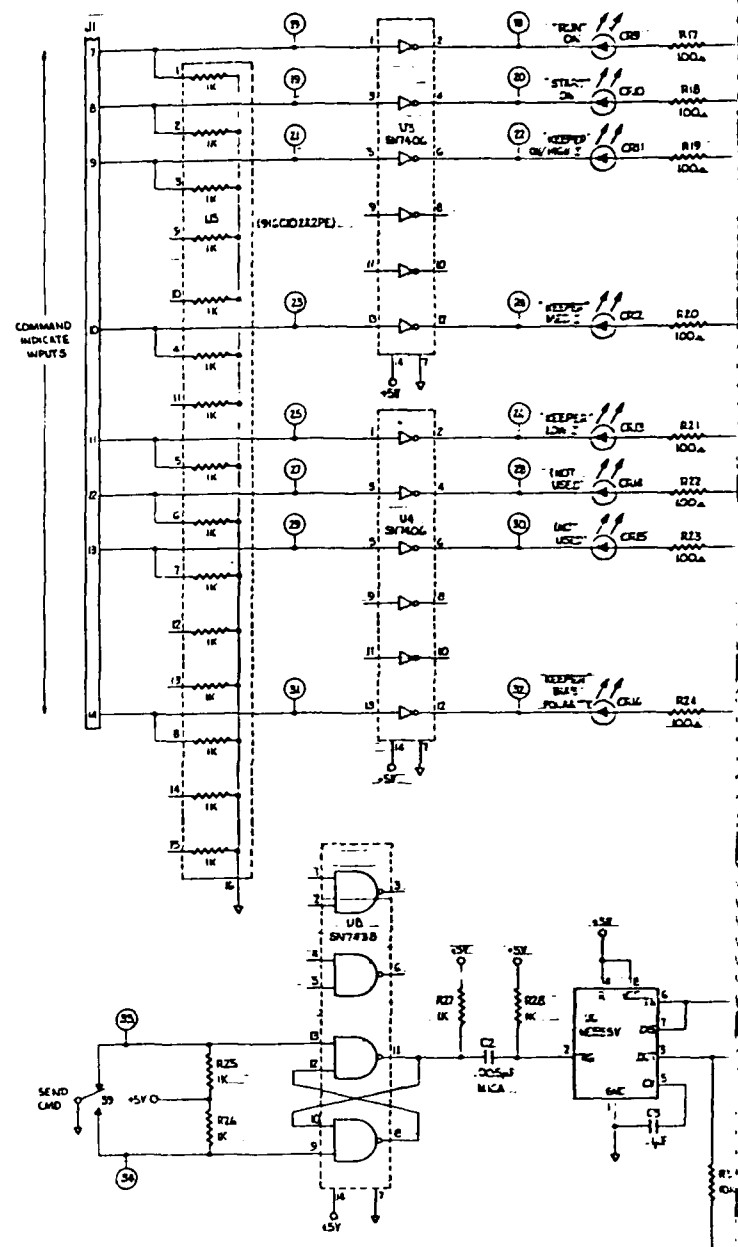
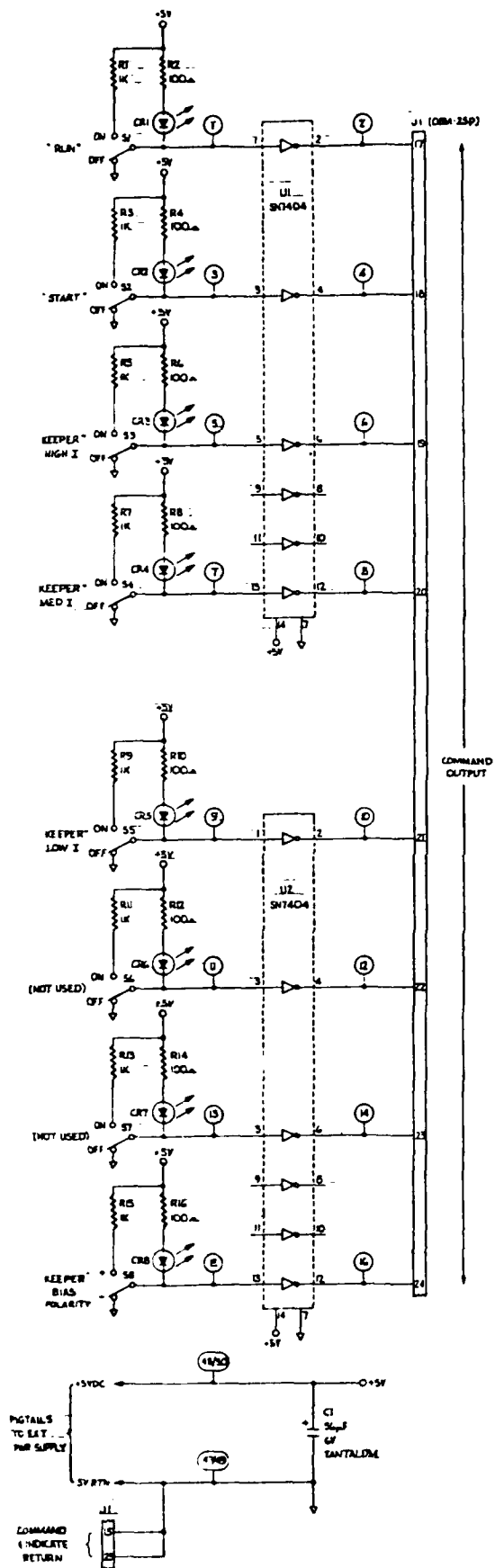
3.3.2.3.2 Output Monitor Telemetry. All of the power supplies are isolated from spacecraft ground through a common 8.08 resistor which acts as a current path for particles flowing into and out of the plasma source. The voltage drop

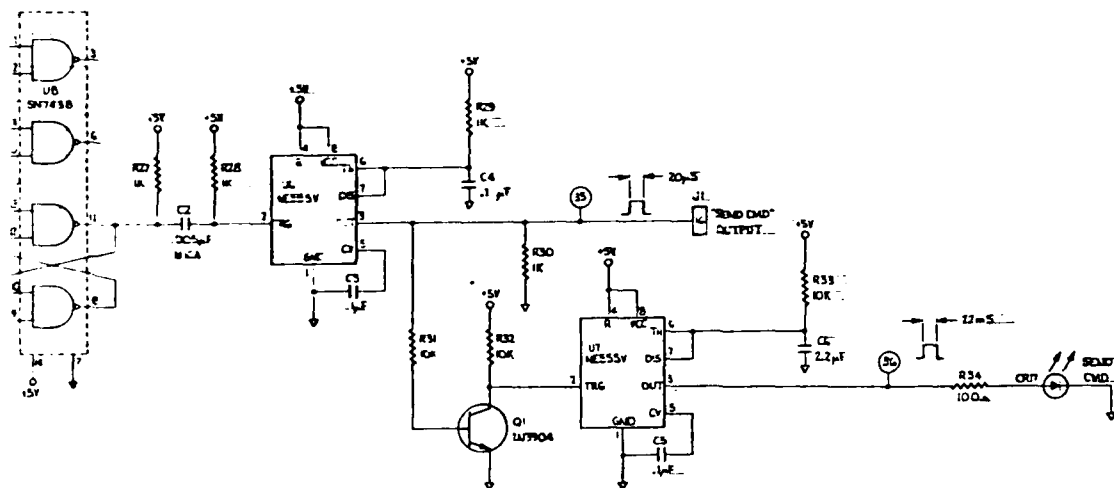
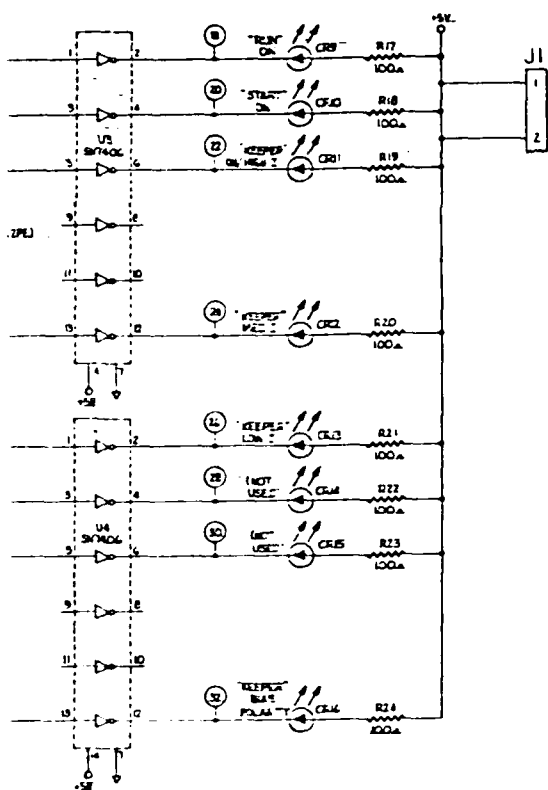
across the resistor provides a means of measuring the plasma source output current and is the input signal to the net current monitor, source output circuitry shown in Fig. 3-23. This circuit provides output for the amplified net current signal and polarity, and the integrated net current signal and polarity. Resistors R5 and R6 form the 8.08 ground isolation common point.

### 3.3.3 Power Processor Boxes


The power processor boxes were fabricated from 0.32 cm and 0.64 cm 6061 aluminum sheet. The four long sides of the two large boxes were salt dip brazed together. The front and rear covers are removable, for servicing, and held in place with stainless steel 6-32 bolts. The nominal box dimensions are 14 cm by 15 cm by 22 cm. Each large box contains 13, 1.9 cm diameter vent holes covered with #40 mesh. There are 8 vent holes on the top of each box and 5 on the rear cover. The connectors on each box are mounted on the front removable cover. The boxes are mounted to the flight deck plate via 8, 1.9 cm long, 8-32 bolts through the base plate mounting holes. The electronics cards are slide mounted.

An exploded view of the contents of Box A is shown in Fig. 3-24 following conformal coating. This box contains the KEEPER supply (top of box), START supply (bottom of box), and the NET CURRENT MONITOR circuitry (the stack in the front of the box). Box A accepts the 28 V input power and the leads from the cathode emitter tube, vessel body and KEEPER electrode. Instructions for removing the contents of Box A are given in Table 3-6.





1. ALL CAPACITORS ARE CERAMIC, 50V

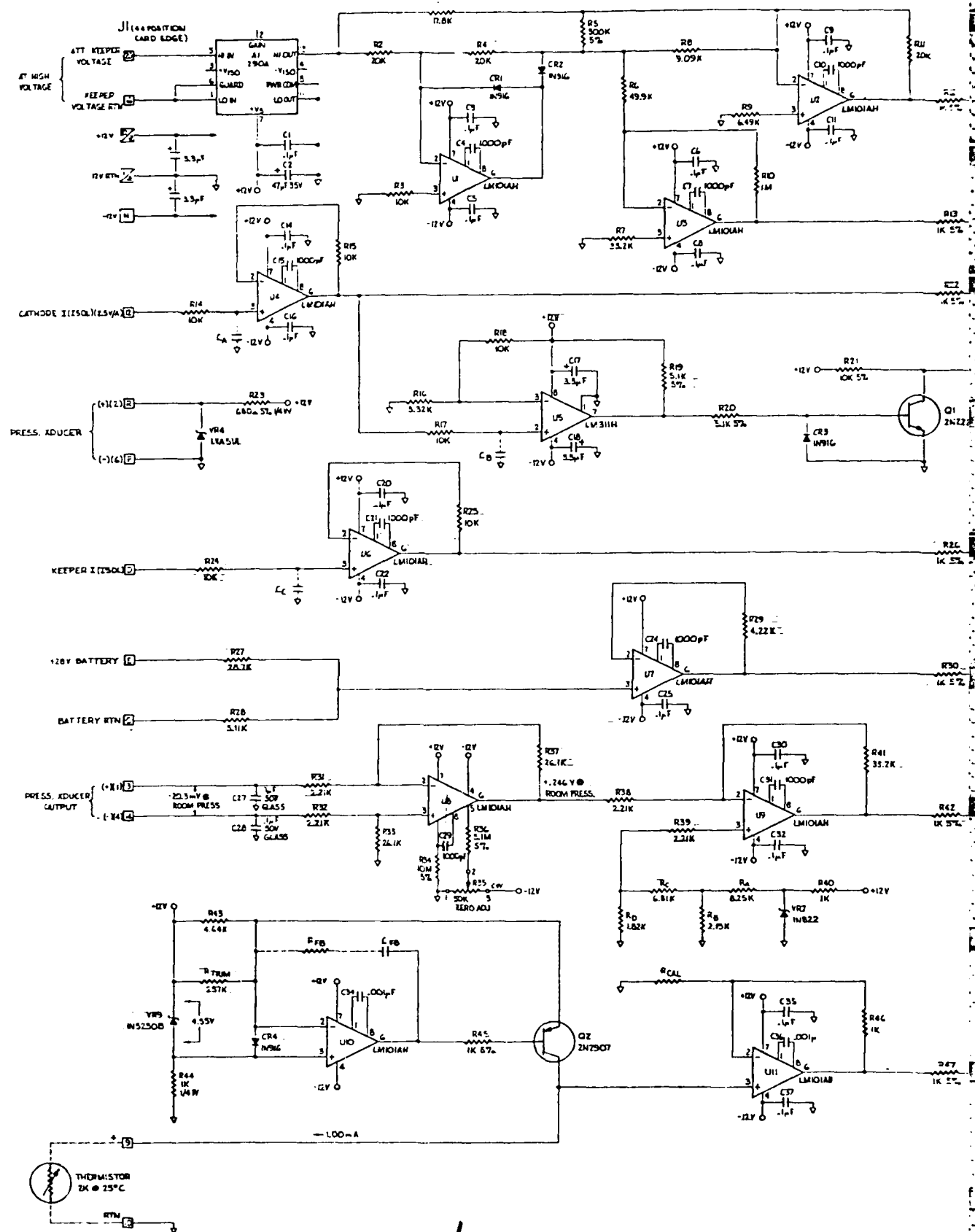
2. SYMBOL  IS SPICE JUNCTION AT A 3-M SCOTCHFLEX 3433-4005 CONNECTOR

3. ALL RESISTORS ARE 5%, 1/4W

NOTES: UNLESS OTHERWISE SPECIFIED

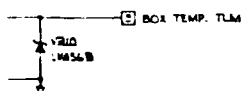
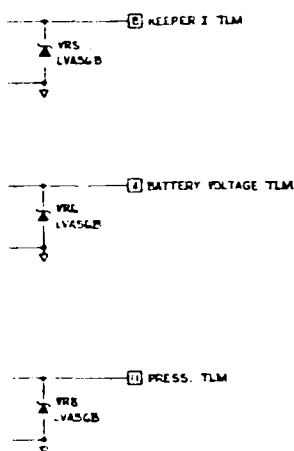
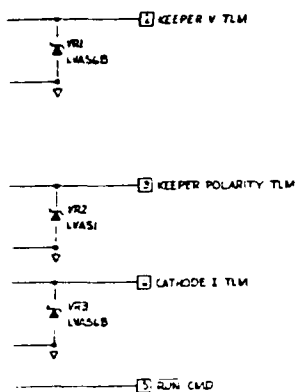
Figure 3-21. Detailed Schematic Of The Ground Test Controller  
(JPL Drawing No. 10111304)

2



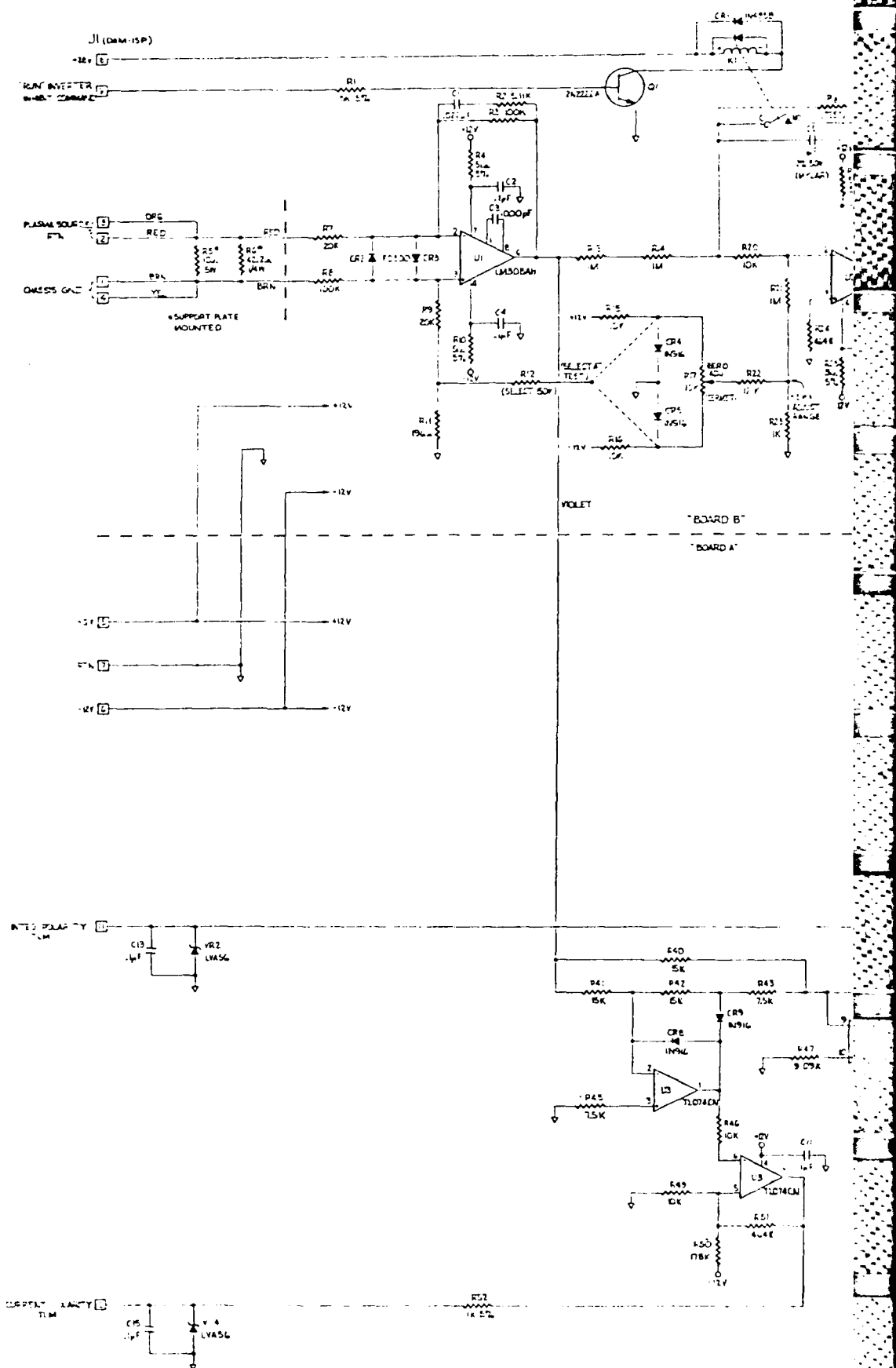


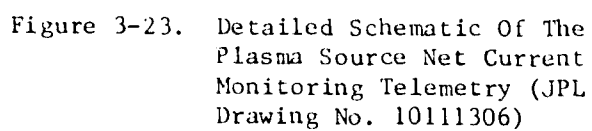




ALL RESISTORS ARE 1% 1/8W  
NOTES: UNLESS OTHERWISE SPECIFIED

Figure 3-22. Detailed Schematic Of The Plasma Source Operations Monitoring Telemetry (JPL Drawing No. 10111307)





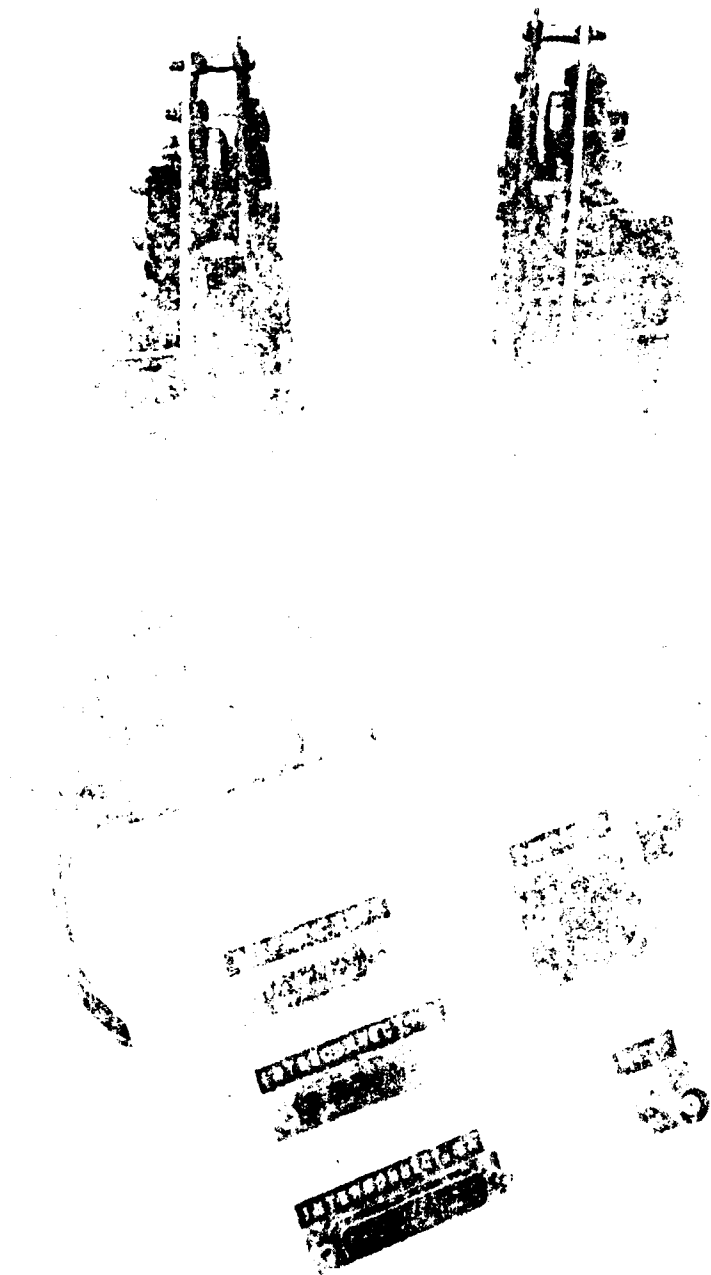


Figure 3-24. Front Cover and Contents of Power Processor Box A

Table 3-6. Disassembly of Box A

Step	Action
1	Remove rear cover (3/32 Allen wrench).
2	Remove Teflon sheets.
3	Remove front cover retaining screws (3/32 Allen wrench).
4	Loosen retaining screws in all three connectors.
5	Remove connectors from net current circuitry and START supply.
6	Slide net current circuitry out from front.
7	Remove connector from KEEPER supply.
8	Slide KEEPER supply out from back of box.
9	Slide START supply out from back of box.

An exploded view of the contents of Box B is shown in Fig. 3-25 following conformal coating. This box contains the HOUSEKEEPING supply (top of box), TELEMETRY card for monitoring source operation (middle of box), the RUN supply (bottom of box), and the CONTROLS circuitry (three-layer stack at the front of the box). Box B accepts the controls and telemetry lines and contains the pressure transducer interface. Instructions for removing the contents of Box B are given in Table 3-7.

#### 3.4 OVERALL PROTOTYPE FLIGHT SYSTEM

The prototype flight plasma source system is shown in the JPL test configuration in Fig. 2-3. Another view of the system is shown in Fig. 3-26. The JPL test configuration duplicates the spacings and dimensions of the SAADS section in the BERT-1 sounding rocket. The power processor boxes are mounted

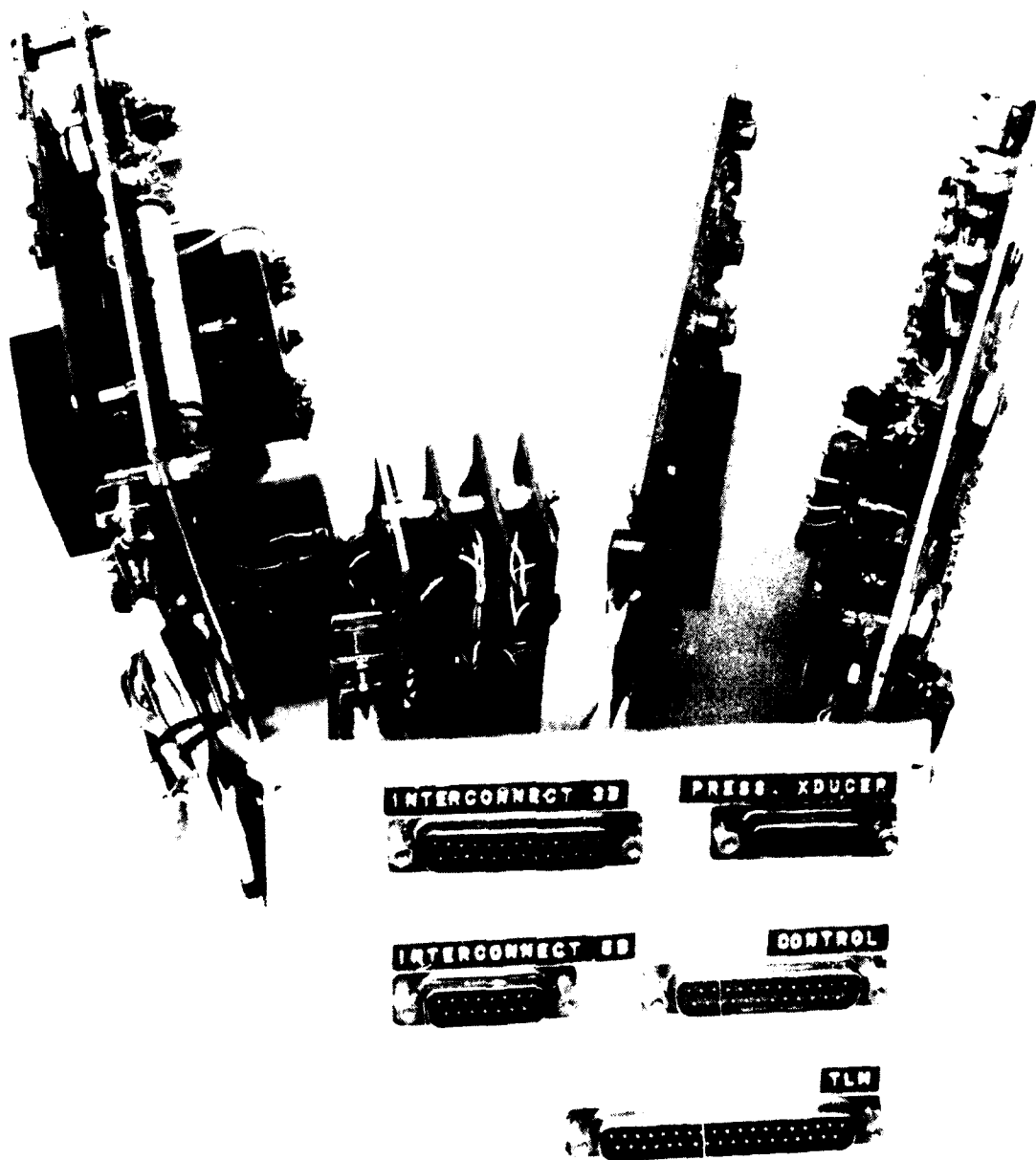


Figure 3-25. Front Cover and Contents of Power Processor Box B

Table 3-7. Disassembly of Box B

Step	Action
1	Remove rear cover (3/32 Allen wrench).
2	Remove Teflon sheets.
3	Remove retaining screws for CTL isolator box in top of Box B (No. 2 Phillips head).
4	Remove retaining nuts (5/32 nut driver) for CTL isolator box on the front cover of Box B.
5	Disconnect CTL isolator box from connector on front cover of Box B.
6	Remove front cover retaining screws (3/32 Allen wrench).
7	Pull front cover back, remove retaining screws from HSKG connector (3/16 slotted screw driver), TLM board connector (3/32 Allen wrench) and CTL board connector (3/16 slotted screw driver).
8	Remove connector from HSKG supply and TLM card.
9	Slide CTL circuitry out from front of box.
10	Remove connector from CTL circuitry.
11	Remove screws (3/16-inch slotted screw driver) from RUN supply connector, remove connector. Set Box B front cover plate aside.
12	Slide HSKG supply out from back of box.
13	Slide TLM board out from back of box.
14	Slide RUN supply out from back of box.

on the top plate with the leads running between the packages and the gas system is mounted on the bottom plate. The open area between top of the gas system and bottom of the power processor plate was to be occupied by a deck plate containing the battery pack for the system. The support vessel was going to be mounted directly to the sounding rocket wall for the flight. This vessel is mounted on a support bracket in the test configuration for convenience. Components which are painted red were to be removed before sounding rocket integration.

Vent holes in the power processor boxes allow the supplies to out-gas quickly. The connector rack, shown on the gas system plate in Fig. 3-26, provides mechanical support for connectors to cables for the KEEPER electrode and support vessel body common point (bottom connector), gas pressure transducer (center connector), and the latching valve (top connector). The output side of the pressure regulator is connected to the input side of the flow metering valve via 0.32 cm outside diameter stainless steel tubing and a AN and swagelok fitting, respectively. The output side of the flow metering valve is connected to the hollow cathode gas inlet via 0.48 cm outside diameter Tygon tubing and swagelok fittings. Two porous, metallic plugs are slip fitted into the Tygon tubing near the hollow cathode gas inlet to force plasma recombination should the plasma back up in the flow tube. This prevents the plasma from grounding and extinguishing the arc discharge.

The external cable routing can be seen in Fig. 2-3. The cathode emitter tube lead runs from Box A directly to the emitter tube where it is lug terminated. The cable is 23 AWG, shielded Teflon cable rated for 200°C. The leads for the keeper electrode and source body are 20 Ga, shielded, Teflon coated wires which run from Box A to the connector rack on the gas system deck plate and then are lug terminated on their respective posts. The cable for the pressure transducer is a shielded, 20 Ga, 4 conductor which runs from Box B to the connector rack on the gas system deck plate. The pressure transducer lead, which is comprised of a five conductor (28 Ga) shielded bundle, is connector mounted in the rack. Two cable bundles carried power and signals between the boxes. Connectors from the SAADS/BERT-1 wiring harness were to mate with the power input connector on Box A, the controls and telemetry connectors on Box B, and the latching valve input on the gas plate connector rack.



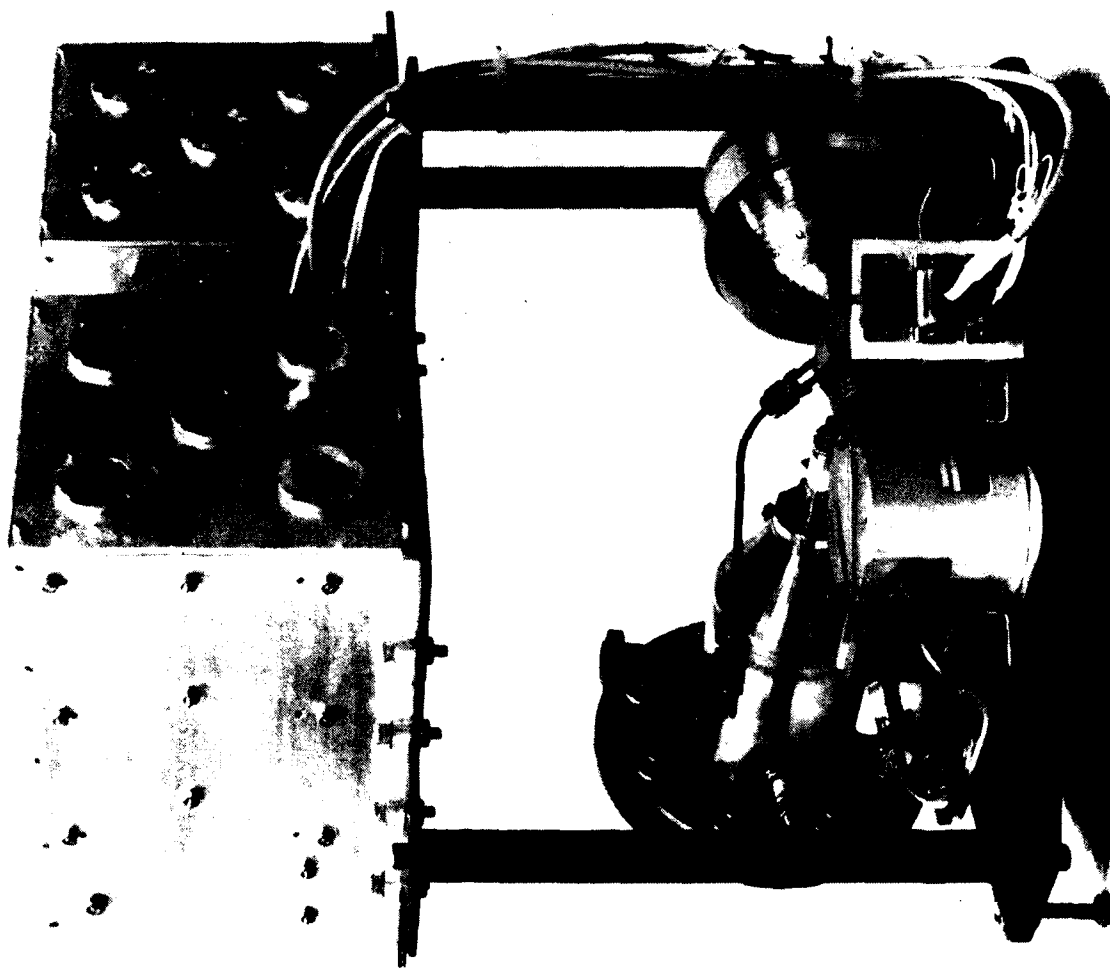


Figure 3-26. Prototype Plasma Source System in JPL Test Configuration

## SECTION 4

### MECHANICAL AND THERMAL TESTING

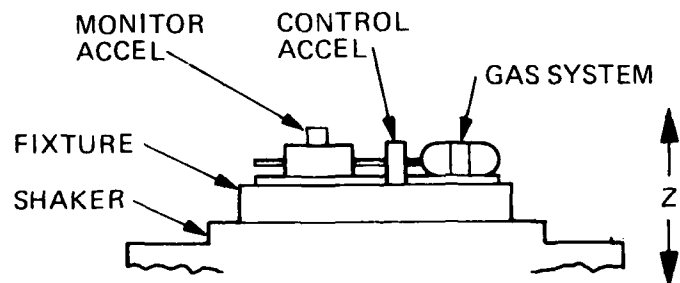
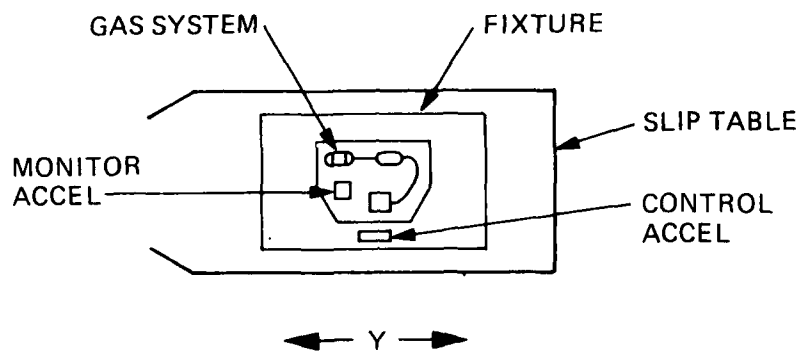
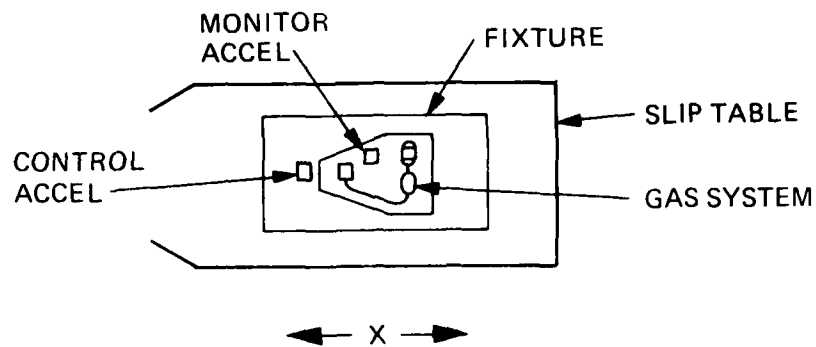
The power processor boxes, gas system and cathode and vessel were subjected to shock and random vibration testing at AFGL. The power processor boxes were also subjected to thermal cycling tests at AFGL. No system performance degradations were noted following the mechanical and thermal testing.

#### 4.1 GAS SYSTEM MECHANICAL TESTING

The gas system was subjected to mechanical testing in the configuration shown in Figs. 3-6 and 3-7 and was mounted on the magnesium flight deck plate. The gas system axes orientations, as defined for mechanical testing, are shown in Fig. 4-1. A photograph of the gas system, mounted on the shake table for shock and vibration testing, along the Z axis, is shown in Fig. 4-2.

A 25 G, 11 ms shock pulse was applied to the gas system along each axis. A typical shock pulse response signal from the control accelerometer is shown in Fig. 4-3. This particular shock pulse was along the Z axis. The shaker at AFGL has no provisions for the use of a monitor accelerometer located on the test article, during shock testing.

The random vibration tests were run for five minutes on each axis and were based on the programmed reference spectrum shown in Fig. 4-4. The spectrum rises at +6 dB/Oct from 20 to 40 Hz and has a flat spectrum at 0.02 GSQR/Hz from 40 to 2000 Hz. Frequencies beyond 2000 Hz were not monitored. Typical vibration test, response signals for the control (on shake table) and monitor (on test article) accelerometers are shown in Fig. 4-5. These particular signals are for vibration along the Z axis. As can be seen



NOTE: MONITOR ACCEL NOT USED DURING SHOCK TESTING

Figure 4-1. Axis Orientations for Gas System Mechanical Testing

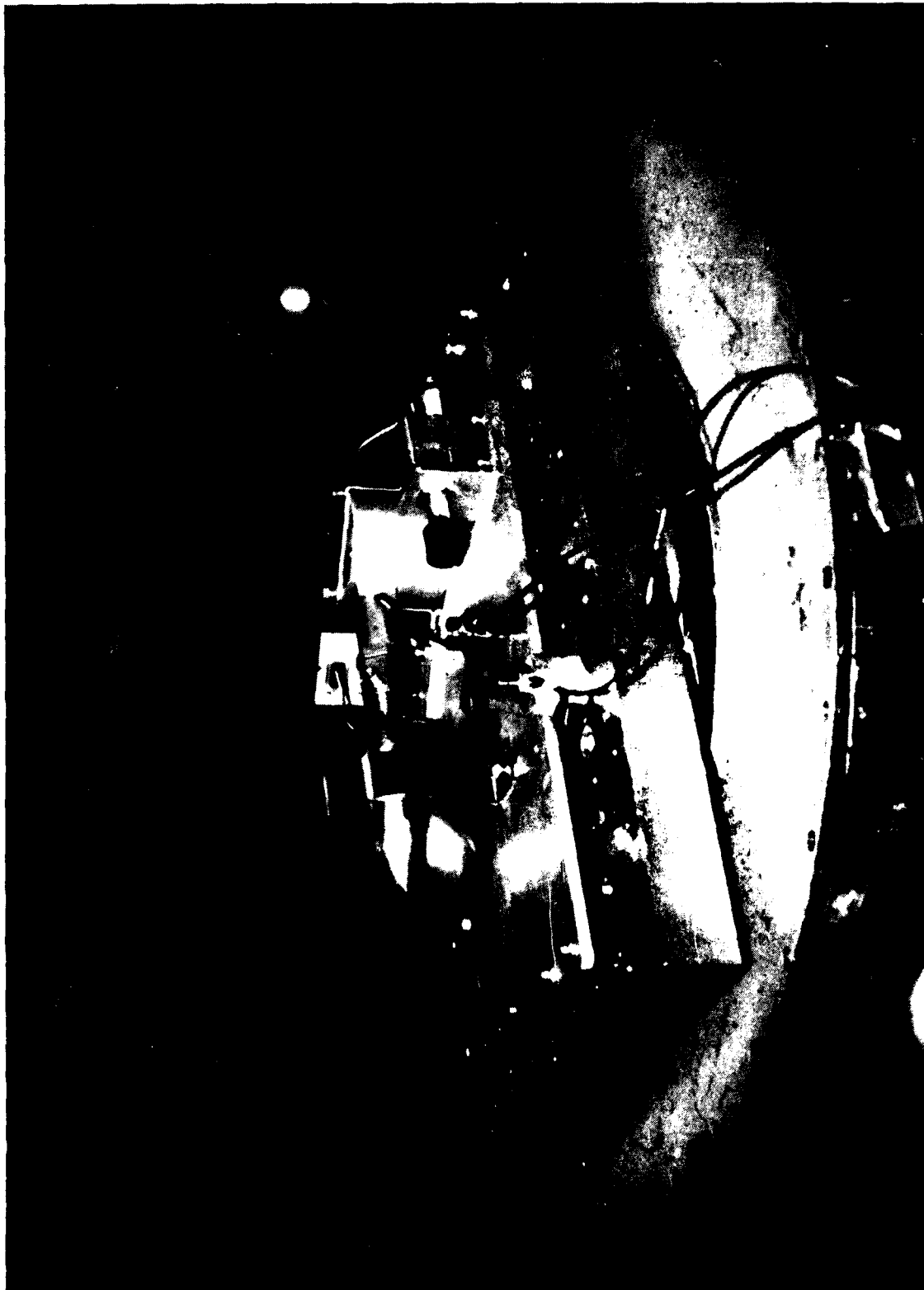


Figure 4-2. Gas System Mounted for Shock and Vibration Testing Along Z Axis

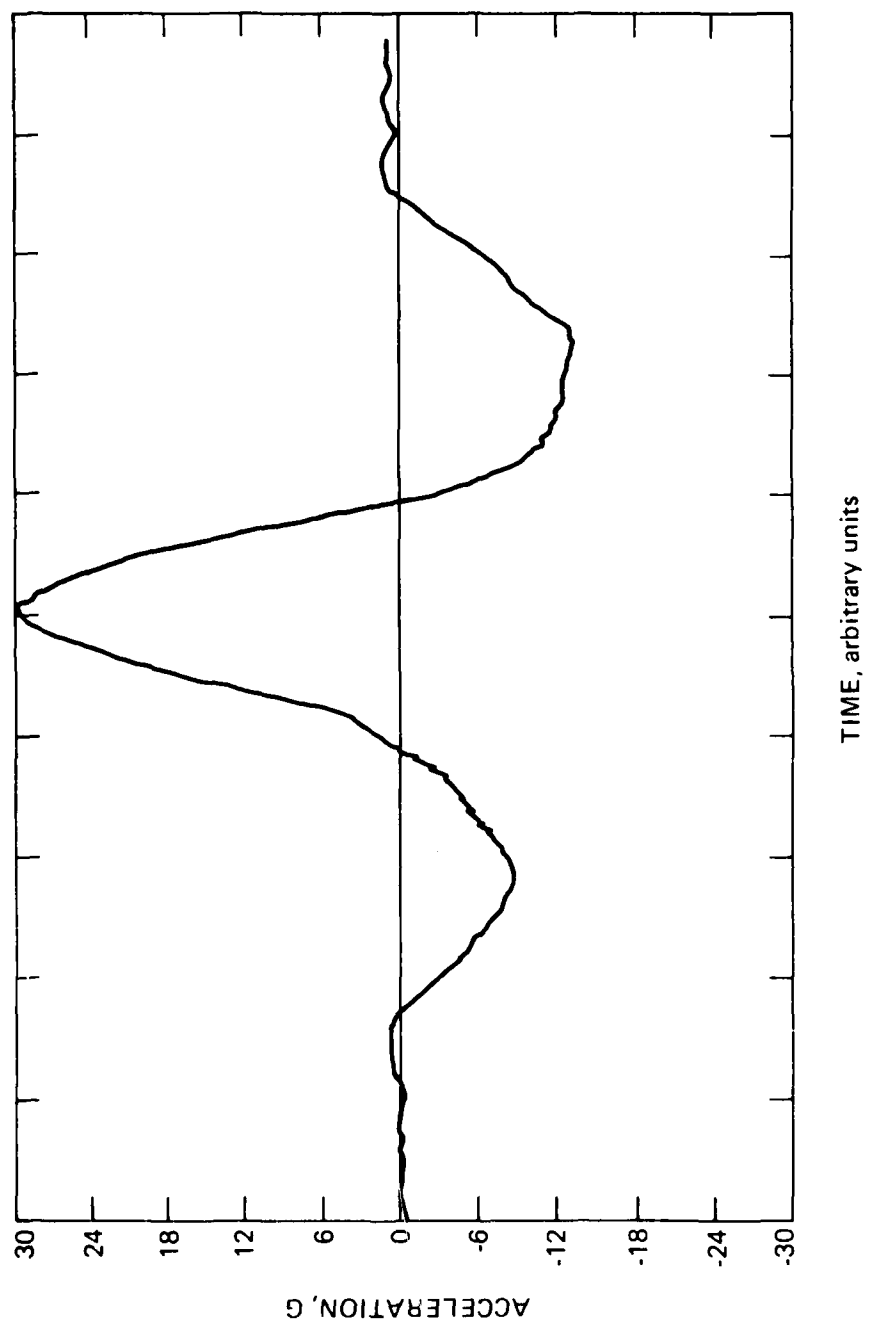


Figure 4-3. Shock Test Pulse Applied Along Z-Axis of Gas System

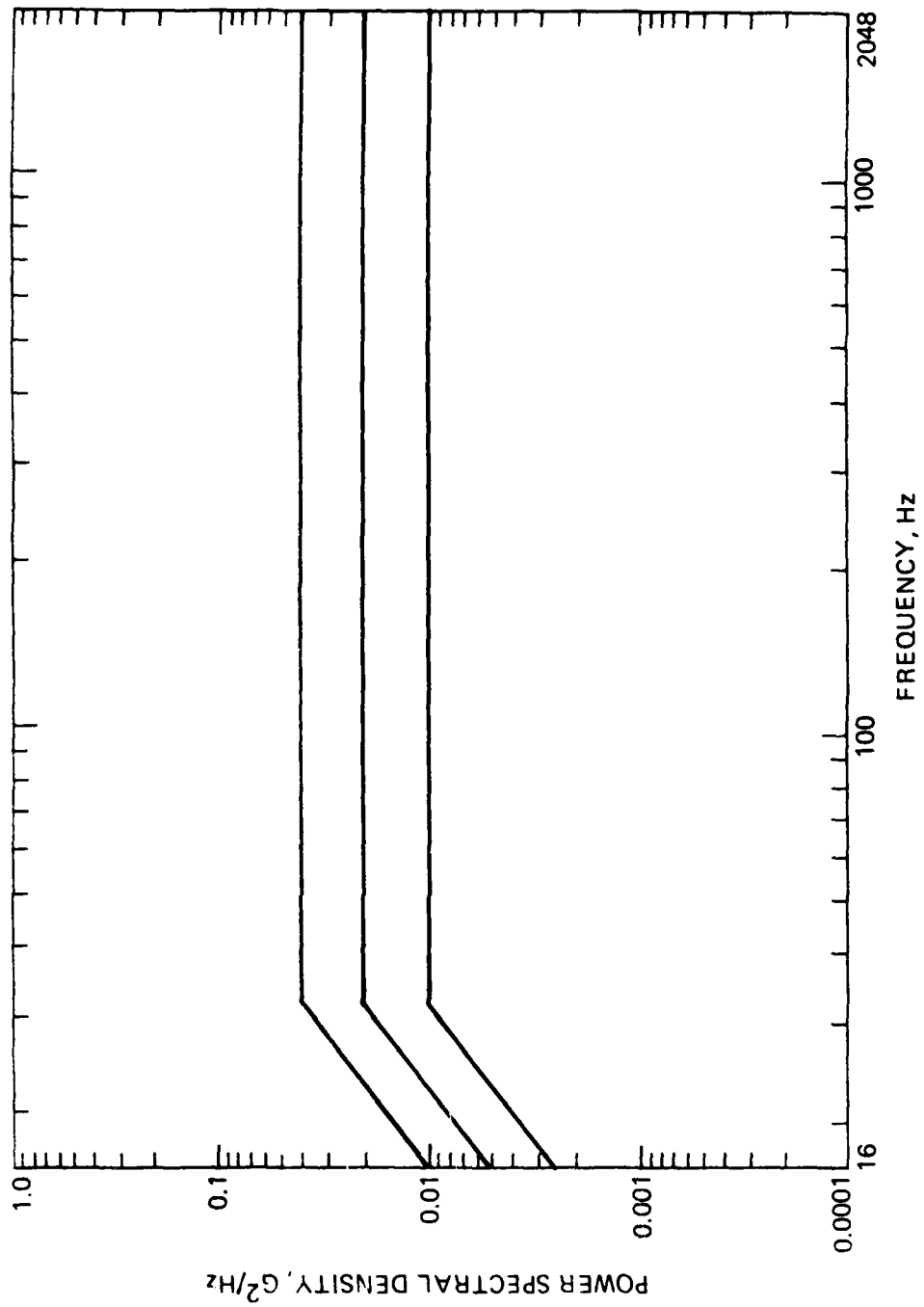


Figure 4-4. Vibration Test Programmed Reference Spectrum

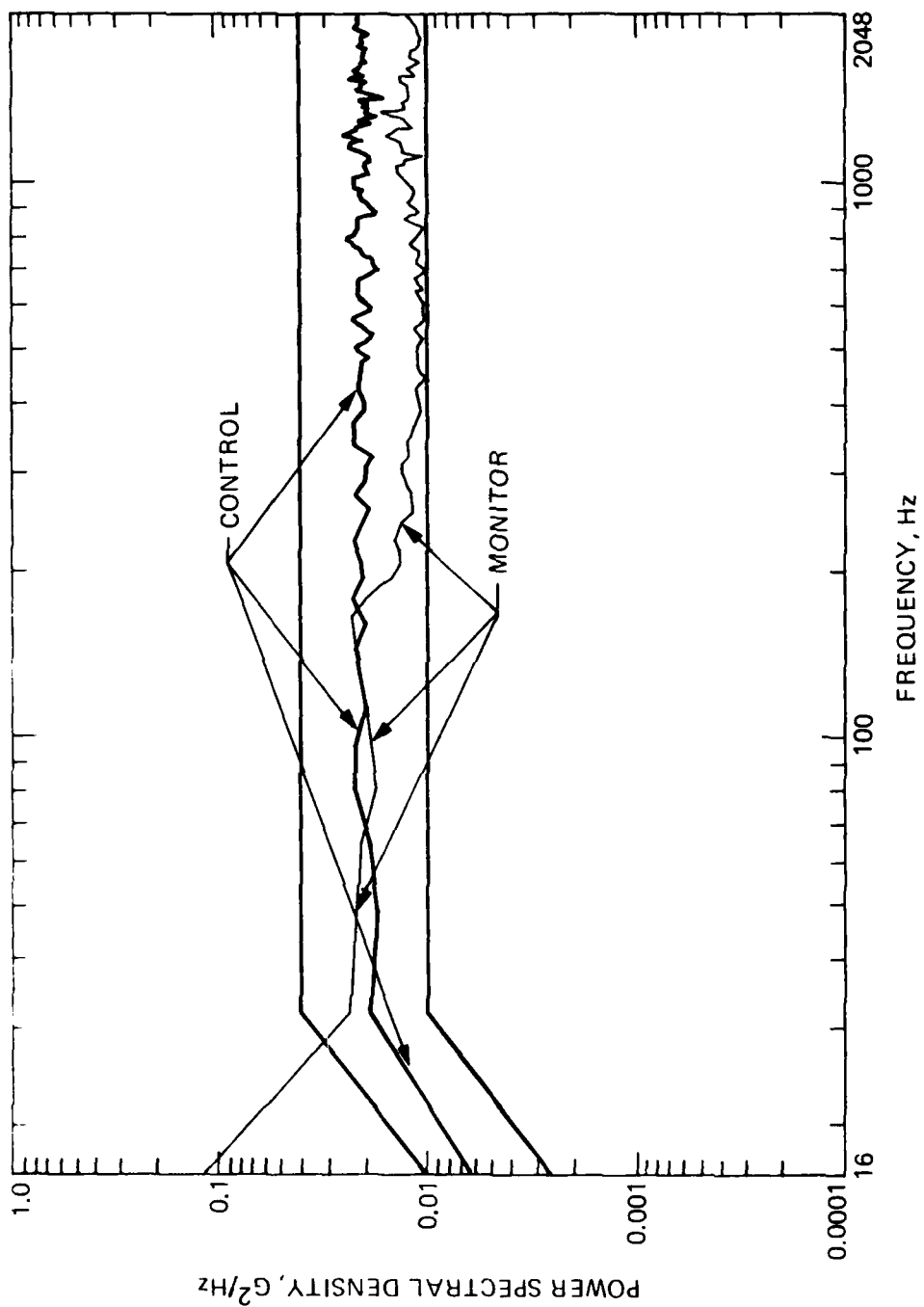


Figure 4-5. Typical Vibration Test Response Signals for the Control and Monitor Accelerometers During Gas System Mechanical Testing

in Fig. 4-2, the monitor accelerometer was located on the magnesium gas system mounting plate far from the plate supports which is the likely cause of low-end frequency ringing.

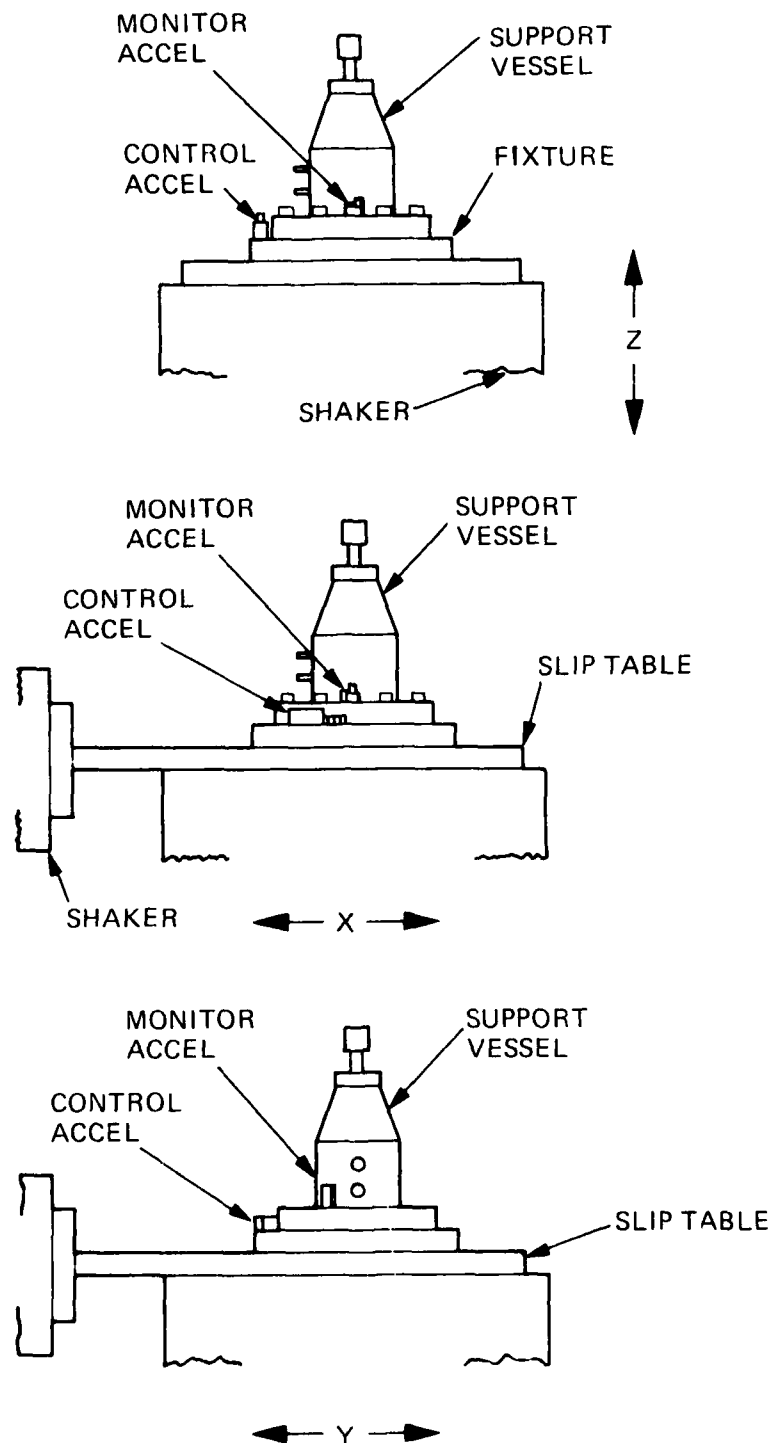
#### 4.2 CATHODE AND VESSEL MECHANICAL TESTING

The flight vessel was three axis, shock and vibration tested at AFGL. The vessel axis orientations, defined for shock and vibration testing, are shown in Fig. 4-6. The support vessel is shown mounted for shock and vibration testing in Fig. 4-7. A 25 G, 11 msec shock pulse was applied to the vessel along each axis, as before. A typical shock pulse, response signal from the control accelerometer is shown in Fig. 4-8. The random vibration tests were run for 5 minutes on each axis and were again based on the programmed reference spectrum shown in Fig. 4-4. Typical vibration test, response signals for the control (on shake table) and monitor (on test article) accelerometers are shown in Fig. 4-9. The resonances shown on the monitor accelerometer curve most likely result from vibrations of the cathode emitter tube which has a non-rigidly supported length of approximately 13 cm.

#### 4.3 POWLR PROCESSOR MECHANICAL TESTING

Each power processor box was subjected to shock and random vibration testing separately. Only typical results for one box will be given. The power processor box axes orientations, as defined for mechanical testing, are shown in Fig. 4-10. Box A (Z axis) is shown mounted on the shaker for shock and vibration testing in Fig. 4-11.





NOTE: MONITOR ACCEL NOT USED DURING SHOCK TESTING

Figure 4-6. Axis Orientations for Support Vessel Mechanical Testing



Figure 4-7. Support Vessel Mounted for Shock and Vibration Testing Along the X-Axis

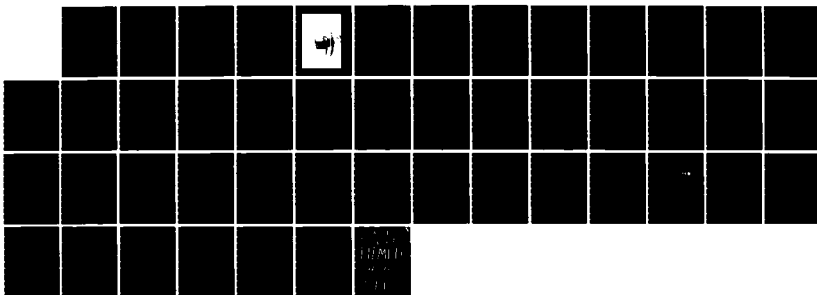
AD-A165 223

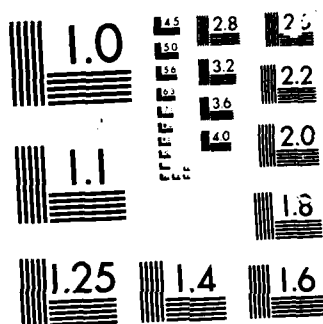
A NEUTRAL PLASMA SOURCE FOR ACTIVE SPACECRAFT CHARGE  
CONTROL(U) JET PROPULSION LAB PASADENA CA  
W D DEININGER ET AL. AUG 85 JPL-D-2734 AFGL-TR-85-0313  
NAS7-918 F/G 22/2

2/2

UNCLASSIFIED

NL





MICROCOPY RESOLUTION TEST CHART  
 1963-A

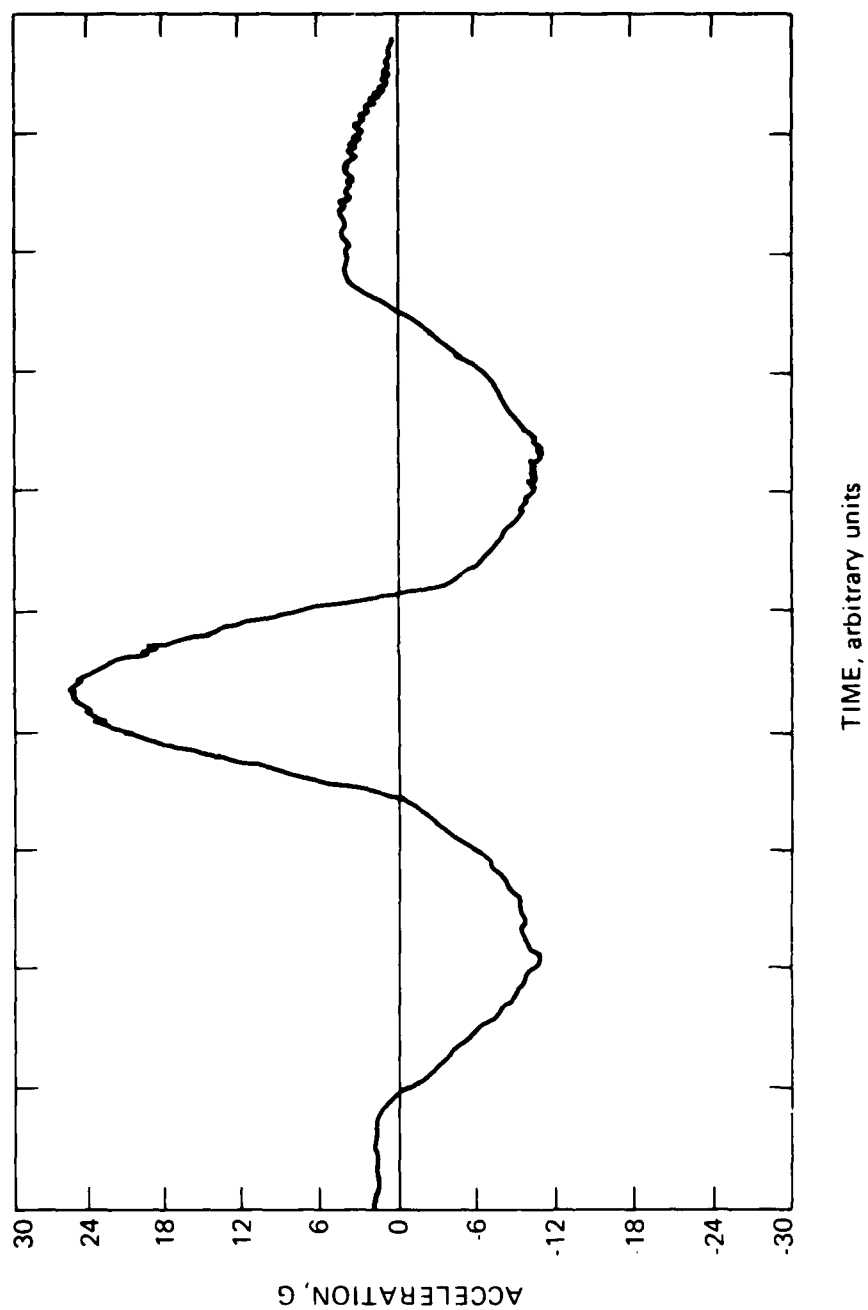


Figure 4-8. Typical Response Signal of the Control Accelerometer During a Shock Pulse

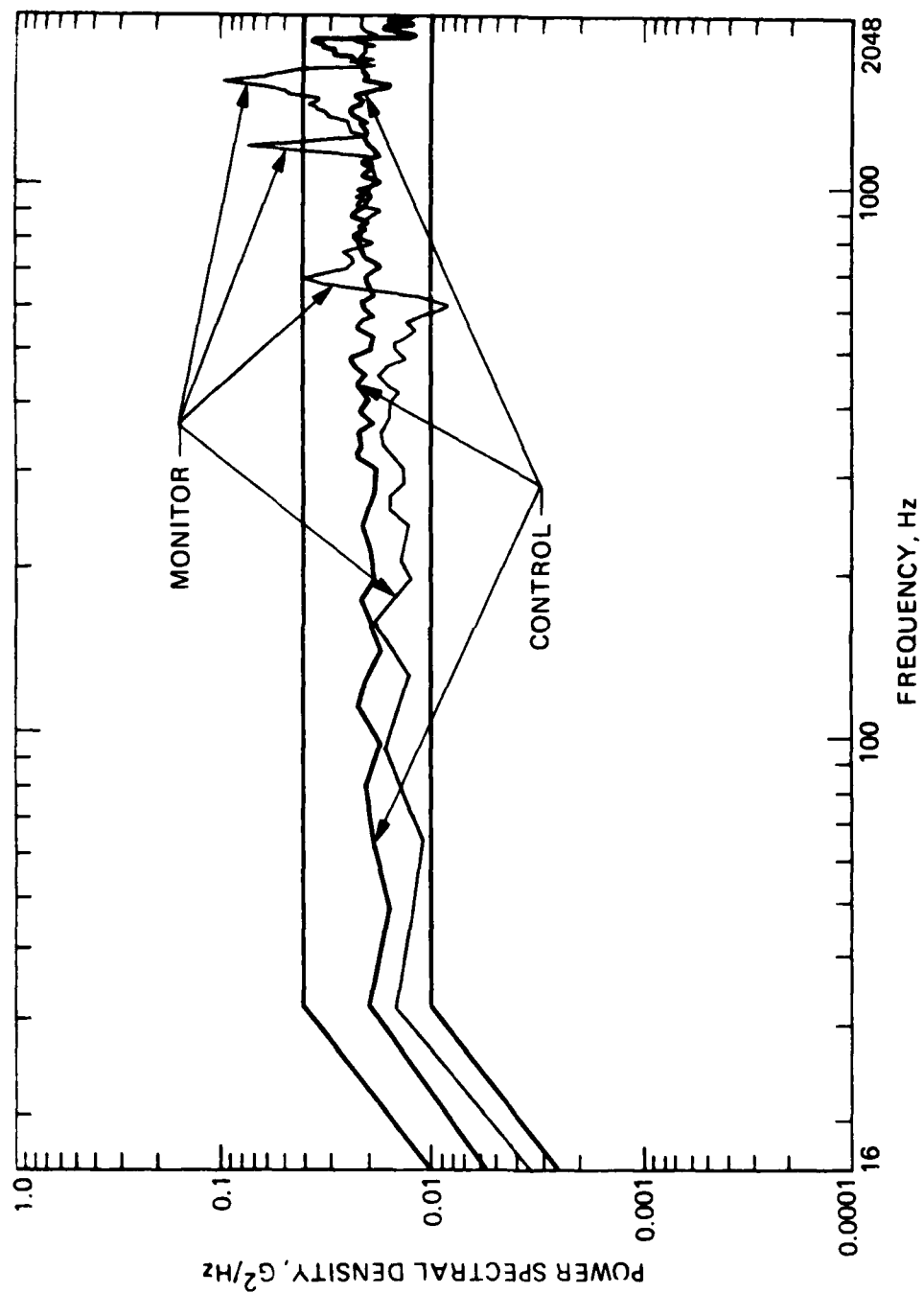
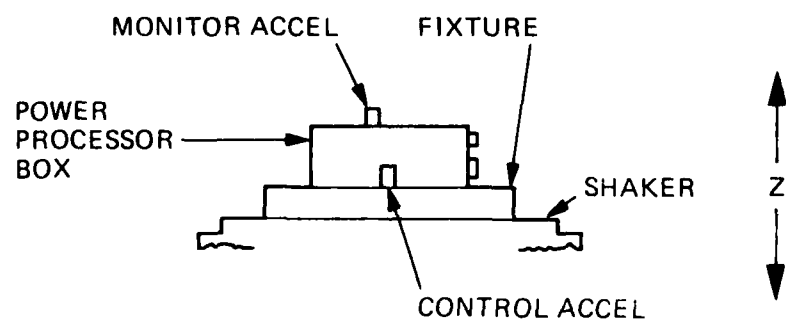
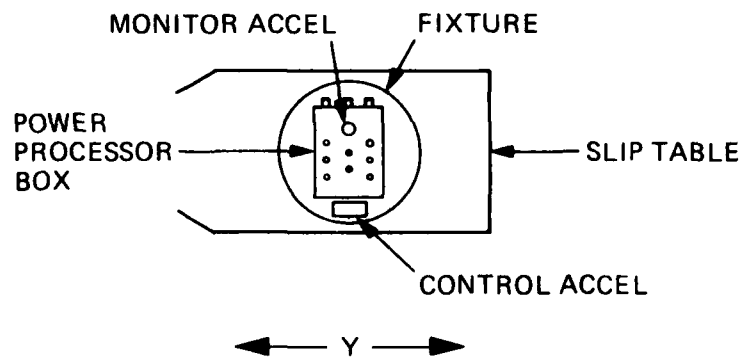
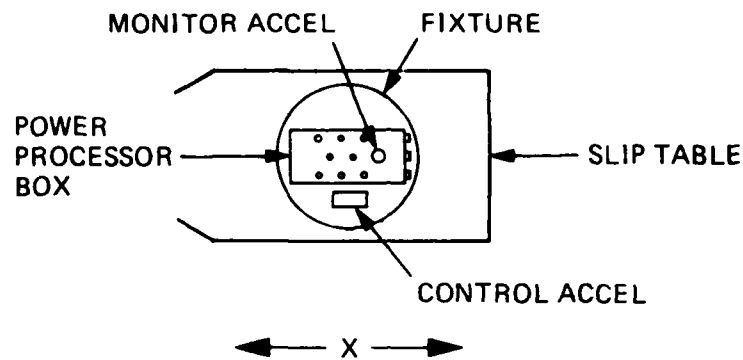


Figure 4-9. Typical Vibration Test Response Signals for the Control and monitor Accelerometers During Support Vessel Mechanical Testing



NOTE: MONITOR ACCELEROMETER NOT USED DURING SHOCK TESTING.

Figure 4-10. Axis Orientations for Electronics Box Mechanical Testing

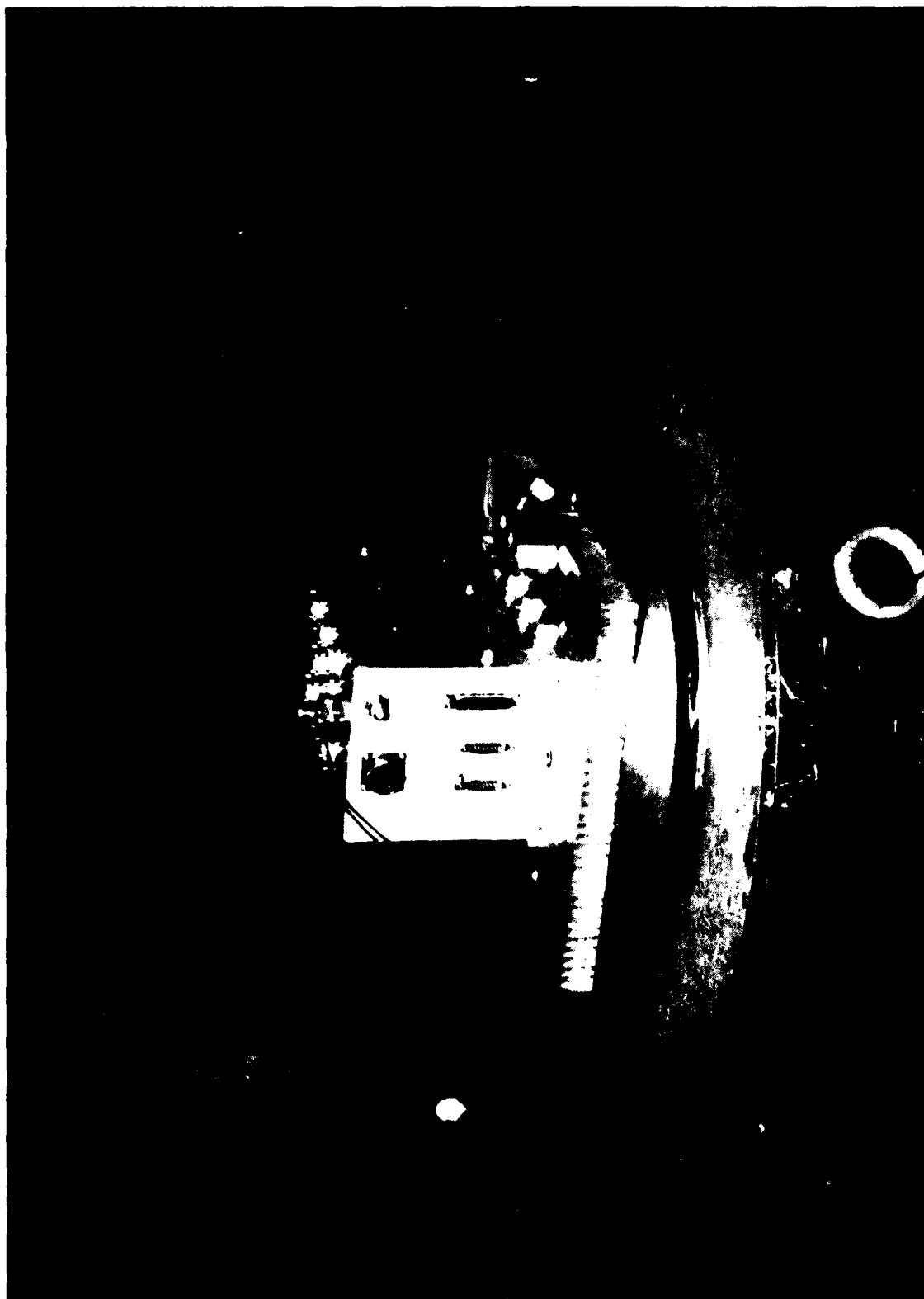


Figure 4-11. Box A Mounted for Shock and Vibration Testing Along the Z Axis



A 25 G, 11 ms shock pulse was applied to each box along each axis. A typical shock pulse response signal from the control accelerometer is shown in Fig. 4-12. The particular shock pulse shown in Fig. 4-12 was along the Z axis of Box A.

The random vibration tests were run for five minutes on each axis of each box and were again based on the programmed reference spectrum shown in Fig. 4-4. Typical random vibration test response signals for the monitor (on test article) accelerometer and the control (on shake table) accelerometer which were obtained in this instance during Z axis vibration testing of Box A are shown in Fig. 4-13.

As can be seen in Fig. 4-11, the monitor accelerometer is located in the middle of the top of the power processor boxes. The top covers of each box have a thickness of approximately 0.15 cm. This surface can act as a "drum head" during the random vibration tests resulting in resonances such as those seen in Fig. 4-13.

#### 4.4 POWER PROCESSOR THERMAL CYCLING TESTS

The power processor boxes were subjected to thermal cycling tests at AFGL. The boxes were placed side-by-side in a Associated Testing Laboratory, Inc., Model SK-3102 refrigerator/oven. The box cabling and a temperature monitor were fed into the refrigerator/oven compartment through a small port on the side. Thermal cycling requirements included a 0 to 60°C temperature envelope and ambient air pressure.

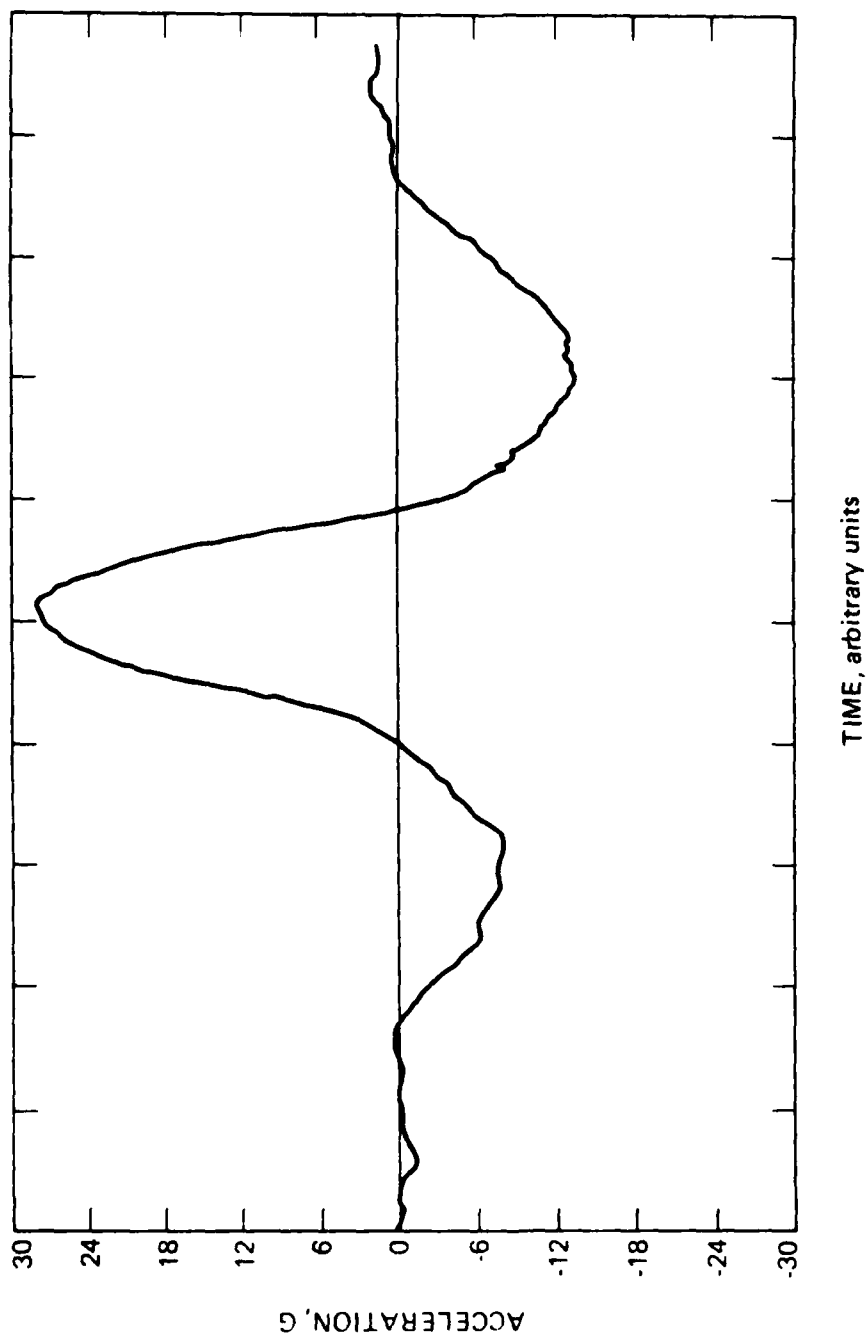


Figure 4-12. Shock Pulse Response Signal for Box a Along the Z Axis

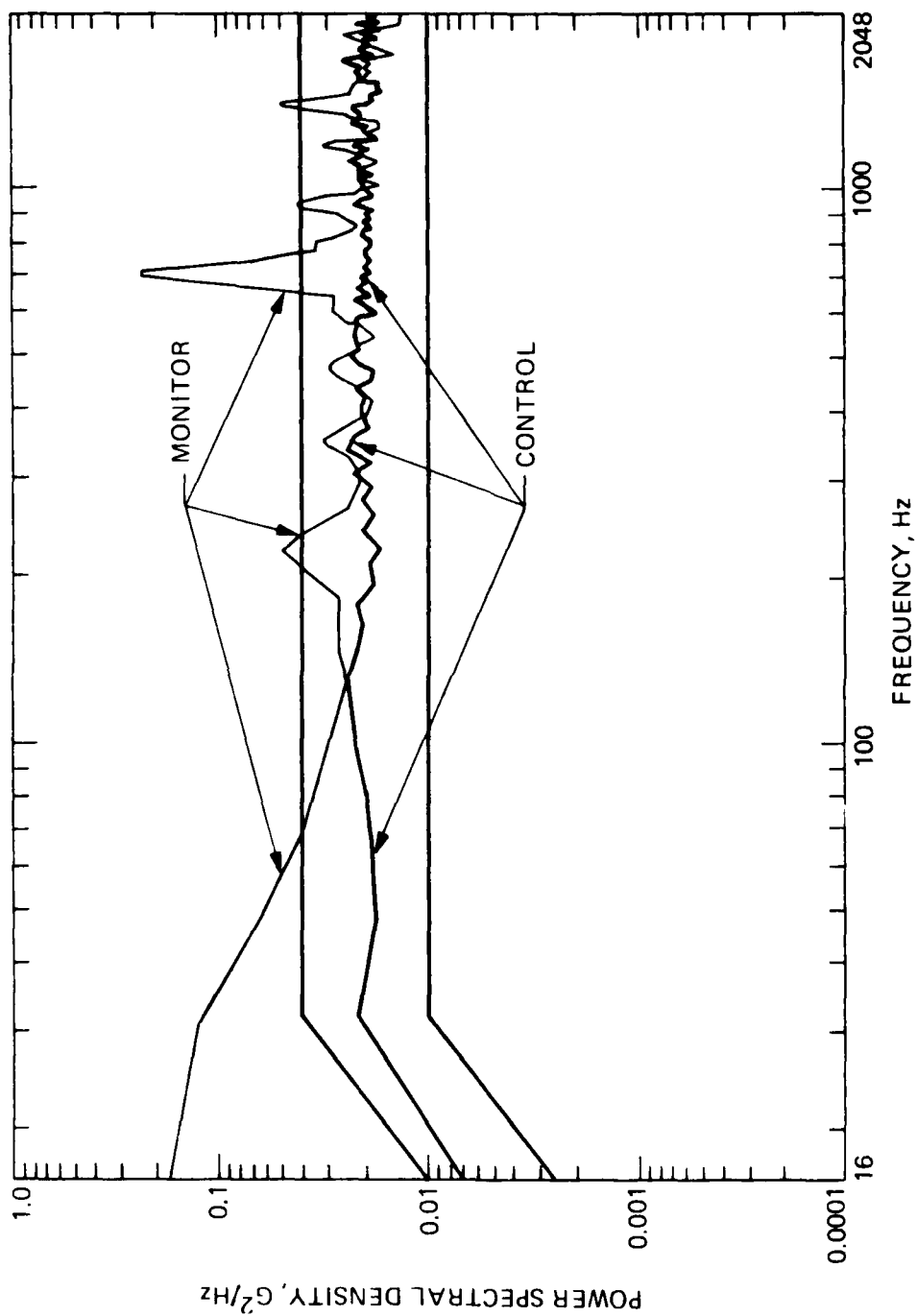


Figure 4-13. Typical Vibration Test Response Signals for the Control and Monitor Accelerometers During Power Processor Mechanical Testing

## SECTION 5

### PLASMA SOURCE OPERATION

The plasma source startup procedure, resistive load checkout procedure and operational testing results are described in this section.

#### 5.1 PLASMA SOURCE START-UP

The plasma source is started and operated when the internal control circuitry receives and processes an appropriate 8-bit word. During the sounding rocket flight, the 8-bit word would have been sent to the plasma source from the SAADS programmer. A controller was built for ground testing to simulate the SAADS programmer (see Section 3.3.2.2.3). All eight of the two position switches across the bottom of the front panel of the controller should initially be in the UP position. The lower row of LEDs should be lighted. The red pushbutton labeled 'SEND CMD' sends an 8-bit word, defined by the positions of the eight switches, to the plasma source for processing. If all of the switches are in the UP position and all of LED's in the lower row are not lighted, the 'SEND CMD' button should be depressed to initialize the controller.

The plasma source is now ready to be started. The starting and operating procedure is given in Table 5-1. Quantities enclosed in quotes, 'XXX', represent specifically referenced switches on the controller console. The keeper polarity should NEVER be changed while the KEEPER power supply is on.

Table 5-1. Starting and Operating Procedure for Plasma Source

Step	Action
1	Open latching valve to begin gas flow.
2	Set eight, two position switches in the UP position.
3	Turn-on power supplies (28 V for plasma source, 5 V for controller).
4	Depress 'SEND CMD' if eight lower LEDS are not lighted.
5	To start, change 'RUN' switch (bit 0) to lower position (Lower LED will go out). Depress 'SEND CMD' (Upper LED will light). The RUN supply is now on.
6	Change 'START' switch (bit 1) to lower position (Lower LED will go out). Depress 'SEND CMD' (Upper LED will light). The RUN and START supplies are on.
7	If starting noise shuts off either/both the RUN and/or START supply(s), the upper LED(s) will go out even though the corresponding switch(es) is (are) still in the down position. Set all switches UP and depress 'SEND CMD' (All lower LEDS on, all upper LEDS off). Repeat Steps 5 and 6 except keep 'SEND CMD' depressed at the end of Step 6.
8	When the telemetry output for the cathode current reaches approximately 4.92 V $\pm 2\%$ and remains there, the cathode is ON (Release 'SEND CMD' if still depressed).
9	Set 'START' switch in UP position (both LEDS on), depress 'SEND CMD' (upper LED off). (The start supply shuts off automatically, this step is a safeguard.)
10	The Keeper electrode can be biased positively (Electron Collection, switch DOWN) or negatively (Ion Collection, switch UP). Select desired Collection Mode, set switch labeled 'KEEPER BIAS' (bit 7) and depress 'SEND CMD'. If the switch labeled 'HIGH CUR' is in the down position <u>DO NOT</u> change 'KEEPER BIAS'. Place switch in UP position and depress 'SEND CMD' first. The switch labeled 'HIGH CUR' serves as the KEEPER power supply ON/OFF.
A. Positive Bias (Switch DOWN)	
Three current collection modes are available when the KEEPER is set for positive bias. These modes are used to enhance plasma source emission by actively extracting electrons. The modes are high (2.0 A) medium (1.2 A) and low (0.3 A) collected electron currents.	

Table 5-1. Starting and Operating Procedure for Plasma Source (Continued)

Step	Action
10 Cont.	<ol style="list-style-type: none"> <li data-bbox="459 390 1356 569">1) To get the high current collection keeper mode, place the switch labeled 'HIGH CUR' (bit 2) in the down position, depress 'SEND CMD'. The keeper is now in the high current collection (2.0 A) mode. To turn the high current mode OFF, place the switch labeled 'HIGH CUR' in the UP position and press 'SEND CMD'.</li> <li data-bbox="459 600 1356 898">2) To get the medium current collection keeper mode, place the switches labeled 'HIGH CUR' and 'MED CUR' (bits 2 &amp; 3) in the down position and depress 'SEND CMD'. The keeper medium collected current (1.2 A) mode is now ON. To turn the medium current mode off, place the switches labeled 'HIGH CUR' and 'MED CUR' in the UP position and depress 'SEND CMD'. Do not change the switch labeled 'MED CUR' to the down position if the switch labeled 'HIGH CUR' is already in the down position.</li> <li data-bbox="459 930 1356 1232">3) To get the low collected current keeper mode, place the switches labeled 'HIGH CUR' and 'LOW CUR' (bits 2 &amp; 4) in the DOWN position and depress 'SEND CMD'. The keeper is now in the low collected (0.3 A) current mode. To turn the low current mode off, place the switches labeled 'HIGH CUR' and 'LOW CUR' in the UP positions and depress 'SEND CMD'. Do not change the switch labeled 'LOW CUR' to the down position if the switch labeled 'HIGH CUR' is already in the down position.</li> </ol>

#### B. Negative Bias (Switch UP)

Only ONE positive current collection mode is available. This bias appears to actively inhibit the electron flow from the hol- low cathode, the collected ion current is on the order of several tens of microamperes. To get the negative bias current mode, place the switch labeled 'KEEPER BIAS' in the UP position and depress 'SEND CMD'. Then place the switch labeled 'HIGH CUR' in the down position and depress 'SEND CMD'. The KEEPER electrode is now biased negatively. To turn the mode off, place the switch labeled 'HIGH CUR' in the UP position and press 'SEND CMD'.

Table 5-1. Starting and Operating Procedure for Plasma Source (Continued)

Step	Action
11	To shut off the plasma source system, set all switches in the UP positions and depress 'SEND CMD'.
12	Close latching valve and shut down power sources.

## 5.2 SYSTEM FUNCTIONAL CHECKOUT

The plasma source system checkout procedure involves running the power processor on a resistive load which simulates the plasma load expected during regular operation. During system checkout the three leads which attach to the plasma source vessel (emitter tube, keeper electrode and vessel body) should be removed from the vessel (see Fig. 3-1). A load of 20 to 30 should be placed between the leads for the keeper electrode and cathode emitter tube for KEEPER power supply checkout. A load of 20 to 30 should be placed between the leads for the cathode emitter tube and the vessel body for RUN power supply checkout. A load of 300 to 360 should be placed between the leads for the cathode emitter tube and the vessel body for START and START/RUN power supply checkout. The load resistors for KEEPER and RUN power checkout should be able to support up to a 120 W power load. The load resistors chosen for START and START/RUN power supply checkout should be able to support up to a 400 W power load.

The operating sequence given in Table 5-1 should be used for plasma source checkout testing on a resistive load. The operational characteristics for plasma source operation on a resistive load are given in Table 5-2. During resistive load testing, the latching valve should remain closed. The starting noise shut/off problem mentioned in Step 7 of Table 5-1 is not a

Table 5-2. Plasma Source Checkout Resistive Load Characteristics

Power Supply	Load	Drop Across Load (V)	Cathode V T/M (V)	Cathode I T/M (V)	Keeper V T/M (V)	Keeper I T/M (V)	Keeper Pol. T/M (V)	Power Supply Current at 28 VDC (A)
RUN	20.7	41.4	3.32	4.92	0.0	0.0	0.0	4.2
RUN	348	73	0.97	0.52	0.2	0.1	0.0	0.8
START	348	298	3.82	2.09	0.0	0.1	0.0	12.7
START/RUN	348	335	4.29	2.37	0.0	0.0	0.0	17.0
KEEPER-HC	20.5	-39.9	0.0	0.0	2.25	4.16	0.0	4.1
KEEPER-MC	20.5	-24.2	0.0	0.0	1.34	2.43	0.0	1.7
KEEPER-LC	20.5	-6.7	0.0	0.0	0.39	0.60	0.0	0.3
KEEPER+HC	20.5	38.4	0.0	0.0	2.16	4.16	5.29	3.9
KEEPER+MC	20.5	22.2	0.0	0.0	1.24	2.43	5.29	1.4
KEEPER+LC	20.5	5.1	0.0	0.0	0.27	0.61	5.29	0.2
KEEP+HC/RUN	20.5/20.7	38.7/41.4	3.35	4.92	2.19	4.13	5.29	8.1
ALL OFF	NONE	--	0.0	0.0	0.0	0.1	0.0	0.0



problem during checkout testing. The three power supplies, START, RUN and KEEPER can be tested independently. As noted in Table 5-2, the KEEPER power supply will exhibit three operational modes in both keeper biases during resistive load testing.

### 5.3 SYSTEM OPERATIONAL CHARACTERISTICS

The starting and operating procedure for the plasma source system is given in Section 5.1. This section discusses the operational characteristics of the plasma source in terms of the telemetry outputs when the source is operating in vacuum and producing a plasma. Calibration charts are provided for each telemetry output when applicable.

#### 5.3.1 Battery Voltage Telemetry

The battery voltage telemetry signal is used to monitor the 28 VDC  $\pm 3$  VDC input voltage provided by the battery pack. A calibration curve is shown in Fig. 5-1. This curve was generated by varying the output voltage of a power supply and monitoring the output telemetry signal.

#### 5.3.2 Box Temperature Telemetry

The box temperature telemetry signal is used to monitor the temperature of the base plate of the RUN power supply in electronics Box A. The RUN power supply has the highest duty cycle and should be the warmest supply of either box. A calibration curve is shown in Fig. 5-2. This curve was generated by using data points obtained during the thermal cycling tests.

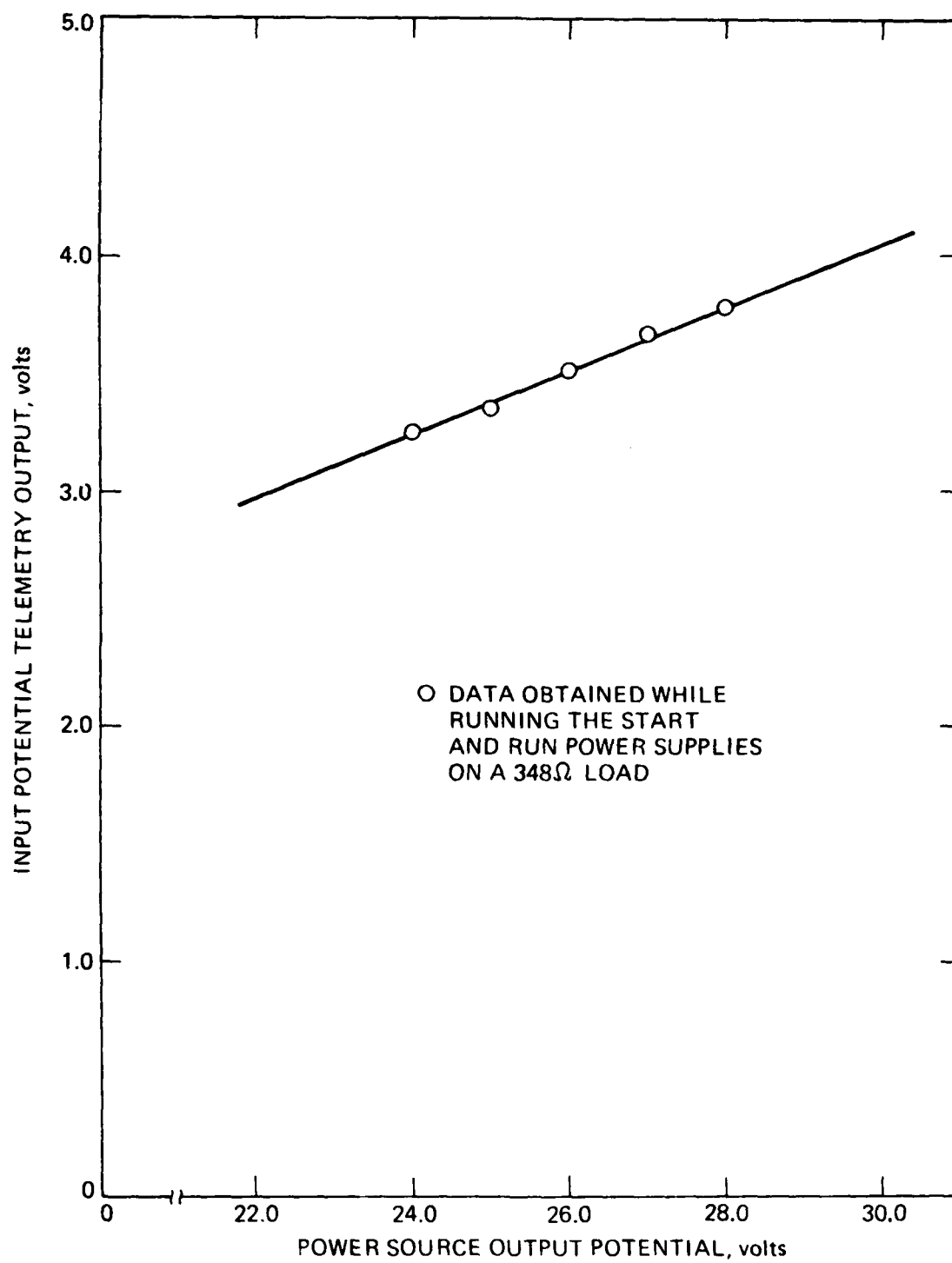


Figure 5-1. Battery Potential Telemetry Output Calibration Curve

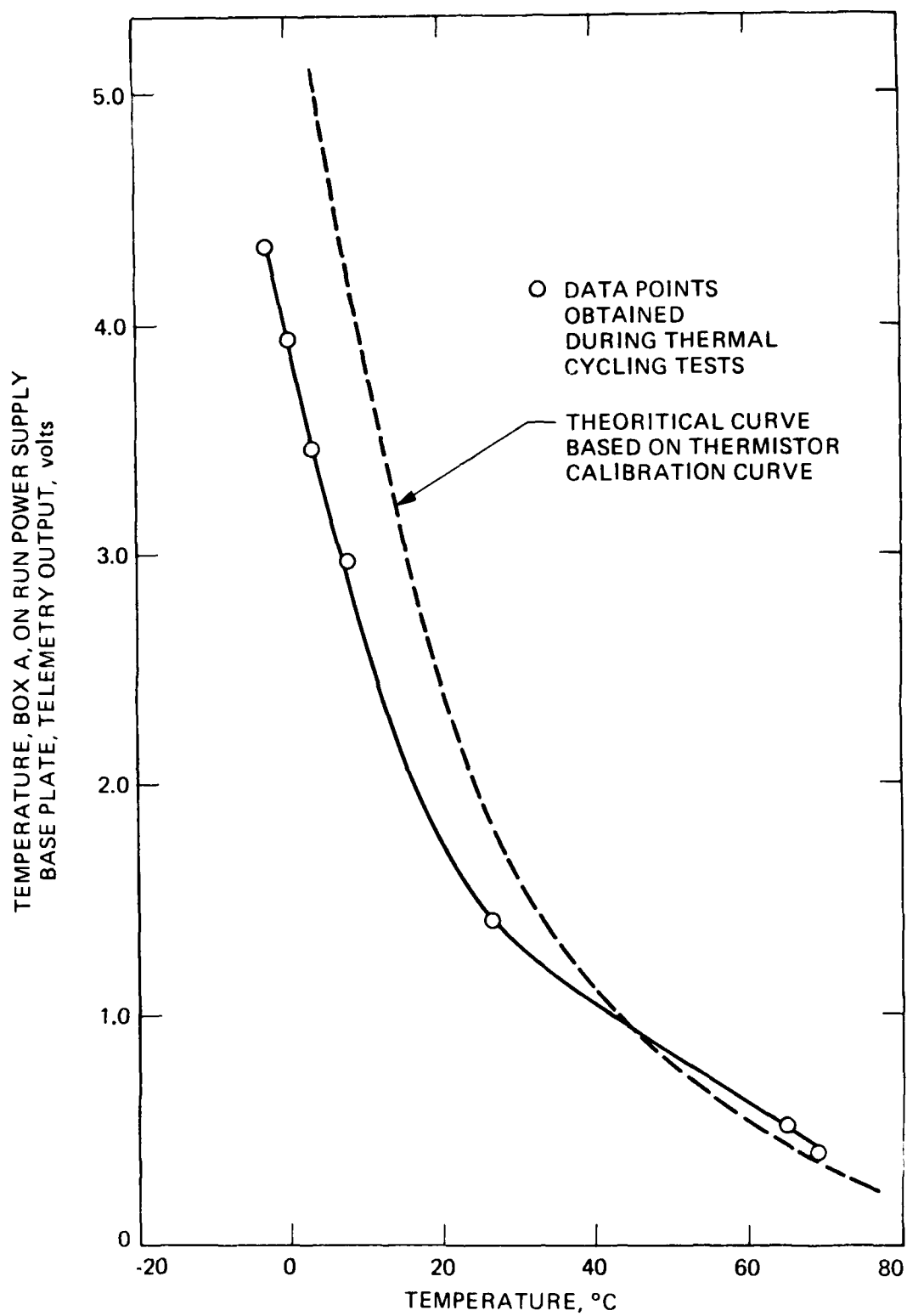


Figure 5-2. Box Temperature Telemetry Output Calibration Curve

Also shown is a curve based on the calibration chart of the thermistor without corrections for conditioning by real electronics.

#### 5.3.3 Gas Pressure Telemetry

The gas pressure telemetry signal is used to monitor the pressure inside the Kr reservoir. A calibration curve is shown in Fig. 5-3. This curve was generated by monitoring the telemetry output as the reservoir was filled. The pressure transducer, which was AFGL supplied equipment, has failed since this curve was plotted (see Reference 21, Section 3-E for details on the failure mode).

#### 5.3.4 Cathode Current Telemetry

The cathode current telemetry signal is used to monitor the current flowing between the cathode emitter tube and barrel during hollow cathode operation. The START and RUN power supplies are constant current sources at 1.0 A and 2.0 A, respectively. As a result, the telemetry output shows only two values; a glow discharge at 1.0 A corresponds to a telemetry output of 2.42 V  $\pm$  5 percent, and an arc discharge at 2.0 A corresponds to a telemetry output of 4.92 V  $\pm$  5 percent. A calibration curve obtained from results of resistive load testing is shown in Fig. 5-4.

#### 5.3.5 Cathode Voltage Telemetry

The cathode voltage telemetry signal is used to monitor the voltage drop between the cathode emitter tube and barrel during hollow cathode operation. This telemetry output has two different sensitivities depending upon whether the cathode is operating in a glow or arc discharge. This was required since actual potential differences between these two cathode modes differ by over an order of magnitude. The sensitivity used is a function of

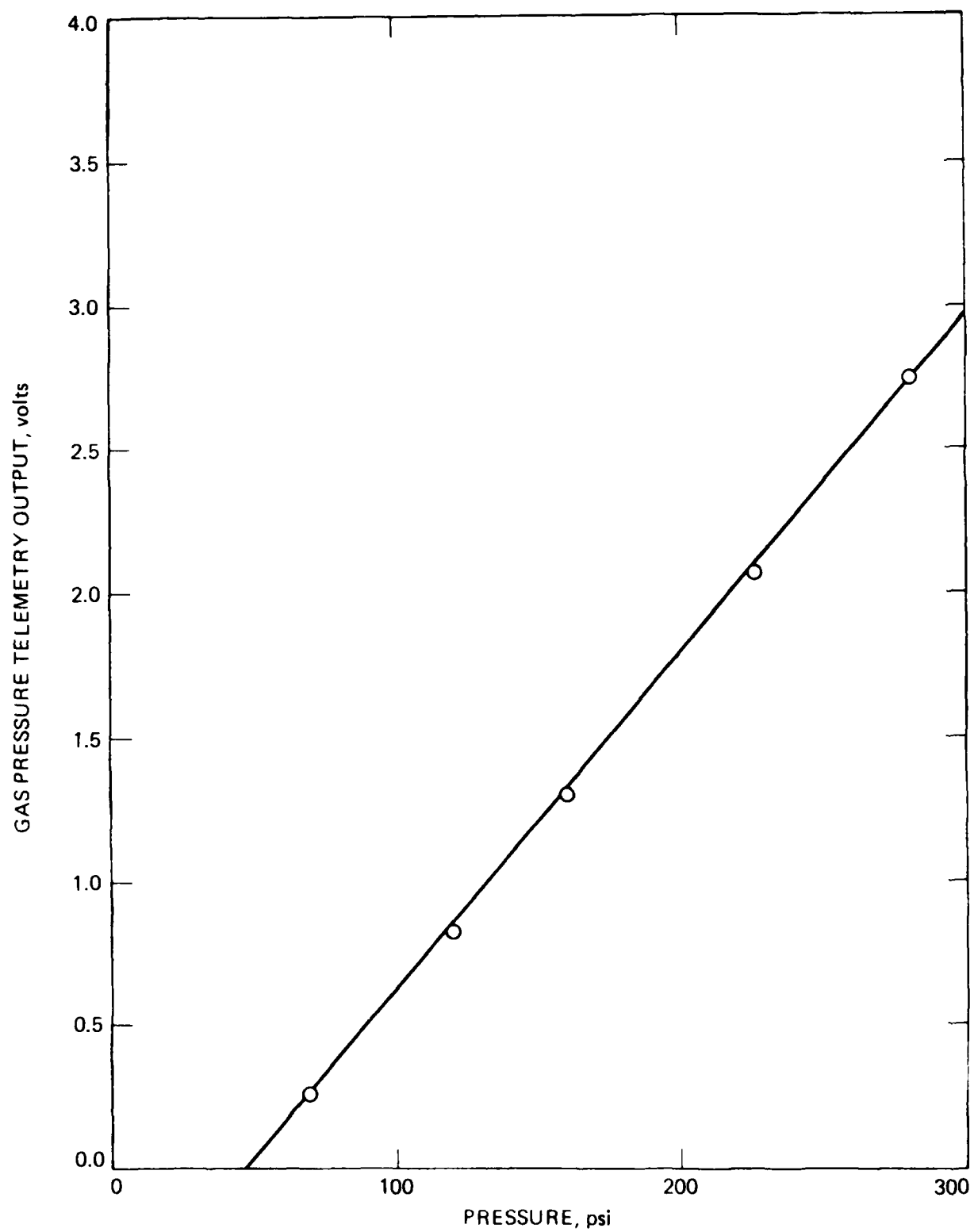


Figure 5-3. Gas Pressure Telemetry Output Versus Read Pressure

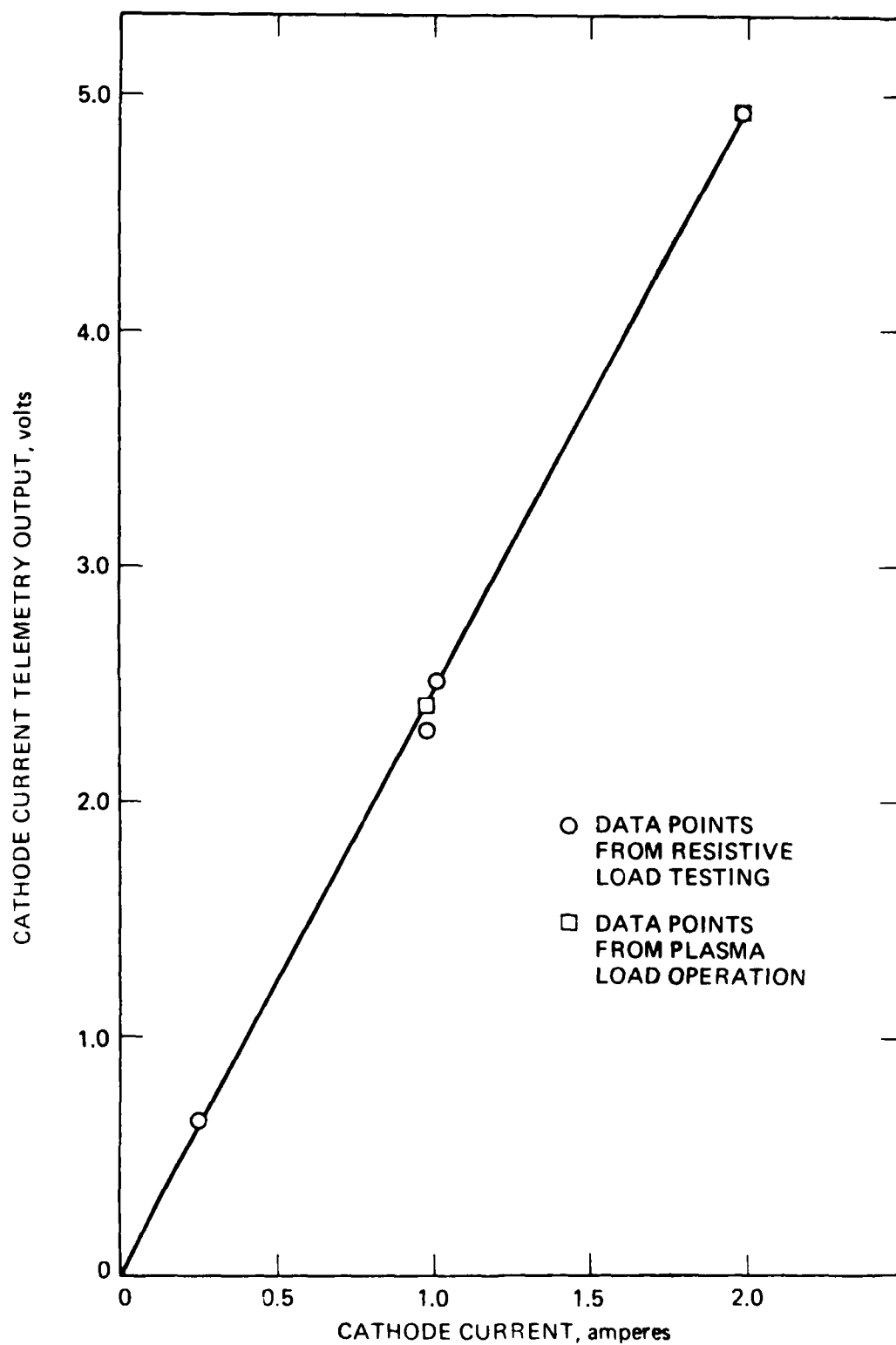


Figure 5-4. Cathode Current Telemetry Output Calibration Curve

the cathode current. Calibration curves for the low sensitivity (cathode current is 1.0 A, range 0-400 V) and high sensitivity (cathode current is 2.0 A, range 0-70 V) cathode voltage telemetry outputs are shown in Figs. 5-5 and 5-6, respectively.

#### 5.3.6 Keeper Current Telemetry

The keeper current telemetry signal is used to monitor the charged particle current flowing from the hollow cathode to the keeper electrode. The KEEPER power supply has three, constant current, operational set points which are 0.3 A, 1.2 A and 2.0 A, for collected electron current. One operational set point exists for collected ion current. A calibration curve for the KEEPER current telemetry output is shown in Fig. 5-7. The data for the curve was obtained while running the KEEPER power supply on a 20.5  $\Omega$  resistive load. The telemetry output values for operation on a plasma load are also noted on the curve and are: for the collected electron low current mode; 0.47 V, for the medium current mode; 2.34 V, and for the high current mode; 4.13 V. The telemetry output value for ion collection is 0.05 V and corresponds to tens of microamperes of collected ion current.

#### 5.3.7 Keeper Voltage Telemetry

The keeper voltage telemetry signal is used to monitor the potential difference between the emitter tube and keeper electrode. The potential between the keeper electrode and emitter tube does not vary much between the three modes for electron collection. The normal keeper telemetry output is between 2 V and 3 V for electron collection. When the keeper is operated to collect ions (negative bias), the normal keeper potential telemetry output is near 5.0 V. A calibration curve for the keeper potential telemetry output

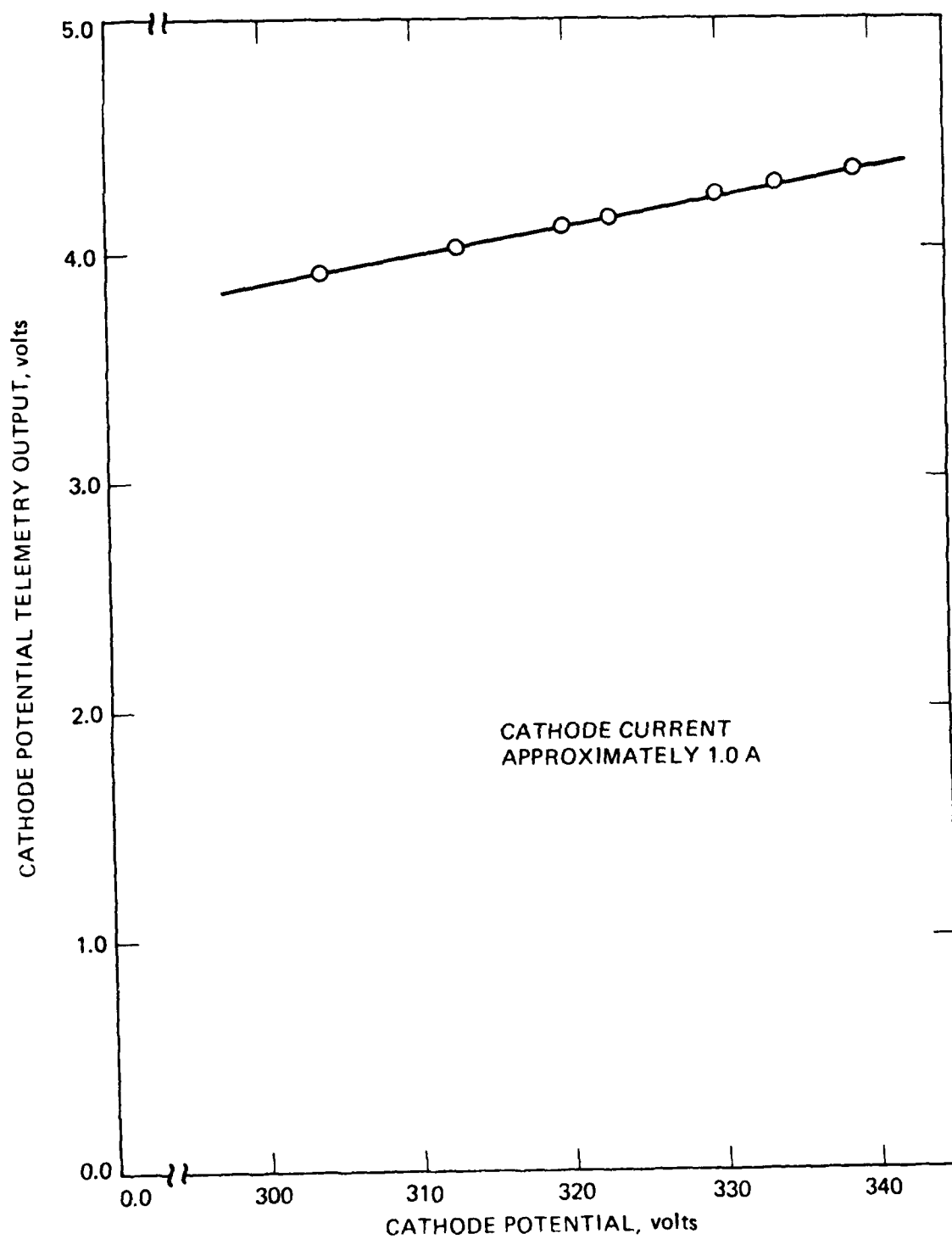


Figure 5-5. Cathode Voltage Telemetry Calibration Curve, Low Sensitivity



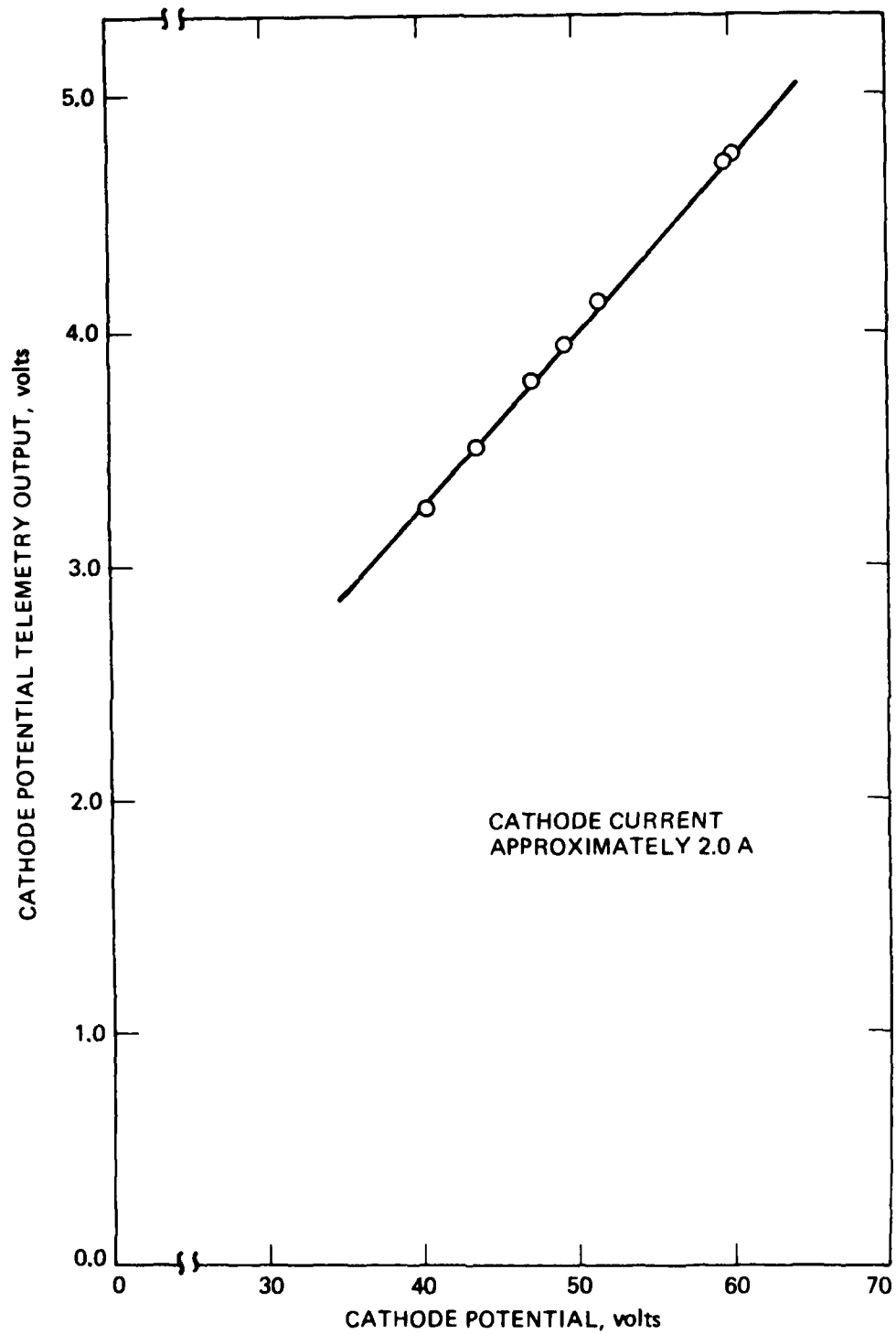


Figure 5-6. Cathode Voltage Telemetry Output Calibration Curve, High Sensitivity

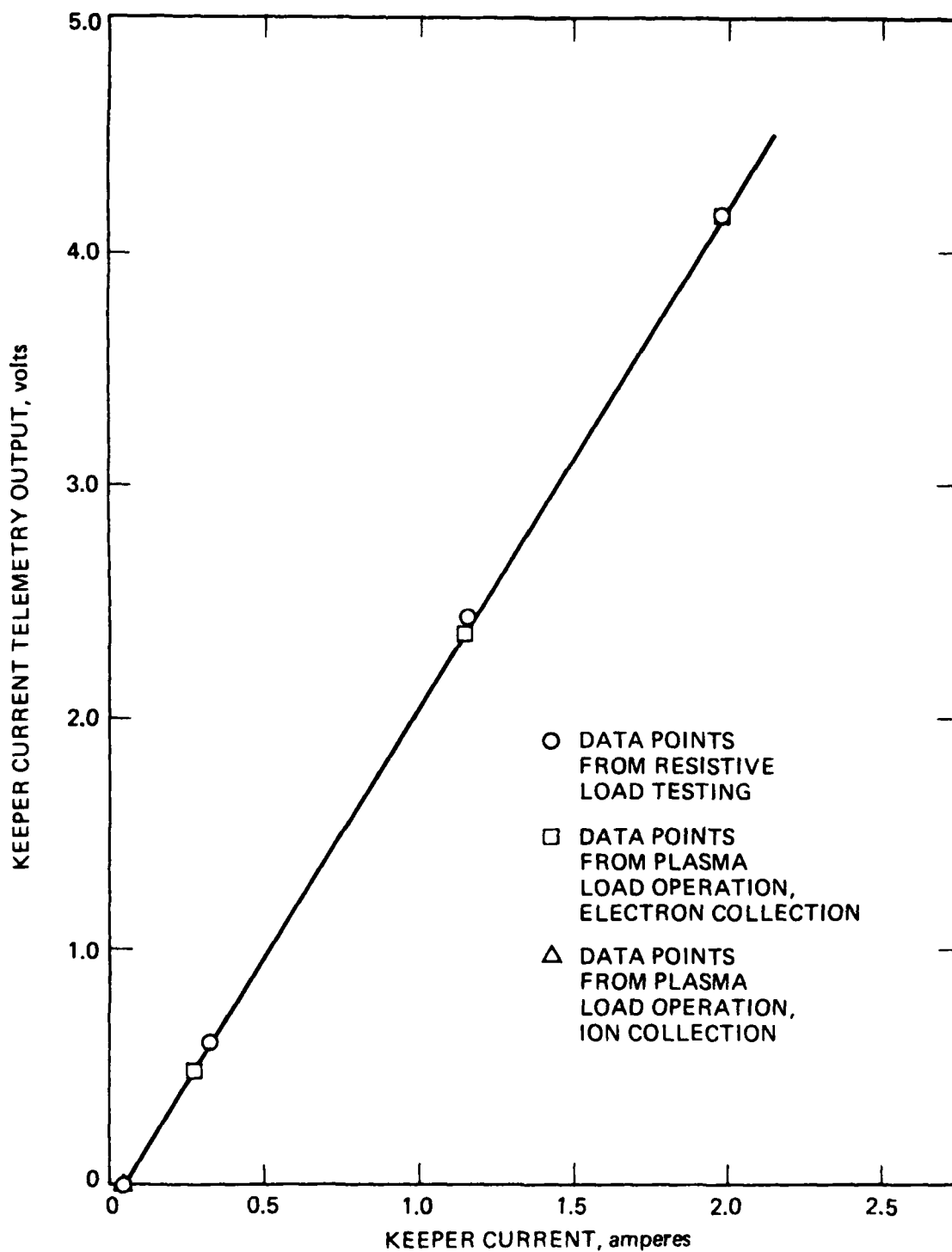


Figure 5-7. Keeper Current Telemetry Output Calibration Curve

is shown in Fig. 5-8. The curve was generated from data obtained while operating the KEEPER power supply on a resistive load. The operating range for plasma load operation is also shown.

#### 5.3.8 Keeper Polarity Telemetry

The keeper polarity telemetry signal is used to monitor the polarity of keeper electrode. When the keeper is biased positively (electron collection), the keeper polarity telemetry output is approximately 0.02 V. When the keeper is biased negatively (ion collection), the keeper polarity telemetry output is approximately 5.28 V. This characteristic is shown graphically in Fig. 5-9.

#### 5.3.9 Amplified Net Current Telemetry

The amplified net current telemetry signal is used to monitor the net charged particle current leaving the plasma source during a discharging event. The current is determined by monitoring the voltage drop through a 8.08 resistor combination which is the common point to spacecraft ground for the entire plasma source system. The amplification circuit has a nominal gain of 25. A calibration curve for this telemetry output is shown in Fig. 5-10 and was obtained through calculations (dotted line). Some experimental data points are also shown. The data points were obtained by placing a biased metal plate directly downstream of the plasma source opening. The electron current extracted by the biased metal plate was monitored and could be varied by varying the plate bias. The electron currents collected by the metal plate are shown with respect to the corresponding amplified net current telemetry outputs as the discreet data points in Fig. 5-10.

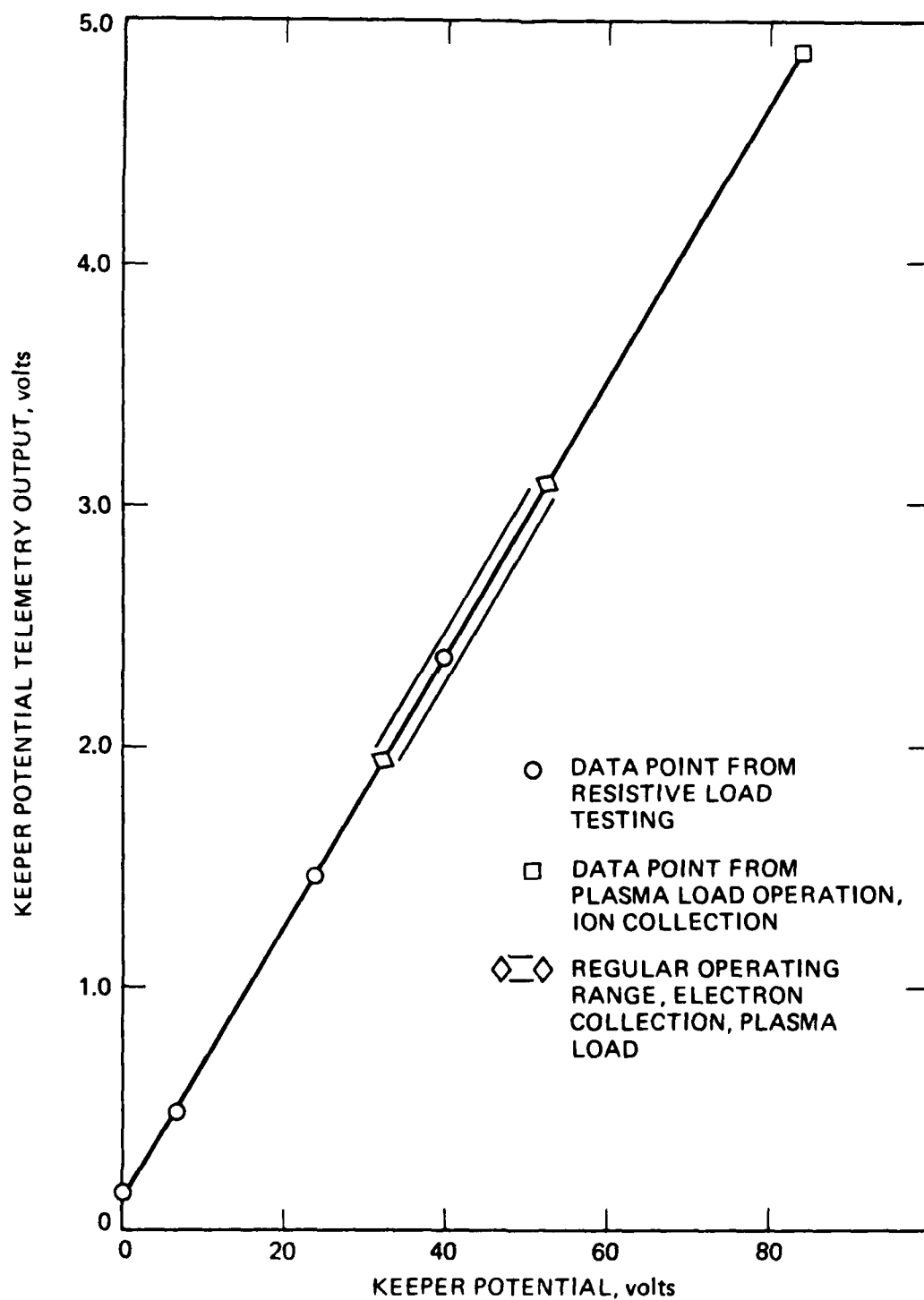


Figure 5-8. Keeper Potential Telemetry Output Calibration Curves

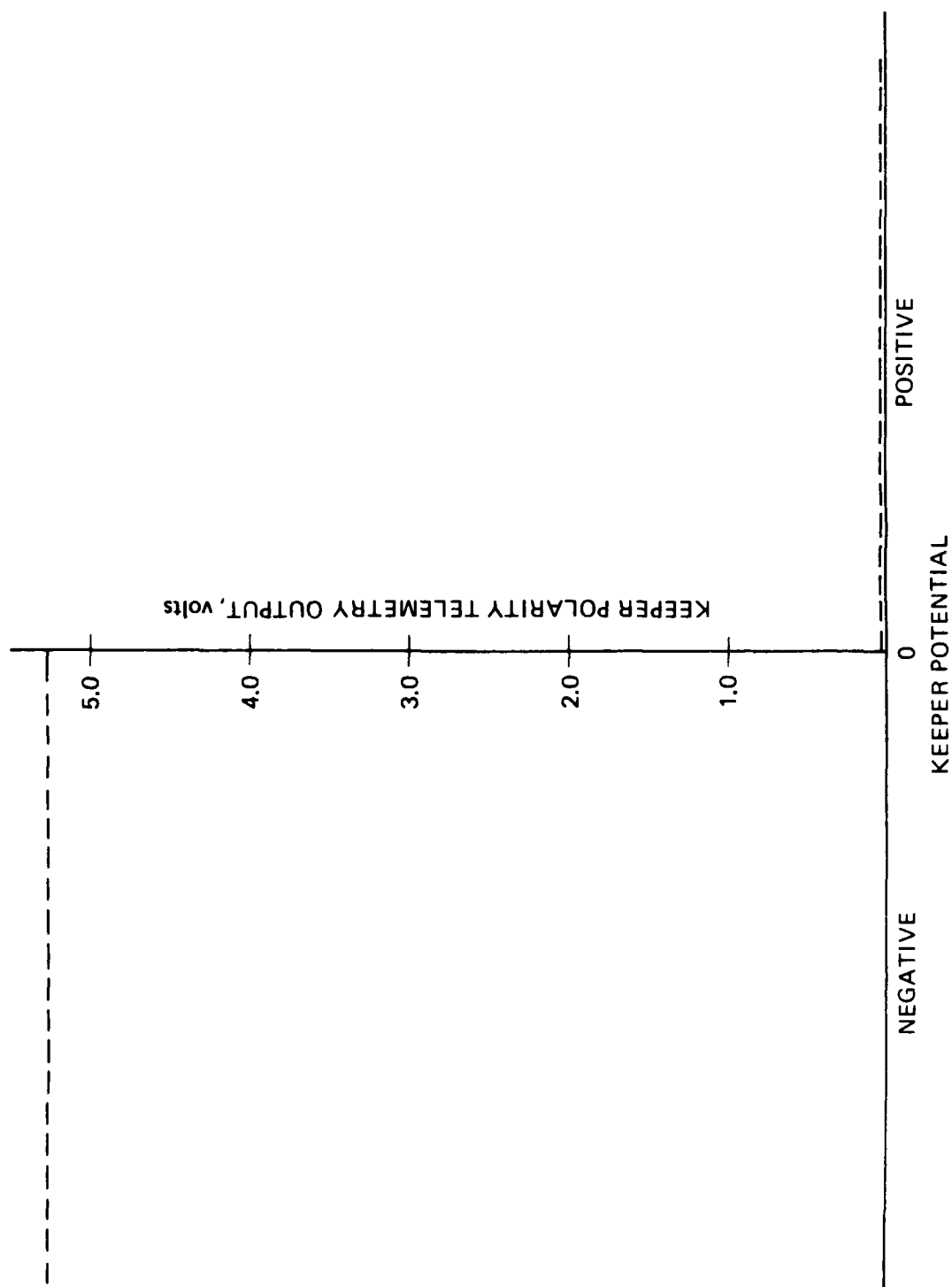


Figure 5-9. Keeper Polarity Telemetry

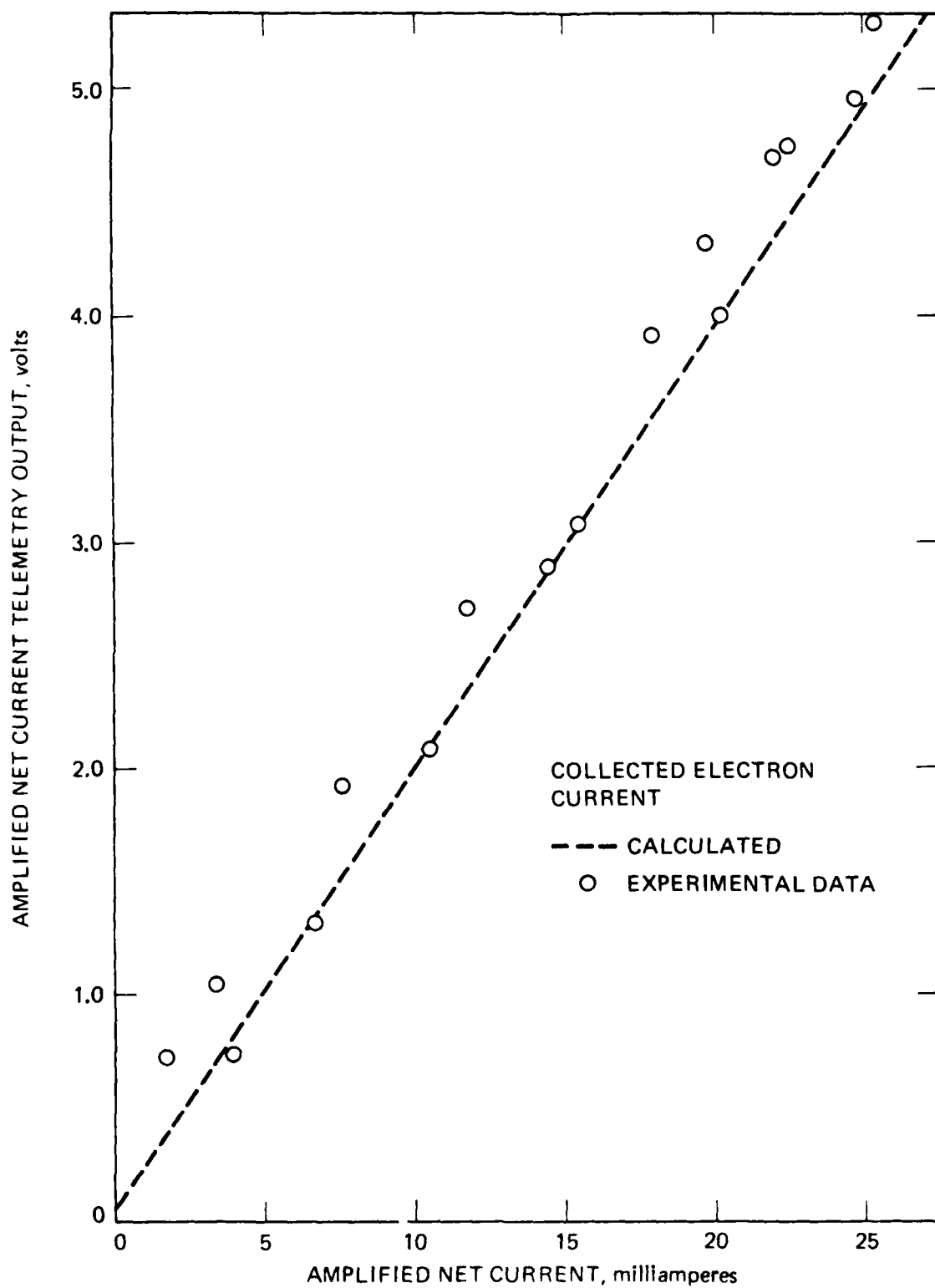


Figure 5-10. Amplified Net Current Telemetry Output Calibration Curve

#### 5.3.10 Amplified Net Current Polarity Telemetry

The amplified, net current, polarity telemetry signal is used to monitor the sign of the net charge leaving the plasma source. The output signal of near 0.0 V means electrons are flowing from spacecraft ground through the 8.08 resistor into the source. An output signal of near 5.0 V means electrons are flowing from the source through the 8.08 resistor, to spacecraft ground. Due to the high electron leakage current from the source to the background plasma, the amplified, net current, polarity telemetry output always indicates a negative net charge leaving the source (electrons coming from spacecraft ground into the plasma source).

#### 5.3.11 Integrated Net Current Telemetry

The integrated net current telemetry signal is used to monitor the total charge (Coulombs) leaving the source during a discharging event. The integrator circuit saturates when approximately 0.44 Coulombs ( $Q_{sat}$ ) of charge have left the source. Table 5-3 shows the time it takes to saturate the integrator due to electron leakage current versus the plasma source operating mode. As can be seen, the integrator saturates in about 6 minutes with the plasma source operating in the high keeper current mode. All other electron leakage currents resulted in longer integrator saturation times. A calibration curve for the integrator telemetry output versus total emitted charge is shown in Fig. 5-11. This curve was generated by biasing the metal plate to collect a specific current and monitoring the time versus the telemetry output to define specific values.

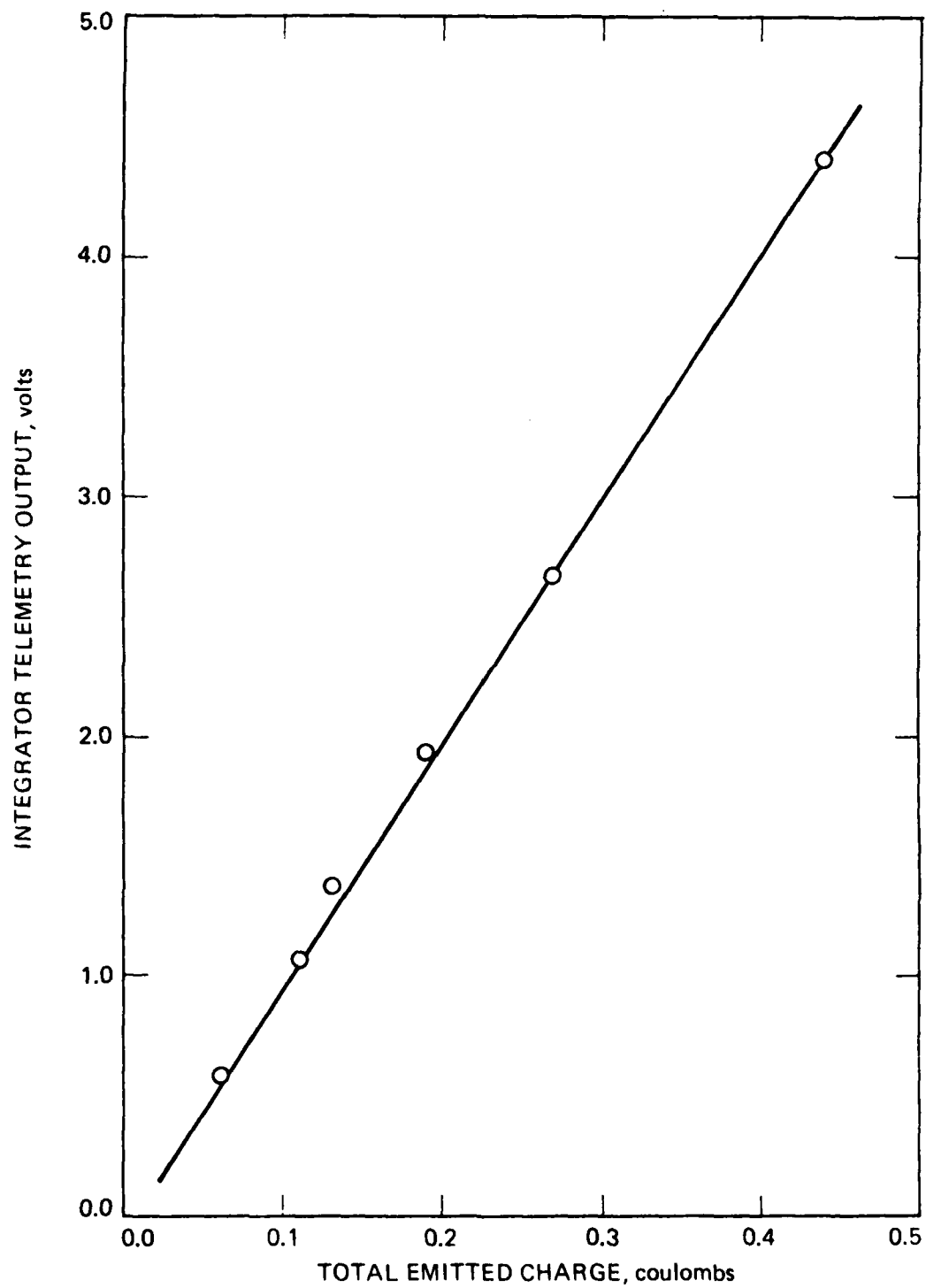


Figure 5-11. Integrated Net Current Telemetry Output Calibration Curve



Table 5-3. Integrator Saturation Times Versus Plasma Source Mode for Various Leakage Currents

Source Mode		Time (S)	Corresponding Leakage Current (mA)
Cathode	Keeper		
On	Off	1975	0.22
On	Lc	724	0.61
On	Mc	460	0.96
On	Hc	360	1.22

#### 5.3.12 Integrated Net Current Polarity Telemetry

The integrated, net current, polarity telemetry output is used to monitor the sign of the net charge being accumulated by the integrator. If the sign of the accumulated charge is positive, the telemetry output will be approximately 0.0 V. If the sign of the net charge is negative, the telemetry output will be approximately 5.0 V. Due to the high electron leakage current from the source, the integrated net current polarity telemetry output always indicates an accumulation of negative charge.

#### 5.4 PLASMA SOURCE SYSTEM TESTING

Plasma source system operational testing has been conducted at both AFGL and JPL. The testing has included determination of the system ON/OFF and keeper operation characteristics. In addition, the system's ability to discharge a capacitively-biased plate was examined along with evaluating how much current could be collected by an actively-biased plate.

#### 5.4.1 Operational Characteristics

The plasma source startup procedure causes the hollow cathode to go from an OFF condition to a high-voltage, low-current glow discharge and then to the ON condition which is a low-voltage, high-current arc discharge. This cathode start sequence is shown in Fig. 2-4. A series of four START-RUN-OFF sequences from the plasma source telemetry outputs are shown in Fig. 5-12. The startup time was on the order of 1.5 s for all four sequences. The small cusp at the beginning of each start sequence in the cathode voltage telemetry output resulted from the activation of the RUN supply. When the START supply was activated, the cathode voltage increased to about 340 V (T/M 3.3V) and the cathode current increased to 1 A (T/M 2.5V) to support a glow discharge. During sequences A and C the cathode potential dropped to about 35 V (T/M 2.5V) and the cathode current increased to 2 A (T/M 4.9V) turning off the START supply and placing the hollow cathode in the ON condition once the cathode emitter tube was hot enough to support thermionic emission of electrons. The keeper voltage increased during sequences A and C since the KEEPER supply is electrically floating, with the cathode emitter tube acting as a common point for it, and the START and RUN supplies. In sequences B and D, the KEEPER supply was activated at the same time as the RUN supply. During the cathode glow discharge, the KEEPER supply saw an open circuit condition with the voltage at about 80 V (T/M 4.9V). Once a cathode arc discharge was initiated, the plasma impedance between the hollow cathode and keeper electrode dropped so that the KEEPER could extract plasma from the cathode and collect a 2.0 A (T/M 4.9V) current at a potential difference of 25 V (T/M 2.0V). This allowed the cathode arc discharge potential to drop to about 20 V (T/M 2.0V). Typical turn off times for the plasma source system were on the order of 2.0 ms as can be seen in Fig. 3-11.

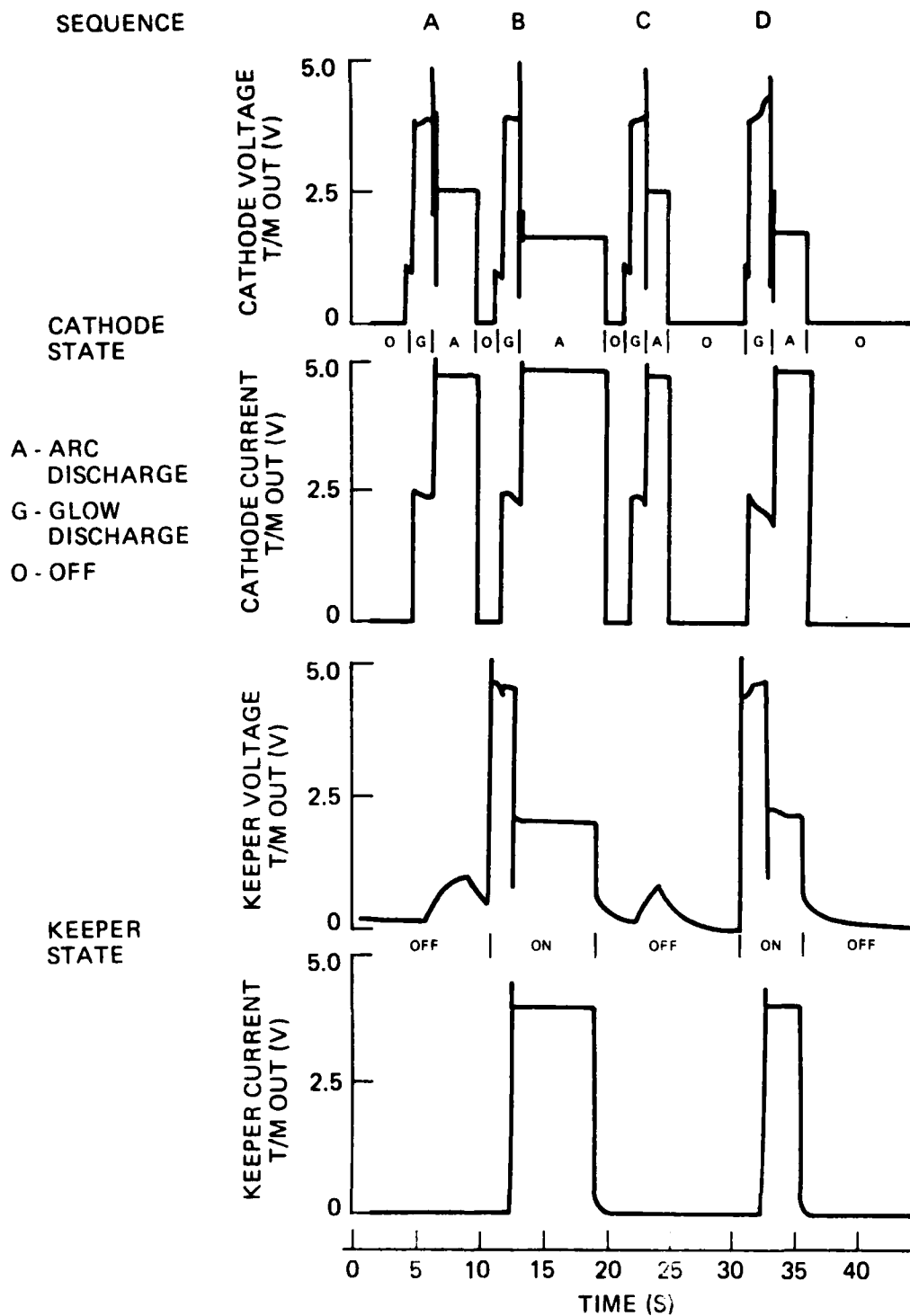


Figure 5-12. Plasma Source ON/OFF Sequence (T/M Outputs)

The plasma source system has 14 operational states which are determined by the status of the cathode and keeper and are defined in Table 5-4. A plasma source system run exhibiting states 1, 6, 9, 8, 7, 11, 12 and 10 (in order of appearance) through the output telemetry signals, is shown in Fig. 5-13. The currents corresponding to the low, medium and high keeper modes are approximately 0.3 A, 1.2 A and 2.0 A of collected electron current, respectively. In the self-heating modes, ion bombardment keeps the cathode emitter tube hot enough to thermionically emit electrons. There is no self-heating mode corresponding to the low current keeper mode because the current is too low to sustain an adequate flow of backstreaming ions to self heat the cathode. Ion currents collected by the keeper in the reverse bias mode (keeper negative) are on the order of, at most, tens of microamperes, and as a result are not detectable on the keeper current telemetry output signal.

#### 5.4.2 Functional Characteristics

Tests were conducted to evaluate how well the plasma source could discharge biased plates. An aluminum plate, 30 cm on a side, was placed 12 cm downstream of the plasma source opening. The plate could be biased by charging a 500 pf capacitor attached to the plate or by applying a bias directly with a variable voltage power supply. The sounding rocket capacitance was determined using the equivalent sphere method whereby the rocket is assumed to be a sphere with a surface area equal to that of the actual sounding rocket. The capacitance is then calculated using<sup>24</sup>

$$C = 4\pi \epsilon_0 R(1 + R/\lambda_D)$$

Table 5-4. Plasma Source Operational States

System State	Cathode Status	Keeper Mode <sup>b</sup>	Command Word Bits <sup>a</sup>							
			0	1	2	3	4	5	6	7 <sup>a</sup>
1	START	OFF	1	1	0	0	0	-	-	-
2	START	(e-) HC	1	1	1	0	0	-	-	1
3	START	(e-) MC	1	1	1	1	0	-	-	1
4	START	(e-) LC	1	1	1	0	1	-	-	1
5	START	(i+)	1	1	1	0	0	-	-	0
6	ON	OFF	1	0	0	0	0	-	-	-
7	ON	(e-) HC	1	0	1	0	0	-	-	1
8	ON	(e-) MC	1	0	1	1	0	-	-	1
9	ON	(e-) LC	1	0	1	0	1	-	-	1
10	ON	(i+)	1	0	1	0	0	-	-	0
11 <sup>c</sup>	OFF	(e-) HC	0	0	1	0	0	-	-	1
12 <sup>c</sup>	OFF	(e-) MC	0	0	1	1	0	-	-	1
13 <sup>c</sup>	OFF	(e-) LC	0	0	1	0	1	-	-	1
14	OFF	OFF	0	0	0	0	0	-	-	-

<sup>a</sup>Bits 5 and 6 not used, "-" under bit 7 means state obtained for either bias

<sup>b</sup>(e-) HC - High current electron collection mode, (e-) MC - Medium current electron collection mode, (e-) LC - Low current electron collection mode, (i+) ion collection mode

<sup>c</sup>Cathode self heating modes, STATE 12 is unstable, STATE 13 not supported

SYSTEM  
STATE

CATHODE  
STATE

KEEPER  
STATE

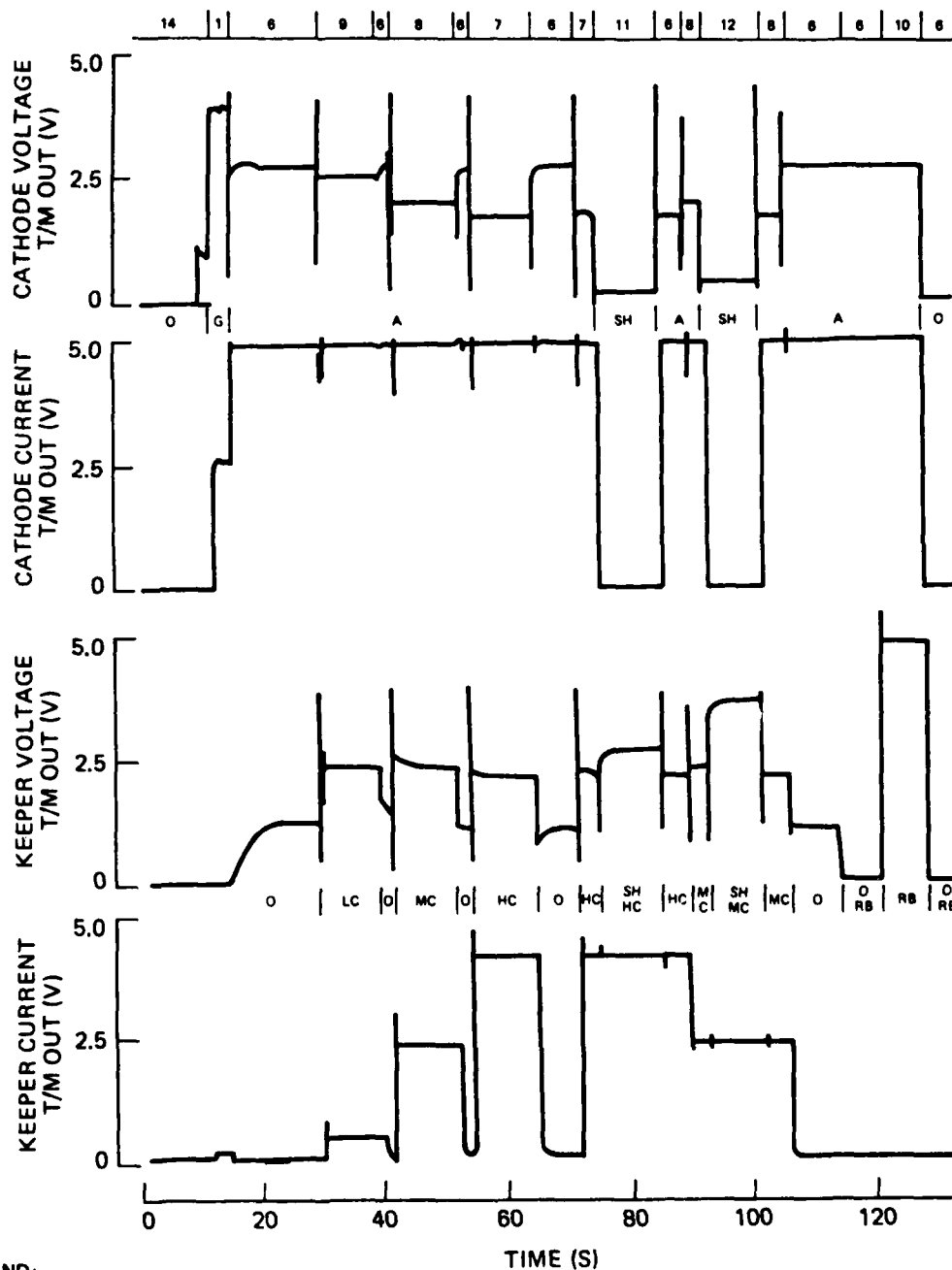


Figure 5-13. Plasma Source Operational States (T/M Outputs)

where  $R$  is the radius of the equivalent sphere (3 m),  $\lambda_D$  is the Debye length and  $\epsilon_0$  is the permittivity constant. Several values of capacitance are given in Table 5-5 for various Debye lengths. A value of 500 pf was chosen since a high-voltage, 500 pf capacitor was readily available though a value of 20 nf is more consistent with the expected sounding rocket capacitance. A high-voltage power supply was used to charge the capacitor through a 22 M charging resistor. The plate biases ranged from  $\pm 100$  V to  $\pm 2500$  V. A typical discharge pulse is shown in Fig. 5-14, which has a pulse duration of approximately 35 ms with a peak discharge current of approximately 17 mA. The initial plate potential was 590 V.

The current which could be extracted from the plasma source was evaluated by biasing the plate directly, with a variable voltage power supply. Then, the plasma source was activated to examine the initial discharge pulse. The current collected by the plate could also be monitored while the plate potential was varied. A typical plate discharge pulse is shown in Fig. 5-15a for a directly biased plate originally at 805 V, as seen in Fig. 5-15b. The pulse width is approximately 10 ms with a peak height of 23 mA. The plate potential was held to about 5 V, while drawing a constant 8 mA electron current. When the power supply output voltage was increased, the plate potential remained constant and the collected current increased.

The plasma source net current monitoring system was also evaluated using the directly biased plate. Typical telemetry outputs are shown for the plasma source net current integrator and amplified net current monitor in the curves of Fig. 5-16 for current collection by a positively-biased plate. These curves were generated while operating the plasma source in the medium current keeper mode. These curves show how, as the collected electron current increases, the slope of the integrator gets steeper. The plate bias and

Table 5-5. Sounding Rocket Capacitance Versus Debye Length

Debye Length (m)	Capacitance (nF)
10.0	0.44
3.0	0.67
1.0	1.34
0.5	2.34
0.1	10.34
0.05	20.35
0.01	100.43

actual values of the collected electron current (see Section 5.3.10) are given for each step of the curve for the amplified net current signal output. The integrator saturates when about 0.44 Coulombs have been emitted from the plasma source. A set of curves showing the electron current collected by the biased plate as a function of plate potential for the five source states where the keeper is also set to collect electrons (states 7-9, 11, 12) is shown in Fig. 5-17. Operation of the plasma source in the high-current keeper mode, pulls the plate potential down the lowest for a given collected current. The self-heating, high-current keeper mode is the next best. The data for the low-current keeper mode end at 100 V since the discharge extinguished itself at this point repeatedly. The low-current keeper mode cannot support a self-heating mode.

Typical net current monitor telemetry outputs are shown in Fig. 5-18 for current collection by a negatively-biased plate (ion collection) located 10 cm downstream of the keeper electrode. The integrator slope



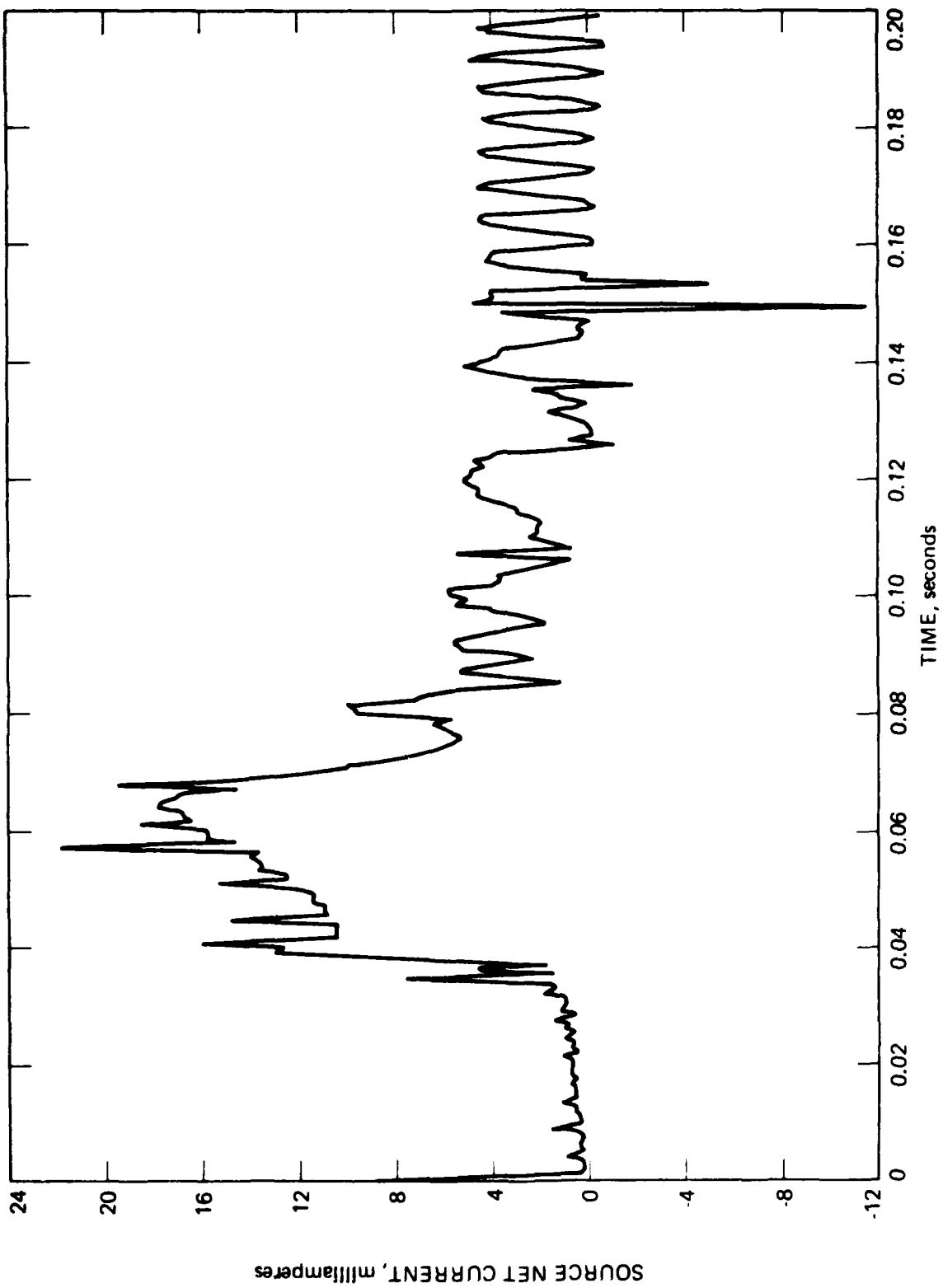


Figure 5-14. Typical Net Current Discharge Pulse

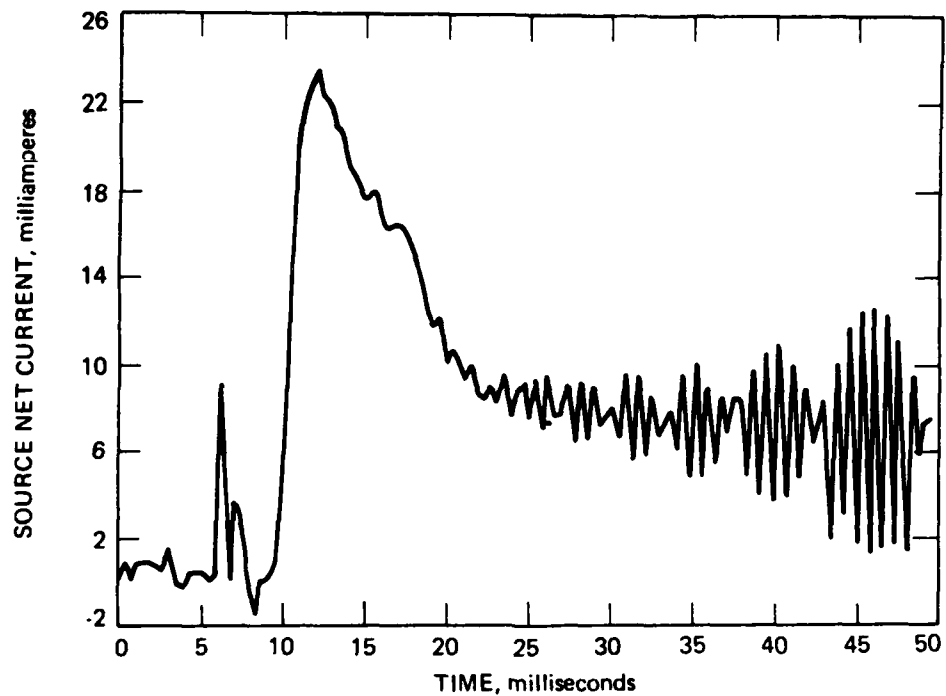


Figure 5-15a. Typical Plate Discharge Pulse

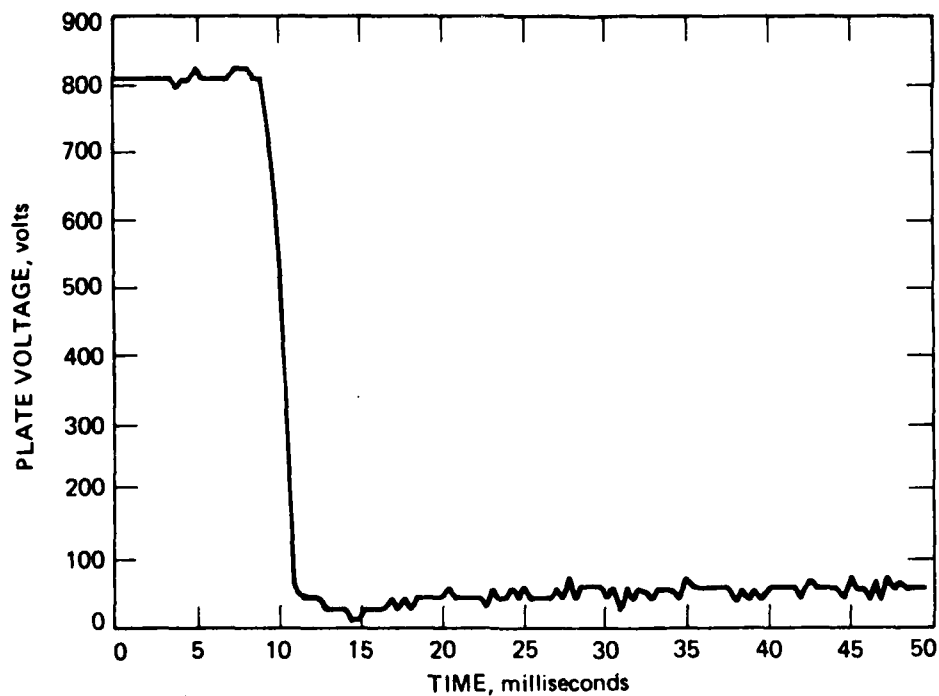


Figure 5-15b. Plate Potential During Discharge Pulse

Typical Plate Discharge Pulse and the Plate  
Potential During the Discharge Pulse

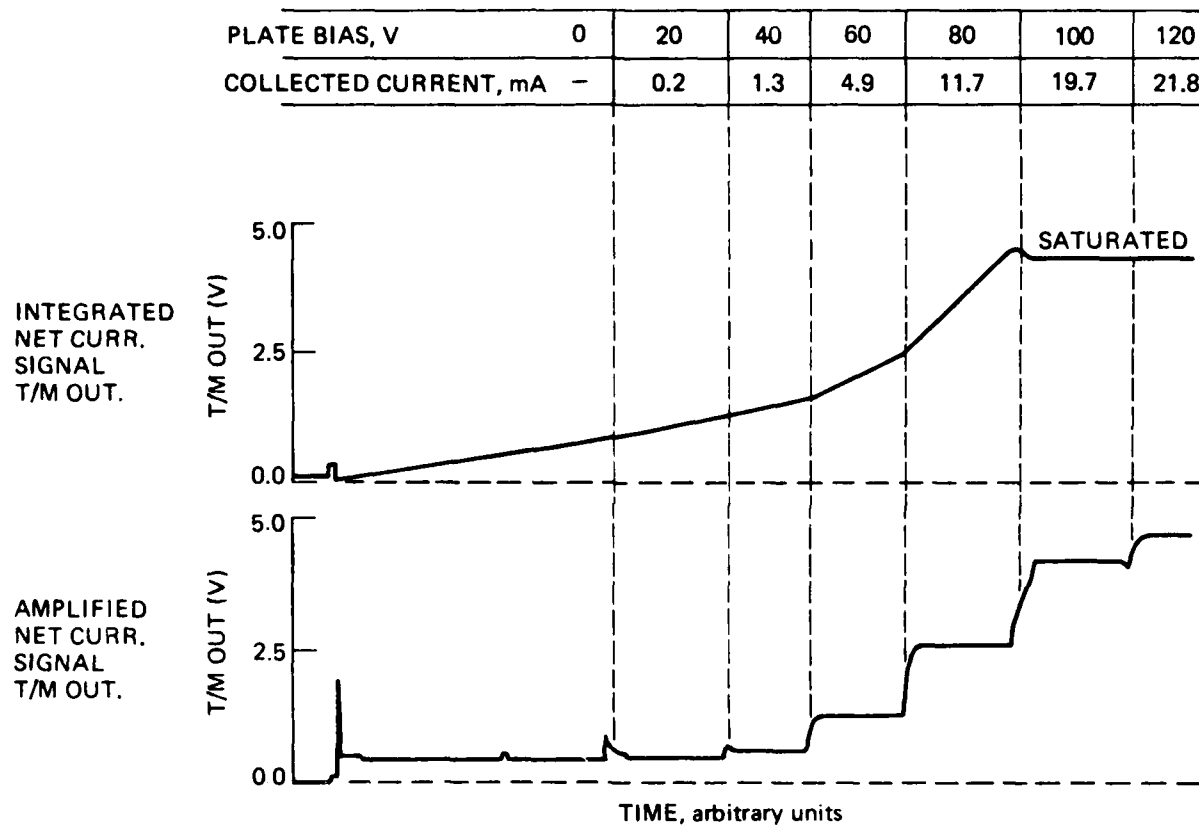


Figure 5-16. Current Collection By a Positively Biased Plate During Plasma Source Operation (T/M Outputs)

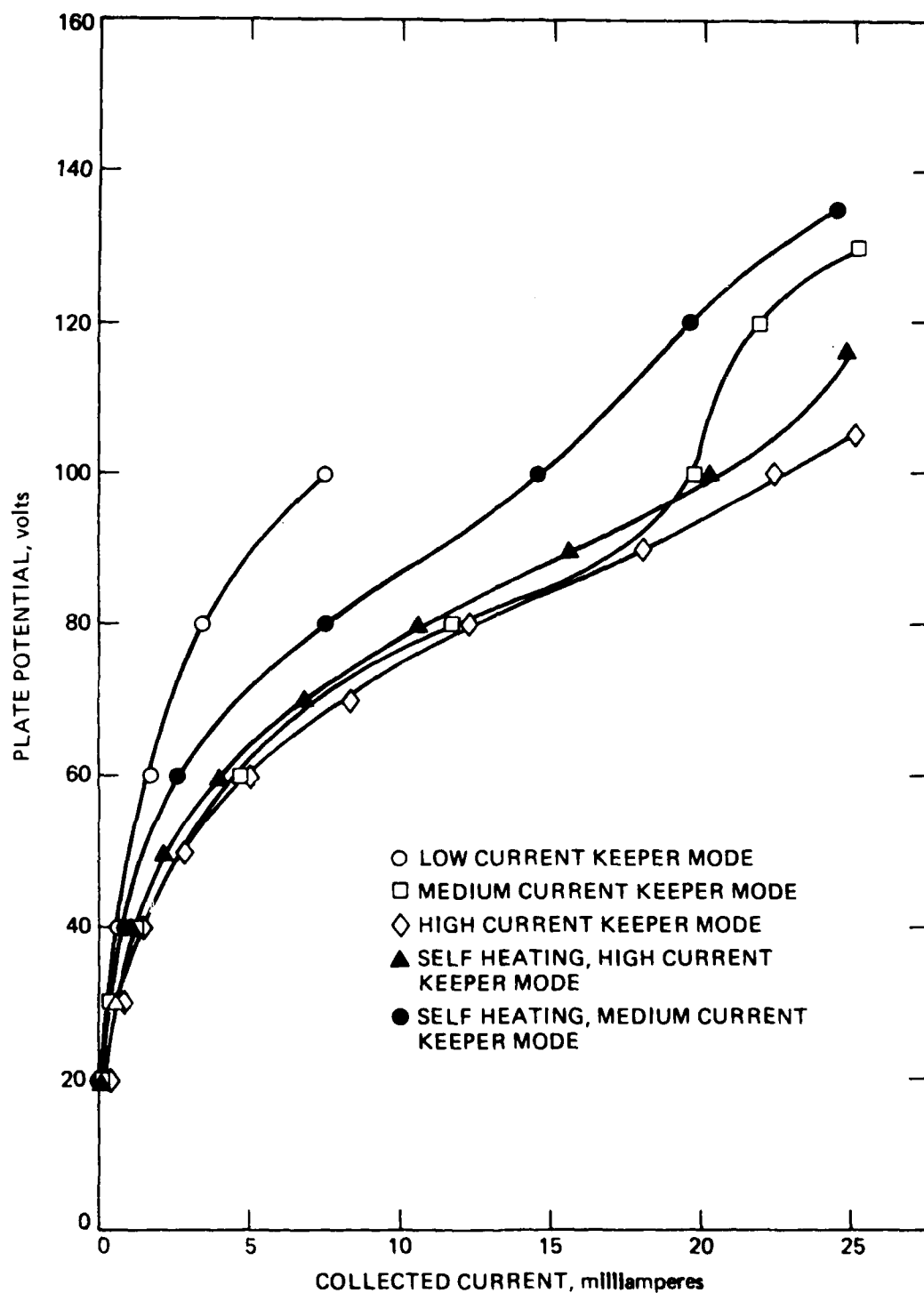


Figure 5-17. Collected Current As a Function of Plate Potential for Various Plasma Source Operating Modes

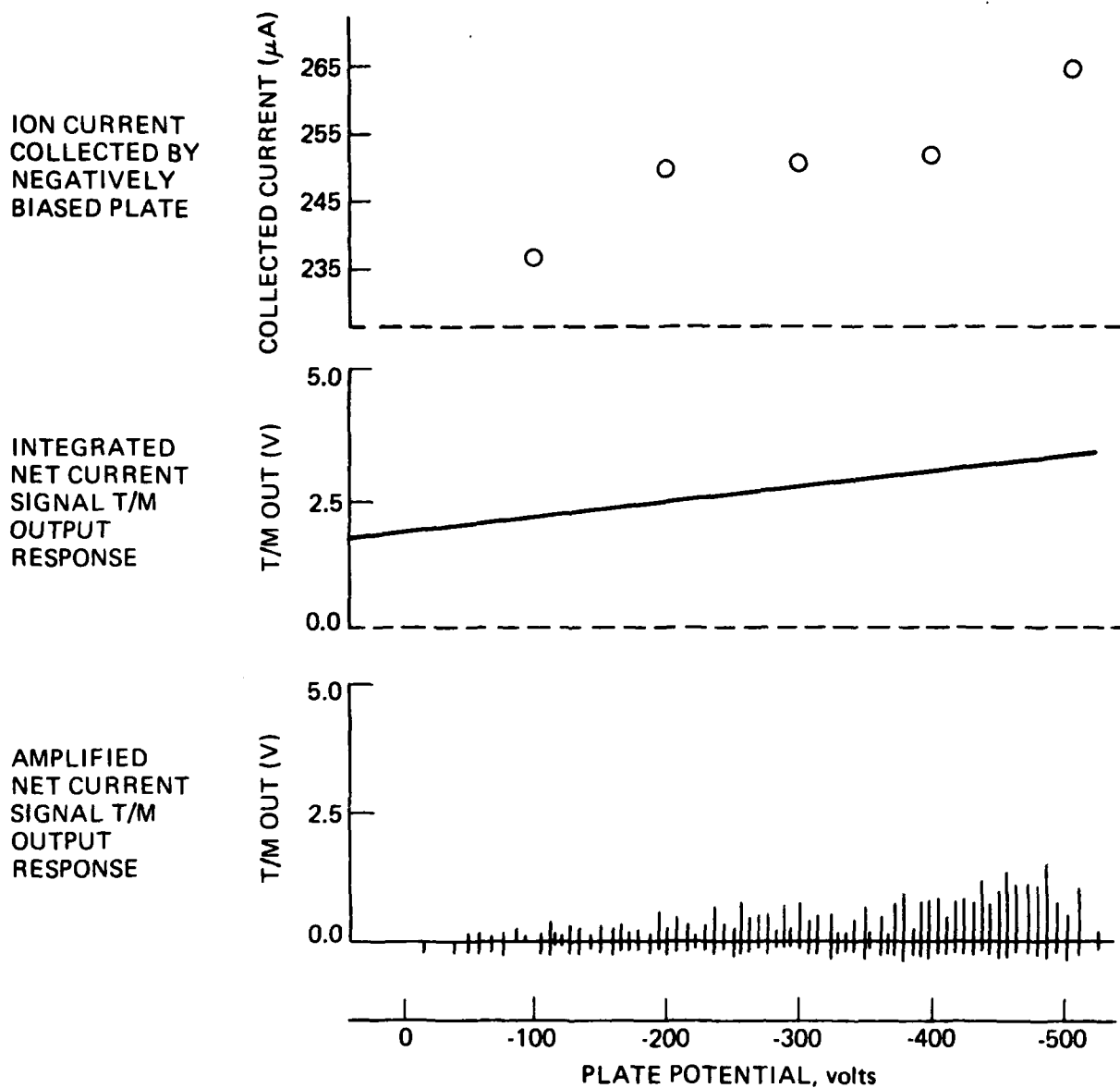


Figure 5-18. Correct Collection By a Negatively Biased Plate During Plasma Source Operation

## SECTION 6

### CONCLUSIONS

A neutral plasma source, for use in active spacecraft charge control, has been developed, fabricated, and characterized and was delivered to the Air Force Geophysics Laboratory on 18 April, 1985. The functional design requirements and actual system characteristics of the plasma source spacecraft discharge device are summarized in Table 6-1. As can be seen by examining Table 6-1, all system requirements have been met or exceeded. In ground simulation tests the plasma source successfully discharged capacitively biased plates, from as high as  $\pm 2500V$ , to ground potential. In addition, actively biased plates could be discharged and clamped at  $+5V$  with respect to ground. Qualification tests completed by AFGL personnel have demonstrated that the plasma source system met the vibration, shock and thermal requirements.

The plasma source had several novel features and characteristics. Fourteen (14) system operational states were available including five (5) electron enhanced modes, an ion enhanced mode and a straight cathode discharge. This device could also be easily run on xenon and argon in addition to krypton. The field enhanced refractory metal (FERM) hollow cathode contained no low work function impregnants to prevent poisoning which could result in complete cathode failure after exposure to air. In addition, the FERM hollow cathode allowed for the plasma generation process to be contained completely within the hollow cathode. No external sustaining electrodes were necessary. The system flexibility should make the device a valuable tool for spacecraft charge control.

Table 6-1. Plasma Source Functional Requirements And Characteristics

Parameter	Requirement	Actual
Startup Time:		
Cold	<5 s	3 - 4 s
Hot	<5 s	<1 s
Working Gas	Krypton	Krypton
Startup Energy	2500 W-s	1904 W-s
Run Power	200 W	196 W <sup>a</sup>
Particle Currents:		
Extracted Electron	>20 mA	20 - 6000 mA
Extracted Ion	>20 $\mu$ A	352 $\mu$ A <sup>b</sup>
Electron Leakage	>2 mA	17 $\mu$ A
Mass	<12.25 kg	12.2 kg
Lifetime		
Total	>450 s	10800 <sup>b</sup>
Duty Cycle (Max.)	0.3	0.001 - 1.0
Starts	>36	350 <sup>b</sup>
<p><sup>a</sup> Value for highest power ion collection mode, State 7 (see Table 5-4)</p> <p><sup>b</sup> Highest value seen during characterization testing, higher values possible.</p>		

## SECTION 7

### REFERENCES

1. Garrett, H. B., "The Charging of Spacecraft Surfaces," Rev. Geophys. Space Phys., Vol. 19, No. 4, pp. 577-616, Nov. 1981.
2. Olsen, R. C., "Modification of Spacecraft Potentials by Thermal Electron Emission on ATS-5," J. Spacecr. Rockets, Vol. 18, No. 6, pp. 527-532, (AIAA Paper No. 81-4348) Nov. 1981.
3. Goldstein, R., "Active Control of Potential of the Geosynchronous Satellites ATS-5 and ATS-6," Paper I-6, Proceedings of the Spacecraft Charging Technology Conference, Editors; C. P. Pike, R. R. Lovell, NASA TM X-73537, pp. 121-130, Feb. 1977.
4. Purvis, C. K., Bartlett, R. O., Deforest, S. E., "Active Control of Spacecraft Charging on ATS-5 and ATS-6," Paper I-5, pp. 107-120, (see Reference 3).
5. Whipple, E. C., Olsen, R. C., "Experiments on Regulation of Electric Charge on Space Vehicles," AIAA Paper No. 79-1506, AIAA 12th Fluid and Plasma Dynamics Conference, Jul. 1979.
6. Olsen, R. C., "Modification of Spacecraft Potentials by Plasma Emission," J. Spacecr. Rockets, Vol. 18, No. 5, pp. 462-469, (AIAA Paper No. 81-4287) Sept. 1981.
7. Coben, H. A., Lai, S., "Discharging the P78.2 (SCATHA) Satellite Using Ions and Electrons," AIAA Paper No. 82-0266, AIAA 20th Aerospace Sciences Meeting, Jun. 1982.
8. Mizera, P. F., "Natural and Artificial Charging: Results from the Satellite Surface Potential Monitor Flown on P78-2 (SCATHA)," AIAA Paper No. 80-0334, AIAA 18th Aerospace Sciences Meeting, Jan. 1980.



9. Reasoner, D. L., Lennartsson, W., Chappell, C. R., "Relationship between ATS-6 Spacecraft Charging Occurances and Warm Plasma Encounters," Spacecraft Charging by Magnetospheric Plasma - Progress in Astronautics and Aeronautics, Vol. 47, pp. 89-102, editor; A. Rosen.
10. Deforest, S. E., "Spacecraft Charging at Synchronous Orbit," Journal of Geophysical Research, Vol. 77, No. 4, 1972, pp. 651-659.
11. Rosen A., "Spacecraft Charging: Environmental Induced Anomalies," J. Spacecr. Rockets, Vol. 13, 1976, p. 129.
12. Balmain, K. G., Cuchanski, M., Kremer, P. C., "Surface Micro-Discharges on Spacecraft Dielectrics", Paper III-7, Proceedings of the Spacecraft Charging Techonology Conference, NASA TM X-73537, Feb. 1977, editors; Pike, C. P., Lovell, R. P., pp. 516-526.
13. Nanevicz, J. E., Adamo, R. C., "Occurance of Arcing and its Effects on Space Systems," Space Systems and their Interactions with Earth's Space Environment - Progress in Astronautics and Aeronautics, Vol. 71, editors; Garrett, H. B., Pike, C. P., pp. 252.
14. Inouye, G. T., "Spacecraft Charging Anomalies on the DSCS-II, Launch 2 Satellites, "Paper No. V-10, Proceedings of the Spacecraft Charging Technology Conference, NASA TM X-73537, Feb. 1977, editors; Pike, C. R., Lovell, R. R., pp. 829-852.
15. Robbins, A., Short, C. D., "Space Environmental Effects on the SKYNET 2B Spacecraft," Paper No. V-11, Proceedings of the Spacecraft Charging Technology Conference, NASA TM X-73537, Feb. 1977, editors; Pike, C. P., Lovell, R. R., pp. 853-863.

16. Shaw, R. R., Nanevich, J. E., Adamo, R. C., "Observations of Electrical Discharges Caused by Differential Satellite Charging," Paper SA-41, Spacecraft Charging by Magnetospheric Plasmas, Progress in Astronautics and Aeronautics, Vol. 47, 1976, editor; A. Rosen, pp. 61-76.
17. Purvis, C. K., Garrett, H. B., Whittlesey, A. C., Stevens, N. J., "Design Guidelines for Assessing and Controlling Spacecraft Charging Effects," NASA TP-2361, Sept. 1984.
18. Rawlin, V. K. and Pawlik, E. V., "A Mercury Plasma Bridge Neutralizer," J.Spacecr. Rockets, Vol. 5, 1968, pp. 814-820.
19. Ward, J. W. and King, H. J., "Mercury Hollow Cathode Plasma Bridge Neutralizers", J. Spacecr. Rockets, Vol. 5, 1968, pp. 1161-1164.
20. Kerslake, W. R., Goldman, R. G., and Neirberding, W. C., "SERT II: Mission Thruster Performance and In-Flight Thrust Measurements," J. Spacecr. Rockets, Vol. 8, 1971, pp. 213-224.
21. Masek, T., "Satellite Positive Ion Beam System," Air Force Geophysics Laboratory, Final Report No. AFGL-TR-78-0141, Oct. 1978. ADA063964
22. Aston, G. and Deininger, W. D., "Test Bed Ion Engine Development," NASA CR-174623, March 1984.
23. Meek, J. M. and Craggs, J. D., "Electrical Breakdown of Gases", Oxford University Press, 1953.
24. Fitzgerald, D. J., "Factors in the Design of Spacecraft Utilizing Multiple Electric Thrusters", AIAA Paper No. 75-404, AIAA 11th Electric Propulsion Conference, Mar. 1975.

END

FILMED

4-86

DTIC